



University of
Stavanger

Faculty of Science and Technology

MASTER'S THESIS

Study program/Specialization: Petroleum Engineering / Reservoir Engineering	Spring semester, 2018 Open access
Writer: MD ASHRAFUL ISLAM KHAN (Writer's signature)
Faculty supervisors: Dr Skule Strand Dr Tina Puntervold Laboratory supervisors: Dr Iván Darío Piñerez Torrijos Alexandr Mamonov	
Thesis title: pH Development Analysis of Alkaline and Low Salinity Water Flooding in sandstone cores	
Credits (ECTS): 30	
Key words: Enhanced oil Recovery (EOR), Smart water EOR, Low salinity EOR, Alkaline EOR, pH screening test, Alkalinity transportation, Sandstone	Pages: 101 Stavanger, <u>15/06/2018</u> Date/year

Acknowledgment

Firstly, I would like to express my gratitude to my supervisors Associate Professor Dr Tina Puntervold and Dr Skule Strand for giving me the opportunity to work in their laboratory. I am thankful for their valuable suggestions and discussion seasons without which it would be impossible to complete this thesis. I am grateful to the entire Smart Water group for their support, endeavor and for giving a friendly working environment where I could express my thinking without any hesitation.

I would also like to thank Alexandr Mamonov, PhD student of UiS, for his support in the laboratory and of course, during writing this thesis. Furthermore, I would like to thank Dr. Iván Darío Piñerez Torrijos, Postdoctoral Fellow, for his support during the experiments. Additionally, I would like to thank laboratory assistant Magnus Sundby Kinn and other students who were working in the laboratory during the semester. Special thank goes to The National IOR Centre of Norway and International Research Institute of Stavanger (IRIS).

Finally, but not the least, I would like to thank my parents and my friends for supporting me in every endeavor during my stay in Stavanger.

Abstract

Low salinity (LS) water flooding has been in the center of interest for conventional oil recovery in sandstone reservoir for more than two decades because of its low cost and potential for increased oil recovery. Though hundreds of researches have been done on LS EOR method, the mechanism behind the oil recovery is still debatable. Recently, Smart Water group of University of Stavanger has proposed a new chemical wettability alteration mechanism where protons (H^+) from LS water replaces metal ions such as Ca^{2+} , Na^+ from the clay surface and made the surface more water wet by releasing polar organic oil components due to a pH increase. As a result, more oil is displaced towards production well and increases oil recovery. As the proton (H^+) is adsorbed, pH of the produced water is increased and using this theory, Aksulu et. al. (2012) established a pH screening test as an experimental tool to check the LS potential for sandstone.

pH of the system can also be increased by injecting alkaline water of high pH instead of creating in situ pH increase by LS water flooding. In this thesis, the transportability of alkalinity and development of pH was investigated for LS and alkaline water flooding. Three outcrop sandstone cores of different mineralogy were used for 12 pH screening tests at different temperatures. In addition with the pH screening test, pressure changes, density changes and ion chromatography tests were done during the flooding to observed the changes of produced water.

pH-screening tests with alkaline water injection showed low potential for extra alkalinity compared with LS water injection. Almost two pH unit of injected high alkaline water is reduced by the minerals and formation water. On the other hand, the results of the pH-screening tests for LS water injection showed a potential for increasing the effluent LS water pH up to two units in comparison to its initial pH-value. Both the LS and alkaline water showed same trend of pH buildup though they had a big difference in bulk pH (almost 5 pH unit). Transportation of alkalinity through a mineral system with large surface area seemed to be challenging due to pH buffering from brine/mineral interactions as well as from chemical interactions involving inorganic cations from the formation water.

It can be concluded after the thesis that an in-situ generation of alkaline conditions in the reservoir by injecting LS water seemed to have a larger potential for EOR purposes than transporting alkalinity by injecting high pH alkaline water through the reservoir.

Table of Content

ACKNOWLEDGMENT	2
ABSTRACT	3
TABLE OF CONTENT	4
LIST OF FIGURES	7
LIST OF TABLES	9
1. INTRODUCTION	10
1.1 OIL RECOVERY	10
1.1.1 Primary oil recovery	10
1.1.2 Secondary oil recovery	11
1.1.3 Tertiary oil recovery- Enhanced oil recovery	11
1.2 DEFINITIONS OF EOR AND IOR.....	11
1.2.1 Importance of EOR.....	12
1.2.2 Different Enhanced oil recovery Methods.....	12
2. OBJECTIVE	15
3 BASICS OF EOR WITH SMART WATER	16
3.1 DISPLACEMENT FORCES.....	16
3.1.1 Microscopic and macroscopic displacement	16
3.1.2 Fluid flow in porous media	17
3.1.3 Capillary forces	19
3.1.4 Gravity force	20
3.1.5 Viscous force.....	21
3.1.6 Interrelation of forces	22
3.1.7 Surface force.....	23
3.1.7.1 Electrical double layer (EDL)	23
3.1.7.2 DLVO theory	25
3.1.7.3 Disjoining pressure.....	25
3.2 WETTABILITY	26
3.2.1 Factors affecting wettability.....	28
3.2.1.1 Mineralogy.....	28
3.2.1.2 Brine composition	28
3.2.1.3 Crude oil composition	29

3.2.1.4 Core restoration	30
3.2.1.5 Pressure and temperature	30
3.2.2 Wettability alteration in Sandstone	30
3.3 MINERALOGY OF SANDSTONE	31
4 SMART WATER.....	35
4.1 CONDITIONS FOR LOW SALINITY WATER FLOODING EFFECT IN SANDSTONE	35
4.2 MECHANISMS OF LOW SALINITY WATER FLOODING	36
4.2.1 Fines migration	36
4.2.2 Reducing IFT similar to alkaline flooding	37
4.2.3 Desorption by pH Increase	38
4.2.4 Multicomponent ion exchange	39
4.2.5 Salting-in Salt-out effect	40
4.3 PH SCREENING TEST	41
5 ALKALINE FLOODING.....	43
5.1 ALKALINE REACTION WITH CRUDE OIL	43
5.1.1 In Situ Soap Generation	43
5.1.2 Emulsification	45
5.2 ALKALINE REACTION WITH FORMATION WATER	46
5.3 ALKALINE REACTION WITH ROCK	46
5.4 RECOVERY MECHANISMS	48
5.4.1 Lowering IFT by generating surfactant	48
5.4.2 Wettability alteration	48
5.4.2.1 Oil wet to water wet	48
5.4.2.2 Water wet to oil wet	48
5.4.3 Emulsification and Coalescence	49
5.4.4 Emulsification and Entrainment	49
5.4.5 Emulsification and Entrapment	49
5.5 ALKALIS USED IN ALKALINE FLOODING	50
5.6 WHY SODIUM CARBONATE IS USED MORE THAN OTHERS?	51
6 MATERIALS AND METHOD	53
6.1 BRINE.....	53
6.1.1 Brine Preparation.....	53
6.2 CORE MATERIAL	54

6.2.1 Core Preparation.....	56
6.2.2 Saturation of Core with Brine	57
5.2.3 Determination of Pore Volume and Porosity.....	58
6.3 CORE FLOODING SETUP	58
6.4 FLUID ANALYSIS	59
6.4.1 pH Measurements.....	60
6.4.2 Density Measurements	60
6.4.3 Ions Concentration Measurement	61
6.5 PRESSURE MEASUREMENT	62
6.6 SCANNING ELECTRON MICROSCOPE (SEM)	62
7 RESULTS	63
7.1 CORE B-22.....	63
7.2 CORE IDAHO GRAY-1	66
7.3 CORE B-01.....	69
8 DISCUSSION	71
8.1 ALKALINITY TRANSPORTING ABILITY	71
8.2 LOW SALINITY WATER FLOODING EFFECT	73
8.3 HIGH SALINITY FORMATION WATER EFFECT ON pH, WETTABILITY AND EOR POTENTIAL	75
8.4 EFFECT OF TEMPERATURE.....	76
8.5 EFFECT OF MINERALOGY.....	79
8.6 EFFECT OF DENSITY.....	80
8.7 EFFECT OF PRESSURE DIFFERENCE DURING FLOODING	81
8.8 ION CONCENTRATION MEASUREMENT.....	81
8.9 SCALE PROBLEMS	83
8.10 COMPARISON BETWEEN LS AND ALKALINE EOR POTENTIAL	84
8.11 ECONOMICAL ANALYSIS	84
9. CONCLUSION	86
RECOMMENDATIONS FOR FUTURE WORK.....	87
NOMENCLATURE	88
REFERENCES.....	90

List of Figures

FIGURE 1: SEQUENCE OF RECOVERY MECHANISM. ADAPTED FROM (AHMED, 2010).....	10
FIGURE 2: EVALUATION AND MATURITY OF DIFFERENT EOR PROCESSES (ELSEVIER, 2016).....	14
FIGURE 3: GRAVITY SEGREGATION (GREEN AND WILLHITE, 1998c).....	21
FIGURE 4: ELECTRICAL DOUBLE LAYER OF A NEGATIVELY CHARGED PARTICLE (MOLNES, 2017).....	24
FIGURE 5: RELATION BETWEEN EDL THICKNESS AND CONCENTRATION (MOLNES, 2017).....	25
FIGURE 6: CONTACT ANGLE MEASUREMENTS THROUGH WATER PHASE (CRAIG, 1971).....	27
FIGURE 7: DIFFERENT WETTABILITY IN MICROSCOPIC LEVEL IN RESERVOIR (SCHLUMBERGER, 2007).....	28
FIGURE 8: IMPACT OF SORTING IN RESERVOIR POROSITY (JAHN ET AL., 2008; MOLNES 2017).....	31
FIGURE 9: CRYSTAL STRUCTURE OF MOST COMMON CLAYS (ADAPTED FROM NICHOLS, 2009).....	33
FIGURE 10: DETACHMENT OF CLAY PARTICLES AND OIL MOBILIZATION (TANG AND MORROW, 1999).....	37
FIGURE 11: ATTRACTION OF DIVALENT CATIONS AND CLAY SURFACE. REDRAWN FROM LAGER ET AL. (2008).....	40
FIGURE 12: ILLUSTRATION OF SALT-IN AND SALT-OUT EFFECT (REZADOUST ET AL., 2009).....	41
FIGURE 13 A TYPICAL pH SCREENING TEST. CHANGE IN EFFLUENT pH VERSUS PV-INJECTED FLUID IN CORE OC1 AT 40, 90, AND 130 °C. THE BRINE FLOODING SEQUENCE WAS HS–LS– HS. THE SWITCHES OF INJECTION FLUIDS ARE INDICATED BY THE DASHED LINES (AKSULU ET AL., 2012).....	42
FIGURE 14: SCHEMATIC OF ALKALINE RECOVERY PROCESS. DEZABALA ET AL. (1982).....	44
FIGURE 15: CHANGE OF IFT OF EXTRACTED OIL (PRODUCED OIL) BY USING ALKALINE SOLUTION (ZHAO ET AL., 2002).....	45
FIGURE 16: pH VALUES OF ALKALINE SOLUTIONS AT DIFFERENT CONCENTRATIONS AT AMBIENT CONDITION: 1, SODIUM HYDROXIDE; 2, SODIUM ORTHOSILICATE; 3, SODIUM METASILICATE; 4, SODIUM SILICATE PENTAHYDRATE; 5, SODIUM PHOSPHATE; 6, SODIUM SILICATE [(NA2O)(SIO2)2]; 7, SODIUM SILICATE [(NA2O)(SIO2)2.4]; 8, SODIUM CARBONATE; 9, SODIUM SILICATE; 10, SODIUM PYROPHOSPHATE; 11, SODIUM TRIPOLYPHOSPHATE; AND 12, SODIUM BICARBONATE (SHENG, 2011).....	50
FIGURE 17: A) A SCHEMATIC DIAGRAM OF WATER FILTRATION SETUP. B) WATER FILTRATION SETUP IN LAB.....	54
FIGURE 18: SEM IMAGE OF CORE B-22.....	55
FIGURE 19: PORE SIZE DISTRIBUTION OF A CORE FROM THE SAME BLOCK AS THE TESTED CORE MATERIAL. DATA PROVIDED BY TOTAL E&P (TORRIJOS, 2017).....	56
FIGURE 20: A) EFFLUENT OF CORE CLEANING WITH KEROSENE. B) WITH HEPTANE.....	56
FIGURE 21: A SCHEMATIC OVERVIEW OF CORE CLEANING SETUP.....	57
FIGURE 22: A SCHEMATIC DIAGRAM OF CORE SATURATION SYSTEM.....	57
FIGURE 23: A) A SCHEMATIC OVERVIEW OF CORE FLOODING SETUP. B) HASSLER CORE HOLDER.....	59
FIGURE 24: A) pH METER, B) DENSITY METER, C) ION CHROMATOGRAPHY.....	62
FIGURE 25: TEST 1: pH SCREENING TEST OF OUTCROP CORE B-22 AT AMBIENT TEMPERATURE. SEQUENCE OF FLOODING: FW - LS – ALK- 1 - LS – FW.....	63
FIGURE 26: TEST 2: pH SCREENING TEST OF OUTCROP CORE B-22 AT 60°C. SEQUENCE OF FLOODING: FW - LS – ALK-1 - LS – FW	64
FIGURE 27: TEST 3: pH SCREENING TEST OF OUTCROP CORE B-22 AT 90°C. SEQUENCE OF FLOODING: FW - LS – ALK-1 - LS - FW	64

FIGURE 28: TEST 4: PH SCREENING TEST OF OUTCROP CORE B-22 AT 90°C SEQUENCE OF FLOODING: FW – ALK-1 - FW - LS – FW ... 65

FIGURE 29: TEST 5: PH SCREENING TEST OF OUTCROP CORE B-22 AT 60°C. SEQUENCE OF FLOODING: FW – ALK-1 - FW - LS - FW .. 66

FIGURE 30: TEST 6: PH SCREENING TEST OF OUTCROP CORE IDAHO GRAY-1 AT 60°C. SEQUENCE OF FLOODING: FW – ALK-1 - FW - LS - FW 67

FIGURE 31: TEST 7: PH SCREENING TEST OF OUTCROP CORE IDAHO GRAY-1 AT 90°C. SEQUENCE OF FLOODING: FW – ALK-1 - FW - LS - FW 67

FIGURE 32: TEST 8: PH SCREENING TEST OF OUTCROP CORE IDAHO GRAY-1 AT 60°C. SEQUENCE OF FLOODING: FW - LS – ALK-2 - LS – ALK-3 – FW 68

FIGURE 33: TEST 9: PH SCREENING TEST OF OUTCROP CORE IDAHO GRAY-1 AT 60°C. SEQUENCE OF FLOODING: FW – ALK-3..... 68

FIGURE 34: TEST 10: PH SCREENING TEST OF OUTCROP CORE IDAHO GRAY-1 AT 60°C. SEQUENCE OF FLOODING: FW - LS- ALK-3 – LS – FW 69

FIGURE 35: TEST 11: PH SCREENING TEST OF OUTCROP CORE B-01 AT 60°C. SEQUENCE OF FLOODING: FW - ALK-1 -FW – LS – FW . 70

FIGURE 36: TEST 12: PH SCREENING TEST OF OUTCROP CORE B-01 AT 90°C. SEQUENCE OF FLOODING: FW - ALK-1 - FW – LS – FW 70

FIGURE 37: OIL RECOVERY TEST ON CORE B-22, WITH 20% WATER SATURATION AND AGED IN CRUDE OIL AT 120°C. FLOODING SEQUENCE WAS FW-LS AT 4 PV PER DAY (TORRIJOS, 2017). 74

FIGURE 38: OIL RECOVERY TEST ON CORE B-21, WITH 20% WATER SATURATION AND AGED IN CRUDE OIL AT 60°C. FLOODING SEQUENCE WAS FW-LS AT 4 PV PER DAY (TORRIJOS, 2017). 74

FIGURE 39: PH-SCREENING TEST AT 60°C AND 90°C OF B-22. 76

FIGURE 40: PH-SCREENING TEST AT 60°C AND 90°C OF IDAHO GRAY-1..... 76

FIGURE 41: COMPARISON OF EFFLUENT PH IN 40°C, 90°C AND 130°C IN SANDSTONE RESERVOIR CORE-2 (RC-2) DURING PH SCREENING TEST AT 4 PV/DAY. THE FLOODING SEQUENCE WAS HS-LS-HS. THE DASH LINES INDICATING THE SLOP OF PH CHANGE (AKSULU ET AL., 2012). 78

FIGURE 42: COMPARISON OF EFFLUENT PH AT 60°C AND 120°C OF B-21 DURING PH SCREENING TEST AT 4 PV/DAY. THE FLOODING SEQUENCE WAS FW-LS (TORRIJOS, 2017)..... 79

FIGURE 43: DENSITY OF THE EFFLUENTS FOR CORE B-22 AND B-1 AT 60°C. THE FLOW SEQUENCE WAS FW - ALK-1 - FW - LS – FW. . 80

FIGURE 44: PRESSURE DROP DURING TEST 7 AT 90°C FOR IDAHO GRAY-1 CORE. FLOODING SEQUENCE WAS FW - ALK-1 – FW – LS – FW. 81

FIGURE 45: CATIONS CONCENTRATION DURING PH SCREENING TEST OF CORE B-22, TEST 01 AT AMBIENT TEMPERATURE. 82

FIGURE 46: ANIONS CONCENTRATION DURING PH SCREENING TEST OF CORE B-22, TEST 01. 82

List of Tables

TABLE 1: CLASSIFICATION OF EOR METHODS (TORRIJOS, 2017).....	12
TABLE 2: CLASSIFICATION OF WETTABILITY BY CONTACT ANGEL.	26
TABLE 3: PROPERTIES OF MOST COMMON CLAY MINERALS (IDF, 1982).	34
TABLE 4: SMART WATER MECHANISM IN LS DISPLAYING HOW ABSORBED ACIDIC AND BASIC MATERIALS FROM CLAY MINERAL CAN BE REMOVED BY DESORPTION (AUSTAD ET AL., 2010).....	39
TABLE 5: PROPERTIES OF SEVERAL COMMON ALKALIS (SHENG, 2011).....	51
TABLE 6: ION COMPOSITION AND PROPERTIES OF BRINE	53
TABLE 7: PHYSICAL PROPERTIES OF CORES.....	54
TABLE 8: MAIN MINERALOGICAL COMPOSITION OF CORES	55
TABLE 9: PH SCREENING TESTS PERFORMED DURING THE THESIS WITH FLOODING SEQUENCE AND TEMPERATURE IN A CHRONOLOGICAL WAY	60
TABLE 10: COMPARISON OF PH CHANGE AT DIFFERENT TEMPERATURE FOR DIFFERENT CORES.	77

1. Introduction

This thesis is an experimental work related to low salinity smart water and alkaline flooding EOR process that is done at the smart water research laboratory in University of Stavanger. Alongside presenting the results obtained during the experiments, the reasons behind the results and the achievements of experiments are discussed. To understand both LS and alkaline EOR process, a detailed literature review was done on their mechanisms and their reactions with rock, oil, brine and water. However, oil recovery stages along with different oil recovery methods were discussed briefly in the introduction part. Basics of EOR such as displacement forces, wettability were discussed in detail in another chapter to understand the EOR mechanism mainly for smart water. In addition, the mineralogy of sandstone was also discussed in the theory part based on different published scientific research papers and books.

1.1 Oil recovery

In conventional oil reservoirs, oil recovery operations can be divided into three stages from a chronological point of view: primary recovery, secondary recovery and tertiary recovery. However, this chronological order can be altered or overlapped depending on reservoir characteristics and economic consideration (Green and Willhite, 1998a). An overview of typical recovery phases of conventional reservoir is shown in figure 1.

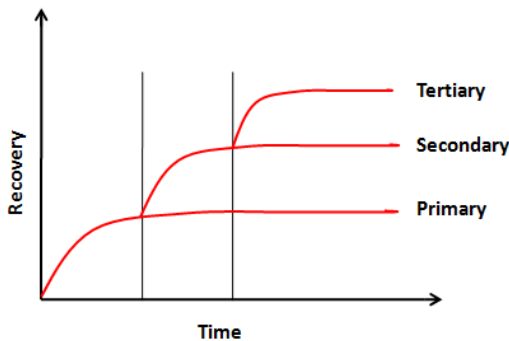


Figure 1: Sequence of recovery mechanism. Adapted from (Ahmed, 2010).

1.1.1 Primary oil recovery

This is the first stage of oil recovery where there is no need of external forces such as injection of fluid. In this stage, hydrocarbon is produced by natural pressure or energy that was naturally stored in the reservoir. There are six different types of natural driving mechanisms that cause primary recovery: Gas

cap drive, solution gas (depletion) drive, rock and liquid expansion drive, water drive, gravity drainage and combination drive. In primary recovery mechanism, total oil recovery is 5-40% in unconventional reservoir (Ahmed and McKinney, 2005).

1.1.2 Secondary oil recovery

When primary recovery mechanism or natural driving forces are not sufficient to produce oil economically then secondary recovery mechanism is used. In this mechanism, mainly water and/or gas are injected to maintain the pressure of the reservoir to produce oil economically. In a very good reservoir condition, oil production could be 70% of OOIP, which is rare. Due to reservoir heterogeneity such as poor distribution of pores, fracture, permeability differences, capillary entrapment, adverse wettability conditions only 20-40% oil can be recovered from total reserve using secondary recovery mechanism (Green and Willhite, 1998a; Muggeridge et al., 2014).

1.1.3 Tertiary oil recovery- Enhanced oil recovery

When primary and secondary recovery methods are not economically viable then tertiary recovery method is used to recover the residual oil that is left after primary and secondary recovery methods. It is also called Enhanced oil recovery (EOR). In this process, fluid is injected to reservoir along with chemical which is not a part of reservoir before. The injected fluid interacts with oil, rock and formation water and change reservoir and fluid properties like interfacial tension (IFT), oil viscosity, wettability, oil mobility etc (Bavière, 1991; Green and Willhite, 1998a). The target of different EOR method is to increase volumetric (Macroscopic) sweep efficiency and displacement (microscopic) efficiency and thus increase ultimate oil recovery (Zolotukhin and Ursin, 2000).

1.2 Definitions of EOR and IOR

Definition of EOR (enhanced oil recovery) was discussed in previous section. According to Norwegian Petroleum directorate, EOR is an advance process, which can reduce oil saturation by improving both microscopic and macroscopic sweep efficiency in the tertiary recovery stage. It is related to changing reservoir and fluid properties.

On the other hand, IOR (improved oil recovery) includes all the recovery mechanism from primary to tertiary. IOR is a combined method of drilling and reservoir engineering to increase oil production that

includes all the method to improve recovery such as IOR, directional drilling, horizontal drilling, infill drilling etc (Torrijos, 2017).

1.2.1 Importance of EOR

Nowadays, though there are several renewable energy sources, the demand for oil is still high. According to International Energy Agency (IEA), 31.1% of total energy is supplied by oil. Discoveries of new oil field was record low in 2017 and the current oil production is dominated by mature fields. To produce more oil, we have to either discover more oil reserves or produce more oil from mature fields by using different IOR method. As the discoveries of new oil fields are declining and most of the mature oil fields are already developed, using different EOR methods can boost the recovery. If we can add 20-30% more recovery by using EOR, it will provide a huge oil reserve for next 2 decades (Torrijos, 2017).

To get more efficient EOR project, it is highly recommended to include EOR strategy during the development plan of the reservoir (Strand, 2005).

1.2.2 Different Enhanced oil recovery Methods

All the enhanced oil recovery methods can be categories into four different groups: Chemical methods, thermal methods, gas injection methods and emerging EOR processes (Taber et al., 1997). All the EOR methods are classified and presented in table 1.

Table 1: Classification of EOR methods (Torrijos, 2017)

Chemical EOR Processes	Alkaline Flooding Surfactant Flooding Polymer Flooding Alkaline/Surfactant/Polymer Flooding (ASP) Solvent flooding Gels for water diversion/shut off
Thermal EOR processes	Steam flooding Cyclic steam stimulation In-situ combustion Hot water flooding

	Steam-assisted gravity drainage
Gas Injection EOR processes	Hydrocarbon injection (miscible/immiscible) CO ₂ flooding (miscible/immiscible) Nitrogen injection Flue gas injection (Miscible and immiscible) Water-Alternating-Gas (WAG)
Emerging EOR processes	Smart Water / Engineered Water Low Salinity Water Flooding Carbonated Water flooding Microbial EOR Enzymatic EOR Electromagnetic heating EOR Surface mining and extraction Nano particles

The most economical and effective EOR methods considering the mineralogy of the reservoir are studied and implemented more. The following figure 2 is showing different EOR processes and their maturity with respect to time. According to figure 2, smart water flooding lies in deploy and repeat section, which is more mature than alkaline water flooding.



Figure 2: Evaluation and maturity of different EOR processes (Adapted from Elsevier, 2016).

2. Objective

The objective of this thesis is to:

- Check which method has larger EOR potential in sandstone: an in-situ generation of alkaline condition in the core by injecting LS water or transporting alkalinity by injecting high pH alkaline water through the core.
- Verify the alkalinity transporting ability of three different sandstone outcrop cores at different temperatures for alkaline and LS water flooding.
- Check the EOR potential of sandstone cores for both LS and alkaline water flooding at different temperatures using pH screening test.
- Find out the mechanism which is the main reason of pH increment in LS EOR and compare with other mechanisms.

3 Basics of EOR with smart water

The performance of the Smart Water EOR depends on several aspects: surfaces forces, displacement forces, the wetting development of the system during Smart Water injection and most importantly mineralogy of the system. Short descriptions of the factors that affect smart water EOR effect are described below.

3.1 Displacement forces

The overall displacement of oil in an EOR method is divided into smaller scale and larger scale. In smaller scale or microscopic scale; viscosity of fluid, wettability, IFT plays the most important role in residual oil saturation. On the other hand, in larger scale parameters such as gravity force, reservoir heterogeneity plays an important role. General descriptions of displacement efficiency at different scales are discussed in next part.

3.1.1 Microscopic and macroscopic displacement

The total displacement efficiency of oil is classified as microscopic and macroscopic displacement efficiency. Total displacement efficiency is a product of those two and can be expressed by the following equation.

$$E = E_D E_V \dots\dots\dots (1)$$

Where, E = Total displacement efficiency, E_D = Microscopic displacement efficiency and E_V = Macroscopic displacement efficiency which is also known as volumetric sweep efficiency. Both microscopic and macroscopic sweep/ displacement efficiency are expressed in fraction. To get higher total displacement efficiency or higher oil recovery, we need to make both microscopic and macroscopic displacement efficiency near to one.

Microscopic displacement efficiency (E_D) represents the mobilization of oil at pore space and typically displayed in the magnitude of residual oil saturation (S_{or}). On the other hand, macroscopic sweep efficiency measure how effective the volumetric sweep is (Green and Willhite 1998a). Microscopic sweep efficiency can be described by the following equation.

$$E_D = \frac{S_{oi} - S_{or}}{S_{oi}} \dots\dots\dots (2)$$

Where,

S_{oi} is initial oil saturation and S_{or} is residual oil saturation.

From equation (2), we can see that to increase microscopic efficiency (E_D), we need to decrease residual oil saturation. The purpose of modern EOR method is to decrease residual oil saturation and increase microscopic sweep efficiency and it is affected by chemical and physical interaction of injected fluid during an EOR process. It can be achieved by lowering IFT or wettability alteration along with many other mechanisms.

On the other hand, macroscopic sweep efficiency is also very important and is affected by reservoir characteristics such as porosity, permeability, reservoir homogeneousness and fluid characteristics such as viscosity ratio, density difference etc. However, non-favorable reservoir geology, large differences in densities and poor mobility ratios can play against favorable displacement efficiencies. Fingering effects, under riding or overriding of the displaced fluid and ultimately low macroscopic sweep efficiency can be the consequences of these effects (Green and Willhite, 1998b; Torrijos, 2017).

3.1.2 Fluid flow in porous media

To understand oil recovery mechanism, it is important to understand how oil flow through the porous media. In 1856, Darcy established a mathematical relationship which describes the mobility of fluid flowing in the porous media of unfractured reservoir and the equation is known as Darcy's law. This law relates the flow rate of fluid through the porous media, the viscosity of fluid and pressure drop that the fluid creates over a given distance and equation (3) expressed the relationship.

$$u = -A \frac{k}{\mu} \frac{dP}{dX} \dots\dots\dots(3)$$

Where,

- u Superficial (Darcy) velocity of the displacing fluid (m^3/s),
- k Effective permeability of the displacing fluid (m^2),
- μ Viscosity of the displacing fluid (Pa.s),
- dP Change of Pressure (Pa/m),

dX Length travelled by fluid (m) and

A Cross-sectional area of the filter medium perpendicular to flow (m^2).

The minus sign of the equation represents the reduction of pressure in the direction of flow. Normally, absolute value of dP is used to achieve a positive value of flow rate.

If two phases co-exist in a displacement process, the mobility ratio (M) depends on the mobility of the displacing fluid phase (λ_D) and the mobility of the displaced fluid phase (λ_d). The mobility of a fluid is the ration of permeability of the porous media and viscosity of that fluid. Both the mobility and mobility ration are expressed by equation (4) and (5) respectively.

$$\lambda = \frac{k}{\mu} \dots\dots\dots(4)$$

$$M = \frac{\lambda_D}{\lambda_d} \dots\dots\dots (5)$$

Mobility ratio (M) is a dimensionless parameter and very important in EOR process. High mobility ratio indicates low sweep efficiency and vice versa. When, M is greater than one, it represents unfavorable mobility ratio and cause viscous fingering. On the other hand, when M is less than one it represents favorable displacement condition. Assuming a piston like flow where water is displacing oil then equation (5) can be rewrite as the following.

$$M = \frac{\lambda_D}{\lambda_d} = \frac{\lambda_w}{\lambda_o} = \frac{\left[\frac{k_{rw}}{\mu_w}\right]_{S_{oi}}}{\left[\frac{k_{ro}}{\mu_o}\right]_{S_{wi}}} \dots\dots\dots(6)$$

Where,

M is the mobility ratio,

λ_D is the mobility of the displacing fluid ($m^2/ Pa.s$),

λ_d is the mobility of the displaced fluid ($m^2/ Pa.s$),

λ_w is the mobility of water ($m^2/ Pa.s$),

λ_o is the mobility of oil ($m^2/ Pa.s$),

k_{rw} is the relative permeability of water (m^2),

μ_w is the water viscosity (Pa.s),

k_{ro} is the relative permeability of oil (m^2),

μ_o is the Oil viscosity (Pa.s),

S_{or} is the Residual oil saturation and

S_{wi} is the irreducible water saturation.

2.1.3 Capillary forces

One of the major driving forces in porous media is capillary force. The dimension and interplay of the geometry of pore spaces, wettability and the interfacial tension generated by the fluids and rocks of a given system affect the capillary force. This force can help or prevent oil production depending on the system. They can be a very important mechanism of oil recovery in fractured reservoir. In oil wet reservoir capillary pressure can be expressed by the following equation.

$$P_c = \sigma \sqrt{\frac{\phi}{k}} J^* \dots\dots\dots(7)$$

Where,

P_c is the capillary pressure (Pa),

σ is the interfacial tension (IFT) (N/m),

ϕ is the porosity, k is the permeability (m^2) and

J^* is the Leverett dimensionless entry pressure.

On the other hand, for the non-fractured reservoir, because of high residual oil saturation, capillary force can cause oil trapping. The difference in pressure across the interface of two immiscible fluids is called capillary force and can be expressed by following equation (Green and Willhite 1998a, Torrijos, 2017).

$$P_c = P_o - P_w = \sigma_{ow} \left(\frac{1}{R_1} - \frac{1}{R_2} \right) = \frac{2\sigma_{ow}\cos\theta_c}{r_c} \dots\dots\dots(8)$$

Where,

P_o is the pressure in the oil phase at interface (Pa),

P_w is the pressure in the water phase at interface (Pa),

σ_{ow} is the Interfacial tension at oil water interface (N/m),

θ_c is the Contact angle between the phases ($^\circ$) and

r_c is the pore radius of capillary (m)

3.1.4 Gravity force

Gravity force plays an important role in oil recovery method. Because of the immiscibility of fluid in the reservoir, the lighter fluid is always subjected to a buoyancy force and can be expressed by equation 9.

$$\Delta P_g = \Delta \rho g H \dots\dots\dots (9)$$

Where,

ΔP_g is the pressure difference of the oil and water interface due to gravity (Pa),

$\Delta \rho$ is the difference in density of the two phases (Kg/m³),

g is the gravitational acceleration constant, 9.8 (m/s²) and

H is the height of the column (m).

Gravity force can generate problems like overriding or under riding (Green and Willhite, 1998b). It is one of the key worry when density differences between to fluids such as oil and water are large (Chen et al., 2000). Gravity segregation can generate override when the density of the displacing fluid is less than the density of displaced fluid. On the other hand, under ride can occur when the density of displacing fluid is higher than the displaced fluid as shown in the figure 3. Gravity segregation can lead to an early breakthrough of injected fluid which will decrease the potentiality of oil recovery by EOR fluid (Green and Willhite, 1998c). Low oil water interfacial tension may also create gravity segregation (Austad and Milter, 1997).

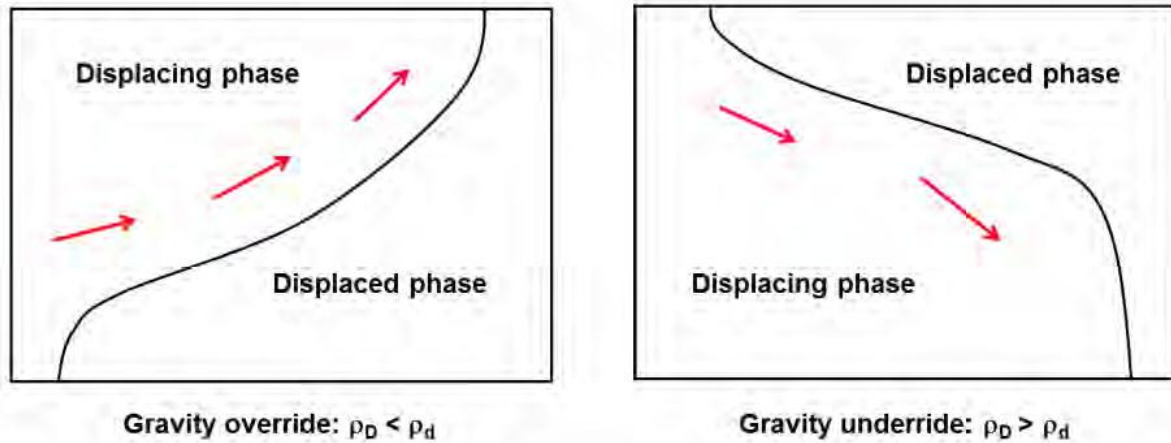


Figure 3: Gravity segregation (Green and Willhite, 1998c)

3.1.5 Viscous force

In porous medium, viscous force depends on the pressure drop that occurs because of flow through the porous medium. To flow through pore space, the viscous force must be greater than the capillary force. The pressure drop for laminar flow can be calculated by Poiseuille's law (Green and Willhite, 1998d). If the porous medium is regarded as a bundle of parallel capillary tube then the pressure drop during flow is-

$$\Delta P = \frac{8\mu L \bar{v}}{r^2 g_c} \dots\dots\dots(10)$$

Where,

ΔP is the difference in pressure over capillary tube (Pa),

μ is the viscosity (Pa·s),

L is the capillary length (m),

\bar{v} is the average flow velocity in the capillary (m/s),

r is the radius of the capillary (m) and g_c is the conversion factor.

3.1.6 Interrelation of forces

In the porous medium, capillary forces cause entrapment of one fluid phase during the displacement process by another phase. When the viscous forces acting on the pore space surpass the capillary forces of trapped fluid such as oil then that oil can be recovered. The oil distribution on the pore space are different in different wetting system. If the system is water wet, then the oil will exist primarily as a discontinuous phase. It can happen due to trapping and/or isolation of droplets by displacing fluid. During smart water flooding, smart water will enter a sufficient number of pores to stop oil flow and the remaining oil will exist as a film around the sand grains (Morrow 1979). In contrast, the smaller pore space may remain empty or saturated with smart water. To mobilize this residual oil in water wet system we need to connect all the oil droplets and create a flow channel. On the other hand, if the system is oil wet then the oil remains around the grains as a film and to recover it we must displaced it to a continues flow system before mobilization. To mobilize the oil from pore space, it is important to understand the effect and correlation of different forces. Numerous researches had been done in the past to correlate the effect of acting forces on mobilizing the residual oil and a dimensionless parameter named capillary number is formulated. It is expressed by N_c and expressed by equation (11).

$$N_c = \frac{V_o \mu_w}{\sigma_{ow}} = \frac{K_o \Delta p}{\phi L \sigma_{ow}} \dots \dots \dots (11)$$

Where,

V_o is the velocity (m/s),

μ_w is the viscosity of smart water (Pa·s),

σ_{ow} is the interfacial tension between oil and water(N/m),

K_o is the effective permeability of oil (D),

ϕ Porosity (%) and

$\Delta P/L$ is the pressure drop due to flow (Pa/m).

High capillary number indicates low oil saturation. However, in some cases, capillary number did not represent residual oil saturation (Armstrong et al., 2014; Guo et al., 2015). Another problem of capillary number is that it does not represent wettability scenarios and the homogeneousness of the reservoir (Torrijos, 2017).

3.1.7 Surface force

The forces that act between charged surface and ionized water is very important to understand to realize the mechanism behind wettability. Four types of forces are believed to act in the saturated charged surface (Israelachvili and McGuiggan, 1988):

- Van Der Waals force, which can occur between all the molecules.
- Repulsive double layer force which occurs because of ionized surface with a net electric charge.
- Solvation force, which takes place because of arranging or ordering of liquid molecules that are tightly confined between two surfaces. The force can be attractive, repulsive or oscillatory.
- Repulsive entropic force, which is the reason either by thermal fluctuations of flexible, fluid-like surfaces or by thermal motions of protruding surface groups (steric forces; polymers etc.)

As these forces function all together in liquid, separate contribution of each force is difficult to recognize (Israelachvili and McGuiggan, 1988). A short description of the forces will be discussed shortly in next section.

3.1.7.1 Electrical double layer (EDL)

Van der Waals force operates alone in very simple system such as non-polar wetting films on surface. In most of the cases, the systems are complex and electrostatic forces are taken into consideration. If Van der Waals force acts alone then it causes all the elements to attach collectively and precipitate. Usually there are some other forces and all the elements dispersed in fluids are normally charged and this charge prevented them from joining together through electrostatic repulsive forces. Rock surface and particles can be charged in three ways:

- Through dissociation of protons or ionization of surface that charge the surface negatively or positively.
- Through adsorption of ions onto an initially uncharged surface which is called ion exchangeable surface.
- Through charge exchanging process between two chemically different surface placed in the vicinity.

The ultimate surface charge of co-ions will be in equilibrium by oppositely charged *counter-ions* in equal quantity (Israelachvili, 2011). By using Stern-Gouy-Chapman theory, the distribution of counterions can be explained. The surface charge of a particle into two distinct layers; a diffuse outer layer and a compact inner layer (Riley, 2010). Stern (1924) described the compact inner layer made of transiently bound counter-ions which is known as the Stern layer shown in figure 4. The diffuse outer layer was illustrated by Gouy and Chapman (Chapman, 1913; Gouy, 1910). They built up a model how the surface charge of a particle is balanced by a diffuse outer layer of ions.

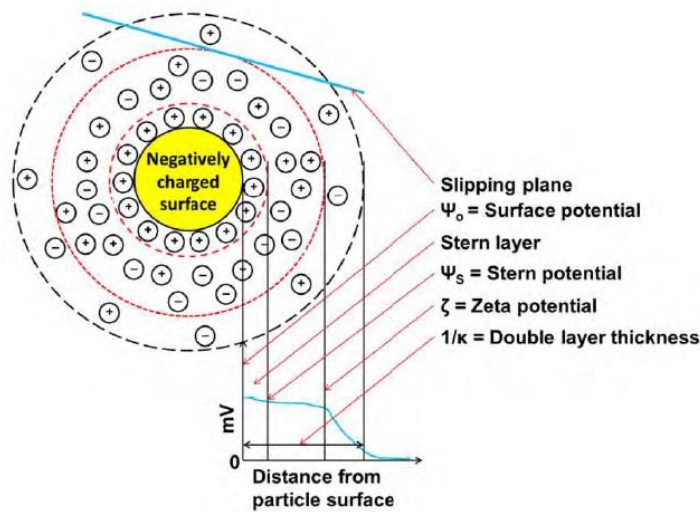


Figure 4: Electrical double layer of a negatively charged particle (Molnes, 2017).

Collectively these two layers are called electrical double layer (EDL). When charged particles come within reach of each other in a liquid medium, their outer layer begins to overlap. As a result, this force overshadows attractive Van der Waals force. Allocation of ions depends on different factors in the EDL such as concentration of electrolyte, formal charge of ions, solvent, and the potential at the boundary between the ion-packed inner layer and the diffuse outer layer. The effect of concentration on the thickness of EDL is shown in figure 5.

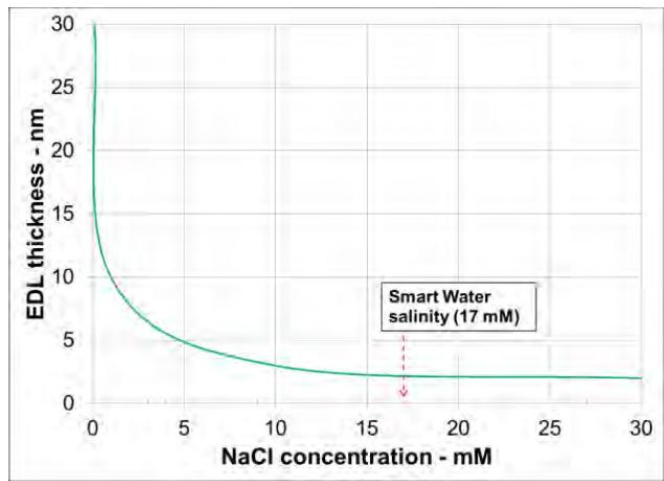


Figure 5: Relation between EDL thickness and Concentration (Molnes, 2017).

3.1.7.2 DLVO theory

DLVO theory was developed by Derjaguin, Landau, Verwey and Overbeek and it is named after them (Derjaguin and Landau, 1941, Verwey and Overbeek, 1955). The attractive van der Waals forces and repulsive forces are united by the existence of double layer (Derjaguin et al., 1987). This theory relates forces involving fluid films and planar substrates. To understand the forces derivative from the present charges at the different solid-fluid or fluid-fluid interfaces, this theory can be used.

3.1.7.3 Disjoining pressure

Disjoining pressure is a force that tends to take apart two interfaces (Hirasaki 1991). Interaction force between the wetting and non-wetting phase is considered necessary to be understood to illustrate the wetting and de-wetting phenomenon of immiscible fluids on rock surface. Why a solid surface favors one fluid over another can be explained by determining the contact angle of the droplet of both fluids on that surface. This contact angle depends on the capillary pressure P_C and the disjoining pressure Π in the wetting film that separates the wetting phase and the solid surface. The disjoining pressure begins to take part in a vital function when the depth of this wetting film becomes smaller than $0.1 \mu\text{m}$. The Laplace- Young equation (equation 12) explains the constancy of these lean separating wetting films:

$$P_C = \Pi + 2\sigma J \dots\dots\dots(12)$$

Where,

P_C is the capillary pressure between wetting and non-wetting phases,

Π is the disjoining pressure,

σ is the interfacial tension between two fluids and

J is the mean surface curvature.

3.2 Wettability

Wettability is one of the most important surface properties in smart water flooding. Wettability determines whether a fluid will stretch on or stick to the surface in the existence of a different immiscible fluid (Zolotuchin and Ursin, 2000). Relative permeabilities, irreducible water saturation, capillary pressure and residual oil saturation depend on the wettability of the rock surface. The success of smart water flooding depends on the wettability because of its consequences on position, flow and allocation of the fluid phases (Anderson, 1986c).

Rock surface can be either strongly oil wet or strongly water wet or in between. Water will inhabit the smaller pores and will get in touch with most of the rock plane in strongly water wet reservoir. In this case, oil will remain as globules at the middle of the bigger pores that can be expanded over several pores. Oil recovery with water flooding is not possible in strongly water wet reservoir after a limited amount of production. On the other hand, in strongly oil wet reservoir, formation water remains in the middle of the big pores as droplets and the oil remain as a thin layer covering the rock surface. Oil also occupies the smaller pores. High oil recovery can be possible by water flooding even after water breakthrough. Whether the reservoir is strongly oil wet or water wet can be measured by contact angle showed in table 2. The angles are measured through the water phase and shown in figure 6.

Table 2: Classification of wettability by contact angel.

Contact angle (°)	Wettability preference
0 – 30	Strongly water-wet
30 – 90	Preferentially water-wet
90	Neutral wettability
90 – 150	Preferentially oil-wet
150 – 180	Strongly oil-wet

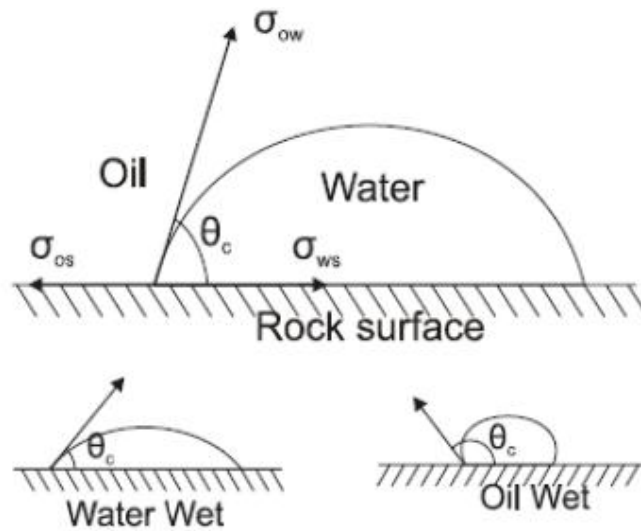


Figure 6: Contact angel measurements through water phase (Craig, 1971)

If the three interfacial tensions (σ_{os} , σ_{ws} and σ_{ow}) are in mechanical stability as shown in figure 6 then Young's equation can be used to express the relation between all the tension and contact angel (Anderson, 1986b).

$$\sigma_{os} = \sigma_{ws} + \sigma_{ow} \cos\theta \dots\dots\dots (13)$$

Where,

θ is the contact angle measured through the denser phase,

σ_{os} is the oil solid interfacial tension,

σ_{ow} is the oil-water interfacial tension and

σ_{ws} is the water-solid interfacial tension.

Due to different pore size, pore distribution and various mineral compositions throughout the reservoir, the wettability will vary. Salathiel introduced mixed wettability in 1973 where smaller pores are filled with only water and the bigger pores are filled with oil (Salathiel, 1973). Frictional wettability was introduced in 1959 in which the smaller pores are fully saturated by oil and bigger pores are fully saturated by water (Fatt and Jr., 1959). Water flooding is mostly effective when the wettability is close to neutral wet but little bit on the water wet site (Jadhunandan and Morrow, 1995; Tang and Morrow, 1997; Yildiz et al.,1999; Zhang and Morrow, 2006). Different wettability are showed in microscopic level in figure 7.

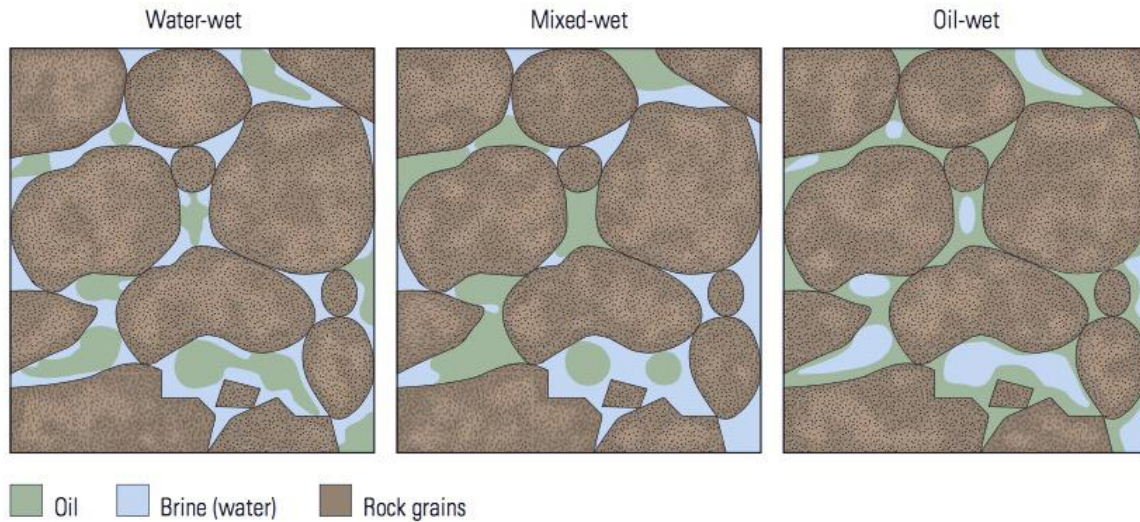


Figure 7: Different wettability in microscopic level in reservoir (Abdullah 2016).

3.2.1 Factors affecting wettability

Wettability is affected by numerous factors, which are strongly related to reservoir mineralogy, crude oil, brine composition and their interaction among each other. The wetting scenario can change dramatically with small changes of any parameters. Thus, it is important to know how they affect the wettability individually.

3.2.1.1 Mineralogy

The interaction between solid and fluid in the reservoir depends on the mineralogy, which controls the adsorption of polar components. At standard reservoir pH condition, a sandstone rock is normally negatively charged. The isoelectric point is about 2.2-2.8 of clays and silicate that influences the negative charge and thus influences the wettability. As a result, the mineralogy directly influences how the fluid both crude oil and formation brine wet the porous surface (Buckley et al., 1998; Jaafar et al., 2014).

3.2.1.2 Brine composition

The chemical composition, salinity and the pH of brine is the most controlling factors in the wetting processes (Anderson, 1986a). The brine composition of both formation and injection water is capable of stimulate surface charge on the rock surface or oil water interface. As the formation water is in an equilibrium state for a long time, change in charge is not experienced in reservoir condition (Buckley,

1994; Buckley and Liu, 1998; Buckley et al., 1998; Buckley and Fan, 2007; Alroudhan et al., 2015). Using different wettability test, many scientists have shown that the changes of the brine parameter such as pH, salinity and composition depends on the oil, rock and brine interaction (Zhang et al., 2007; Morrow and Buckley, 2011; RezaeiDoust et al., 2011).

Wettability alteration in sandstone has been a center of interest in current years in petroleum industry and there are many theories to understand the wettability change in case of low salinity water flooding. Wettability alteration by increasing the pH is one of the most discussed topics (Austad et al., 2010; Morrow and Buckley, 2011; Didier et al., 2015; Shi et al., 2016). Many experiments have established that the pH has a significant function in the development of protonation and deprotonation of polar components in the oil phase which affects the attraction towards sandstone surface and changes the initial wetting (Buckley et al., 1989; Austad et al., 2010; Brady et al., 2015; Torrijos, 2017).

3.2.1.3 Crude oil composition

As crude oil is one of the most complex mixtures of organic compounds, understanding the influence of it in wettability is difficult to explain though scientists have taken limitless attempts to know it better. Jill S. Buckley found that asphaltenes and resins of crude oil have the highest impact on wettability on the surface of rock (Buckley, 1995; Buckley et al., 1998; Buckley, 2001). Asphaltenes have the highest molecular weights, other than resins have higher levels of NSO compounds. NSO compounds contain nitrogen, sulphur and oxygen. Therefore, resins are more polar than the asphaltenes. The resin fractions that are NSO rich have higher surface activity, and as a result may influence the wetting behavior of the oil (Aksulu et al., 2012; Standnes and Austad, 2000). The oil-water interphase becomes charged when they have been exposed to water and exposes the electrical characteristics of the organic compounds. It depends on the type of compound and its concentration. Crude oil is adsorbed onto the mineral surface when opposite charges interact by intermolecular or interionic forces as both positive and negative charge can be present in the interface (Buckley et al., 1998; Hirasaki, 1991). Buckley et al. (1998) mentioned the main mechanism of interaction credited to:

- Polar interactions that dominate in the absence of water film between oil and solid.
- Surface precipitation that depends mainly on crude oil solvent properties, with respect to the asphaltenes.
- Acid/base interactions that control surface charge at oil-water and solid-water interfaces.

- Ion binding or specific interactions between higher valency ions and charged sites.

Additional aspects such as water chemistry and mineralogy are also responsible for when determining if a crude oil is able to alter the wettability of a surface, because they enforce significant assistance to the interactions between the oil and the rock surface (Austad et al., 2013; Morrow et al., 1998; Molnes, 2017).

3.2.1.4 Core restoration

Core restoration consists of three basic steps: core cleaning, core saturation and aging. During these processes, it is always a big challenge to restore the same wettability as before in the reservoir. Numerous investigations have been done to recognize initial wettability and develop core restoration techniques, although there is a need of universal agreement to assess which is the best procedure to go after. Nevertheless, a mixture of latest screening methods could assist to diminish the ambiguity in the assessment of initial wetting, which is of high significance in the EOR field (Torrijos, 2017).

3.2.1.5 Pressure and temperature

Solubility of polar active components in crude oil increases as pressure and temperature increase. Because of the reduction in the solubility of wettability altering components, it has been experienced that the cores behave more oil wet at atmospheric condition. The change in pressure could cause fluid ejection from the porous media during the removal of core material from reservoir (Anderson, 1986c). However, some other experiments have verified that pressure effect does not affect the wettability such as Wang and Gupta (1995). Rao (1999) found that quartz surface become more oil wet when temperature increases. Berea sandstone also became more oil wet when the aging temperature was increased (Jadhunandan and Morrow, 1995).

3.2.2 Wettability alteration in Sandstone

Wettability alteration in sandstone is difficult to evaluate because of the variety of mineralogy and geochemical complexity. Wettability of sandstone can vary from strongly water-wet to strongly oil-wet and for that reason a cautious assessment of initial wettability of the core is important to have a successful procedure of wettability alteration (Torrijos, 2017).

3.3 Mineralogy of sandstone

The focal point of this thesis is to understand the transportation of alkalinity of different brines in sandstone using pH-screening test. Therefore, it is very important to understand the mineralogy of sandstone. Sandstone is a sedimentary rock formed by the deposition of clastics and detritus through lithification. Clastics and detritus was formed from other rock by weathering or erosion and transported by the natural energy like water and wind. The porosity, permeability and sorting depend mainly on the transporting system, depositional environment and the property of mother rock. Those parameters are very important reservoir properties and determine how good the reservoir is. Sorting impact on different reservoir properties are demonstrated in figure 8 below:

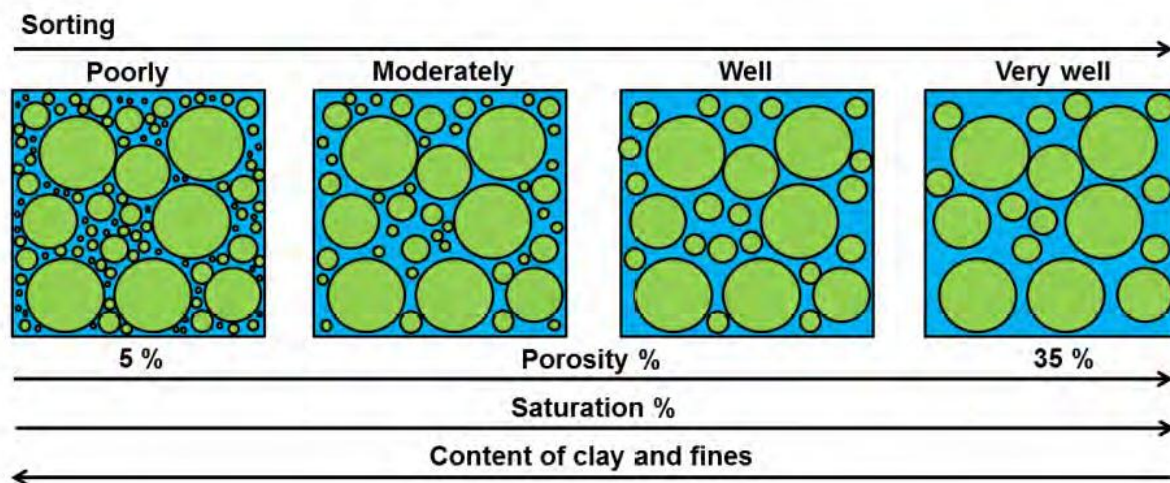


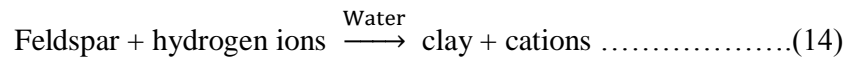
Figure 8: Impact of sorting in reservoir porosity (Jahn et al., 2008; Molnes 2017)

Sandstone are composed of many different minerals as they are eroded, transported and deposited from numerous rock system. Most common minerals are clays, micas, feldspars and quartz. They are discussed briefly below:

Quartz: Quartz is the most common mineral found in sandstone that contributes around 60-70% of all sandstone of the world because they are highly resistant to weathering. Quartz is a silicate mineral consisting of silicon and oxygen (SiO_2). According to Carroll (1959), silt fraction of quartz ranging with size 2 to 63 μm and has a cation exchange capacity (CEC) of 0.6 cmol kg^{-1} , compared to clay fraction of quartz with size lower than 2 μm and CEC of 5.3 cmol kg^{-1} .

Micas: Micas are eroded from igneous, metamorphic and other sedimentary rock, abundant in sandstone and are phyllosilicates. Micas can be classified in two categories: biotite and muscovite. Biotite is white in color and muscovite is brown (Nichols, 2009; Pettijohn, 1975).

Feldspars: Feldspar is a silicate mineral eroded from igneous rock mainly from granites. They are softer than quartz and more vulnerable to weathering during transportation and degradation. In contact with hydrogen ions, they change to clays by hydration process as described in equation 14 (Velde and Meunier, 2008).



Feldspars are mainly consisted of silicon and oxygen, though calcium, potassium and sodium may also be present there and the type of feldspar is dependent on those ions. Feldspars can be classified as potash feldspars (KAlSi_3O_8), albite ($\text{NaAlSi}_3\text{O}_8$) and anorthite ($\text{CaAl}_2\text{Si}_2\text{O}_8$) (Crundwell, 2015; Nichols, 2009). Albite is one of the last feldspars to crystalized from magma at lower temperature and is found near the surface. On the other hand, anorthite formed in higher temperature. Major diversity among these three feldspars is the crystal structure, which depends on temperature of molten rock solidification, its cooling rate and geothermal history.

Clays: Clays are mainly aluminum silicate and a product of weathering from silicate mineral like silicates. They are mainly composed of aluminum and silica with frequently containing large amount of magnesium, iron, sodium and potassium. Normally, clays are consisted of two building units: tetrahedral silica sheets and octahedral aluminum sheets. These sheets are connected together by sharing oxygen ions between Si^{4+} and Al^{3+} ions. Though these two ions are the major inhabitants in the space between two layers, other cations may also be present to ensure charge balance. Two-layer system is known as kandite group while three-layer system is known as smectite group (Nichols, 2009; Worden and Morad, 2003). The four most common clay minerals found in sedimentary rocks are shown in figure 9 (Molnes, 2017).

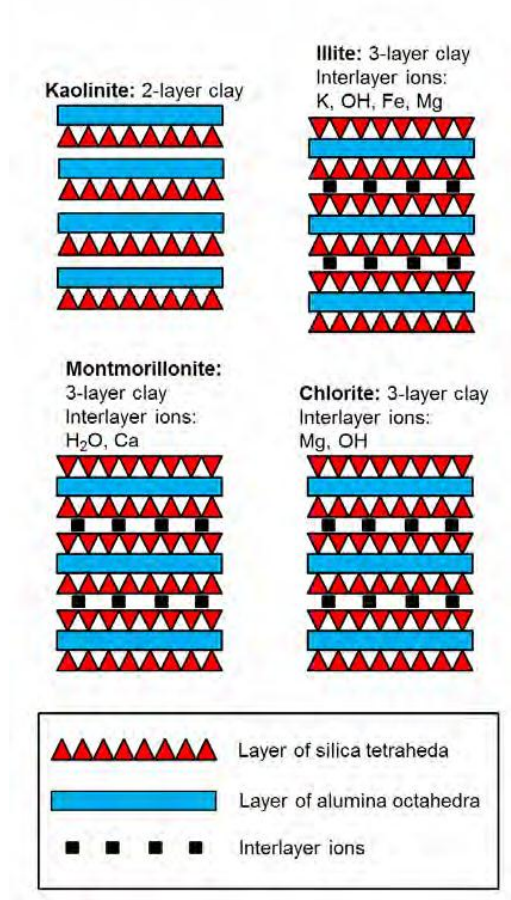
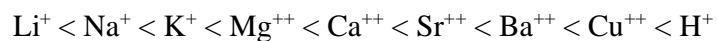


Figure 9: Crystal structure of most common clays (Adapted from Nichols, 2009)

Kaolinite ($\text{Al}_2\text{Si}_2\text{O}_5(\text{OH})_4$) is consisted of one tetrahedral and one octahedral layer though O-H-O bonds and described as 1:1 layer structure. Montmorillonite is consisted of one octahedral sheet and two tetrahedral sheets, therefore, known as 2:1 layer structure. It can absorb water within this structure and can swell. For this reason, it is also known as swelling clays. On the other hand, illite is also consisted of 3 layers, two tetrahedral and one octahedral layers, but opposing tetrahedral layers are bound together with O-K-O bonds. As the bond is very strong, it prevents swelling of the clays. Chlorite is also one kind of clay that is made of layers but a different structure. It has 2:1:1 structure that consists of a 2:1 layer (tetrahedral-octahedral-tetrahedral) which is negatively charged and an octahedral layer that is positively charged (Nichols, 2009; Worden and Morad, 2003).

Clay minerals have a distinguishing feature that separates it from other minerals. They have a negative charge at the edge of every unit cell, which enable them to interact with the surrounding to stabilize the charge. This ability is measured by cation exchange capacity (CEC) of a clay mineral (Velde and Meunier, 2008). It measures the ability of the mineral to attract and take cations from the surrounding. The ability to attract the cations towards clay minerals is shown below (Yong et al., 2012):



For example, this sequence implies that when the same concentrations of Na^+ and Ca^{++} exists, the Ca^{++} cations will be better at displacing Na^+ from the clay surface than Na^+ will be at displacing Ca^{++} . However, if the concentration of the high replacing power cations is low than this sequence can be broken (RezaeiDoust, 2011; Molnes, 2017). Properties of most common clay minerals are summed up in table 3 below.

Table 3: Properties of most common clay minerals (IDF, 1982).

Property	Kaolinite	Illite	Chlorite	Smectite
Structure	1:1	2:1	2:1:1	2:1
Particle size (μm)	0.5-5	Highest 0.5	0.1-5	0.1-2
CEC (meq/100g)	3-15	10-40	10-40	80-150
Typical surface area BET (m^2/g)	15-25	50-110	140	30-80

4 Smart water

Smart water is a brine that is injected not only to maintain the reservoir pressure but also to improve oil recovery by changing wettability of the rock. Water flooding is being used for centuries to produce oil and in this process, a huge amount of residual oil is being left in the reservoir. Since last two decades, a new era of oil recovery has opened with low salinity water flooding. Under the umbrella of “smart water”, oil companies and scientists have improved this technique by modifying the ion of the injected water according to the reservoir properties. This injected water is known as low salinity water or engineered water or modified water or smart water flooding. Even if sea water and modified sea water of high salinity can be called smart water if it changes wettability and increases recovery in carbonate rocks. However, this method increases oil recovery less than other chemical processes (Such as ASP flooding) in some cases, but the cost effectiveness of this method made it popular at recent low oil price scenario.

4.1 Conditions for Low salinity water flooding effect in sandstone

In some cases, low salinity water flooding showed very good recovery in laboratory but few cases they did not show any significant effect. To maximize the low salinity water flooding effect, many researchers had proposed some conditions for effective flooding and they are presented below:

- Clays must be present in the porous medium of sandstone. Organic compounds such as acids and/or bases must be present in the crude oil (Tang and Morrow, 1999).
- Divalent cations such as $\text{Ca}^{++}/\text{Mg}^{++}$ must be present in the formation water and the reservoir must have formation water (McGuire et al., 2005; Lager et al., 2007)
- The pH of the produced water normally increases about 1-3 pH unit when low salinity brine of 1000-2000 ppm is injected, but the low salinity EOR effect also observed for 5000 ppm brine (Tang and Morrow, 1999; RezaeiDoust et al., 2011).
- Most of the researchers found that low salinity water is effective when the reservoir temperature is under 100°C (Aghaeifar et al., 2015).

4.2 Mechanisms of low salinity water flooding

All the experiments related to low salinity water flooding proposed that the prospective for oil recovery depends on the interaction among crude oil, brine and rock. Many researchers have experienced increased oil recovery using low salinity water and proposed different mechanism. Sheng (2014) found eighteen mechanisms of low-salinity water flooding as follows: (1) fine migration (Tang and Morrow, 1999); (2) mineral dissolution (Buckley and Morrow, 2010); (3) limited release of mixed-wet particles (Buckley and Morrow, 2010); (4) increased pH effect and reduced interfacial tension (IFT) (McGuire et al., 2005); (5) emulsification / snap-off (McGuire et al., 2005); (6) saponification (McGuire et al., 2005); (7) surfactant-like behavior (McGuire et al., 2005); (8) multi component ion exchange (MIE) (Lager et al., 2006); (9) double layer effect (Ligthelm et al., 2009); (10) particle-stabilized interfaces / lamella (Buckley and Morrow, 2010; Morrow and Buckley, 2011); (11) salt-in effects (RezaeiDoust et al., 2009); (12) osmotic pressure (Buckley and Morrow, 2010); (13) salinity shock (Buckley and Morrow, 2010); (14) wettability alteration (more water-wet) (Buckley and Morrow, 2010); (15) wettability alteration (less water-wet) (Buckley and Morrow, 2010); (16) viscosity ratio (Buckley and Morrow, 2010); and (17) end effects (Buckley and Morrow, 2010). (18) clay hydration and swelling (Boston et al., 1969). In addition to this, “desorption by pH increase” suggested by Austad et al. (2010) is one of the widely accepted mechanisms for LS EOR. All the mechanisms are related to each other. In next section, major mechanisms and their working conditions will be discussed.

4.2.1 Fines migration

Tang and Morrow (1999) were among the first researchers who recognized the low salinity impact on oil recovery. With the fine migration theory, they had tried to explain the low salinity effect. The theory suggested that electrostatic interaction between clay particles are higher in low salinity brine than high salinity that guides to expansion of the double layer. Thus, clay particles will be isolated from the rock surface.

Figure 10 shows the discharge of clay particles and oil mobilization. Later, it was found that the fines were kaolinite particles from the rock and they cause pressure drop. The discharge of particles can block the pore space and reduce permeability that might cause serious reservoir damage. Although, evidence of mine migration was not found in several researches (Lager et al., 2008; Aksulu et al., 2012). On the other hand, cores that do not have kaolinite also showed LS effect that make the fine

migration theory questionable (Cissokho et al., 2009). This theory cannot explain the increased wetness at given pH with LS compared to HS (Aksulu et al., 2012).

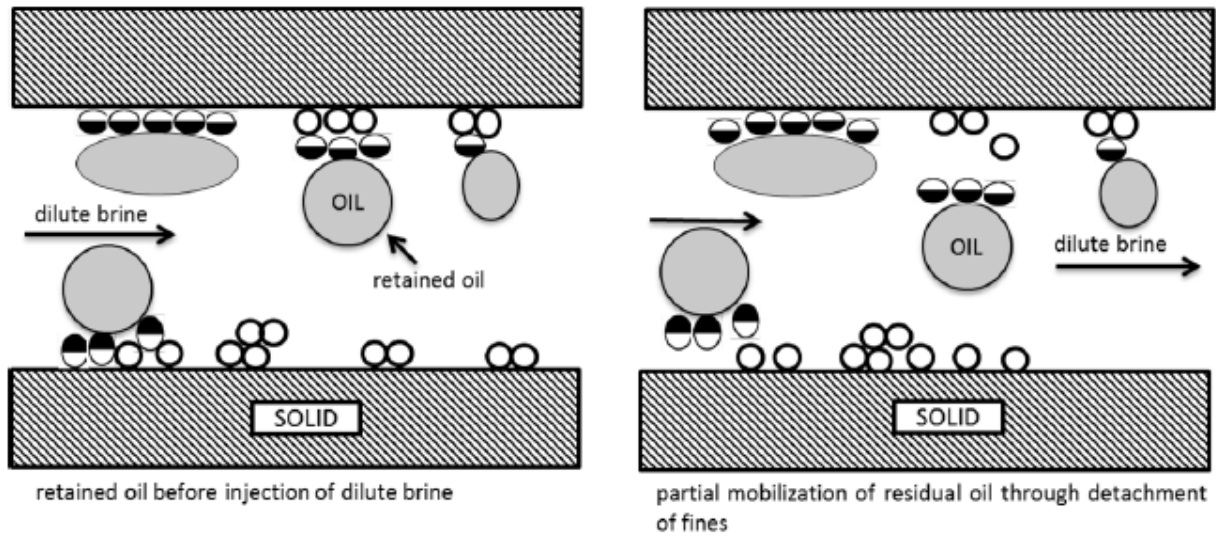
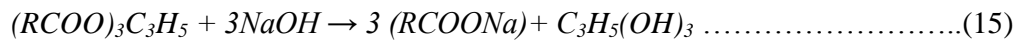


Figure 10: Detachment of clay particles and oil mobilization (Tang and Morrow, 1999)

4.2.2 Reducing IFT similar to alkaline flooding

McGuire et al. (2005) argued that brine rock interaction during LS brine is similar to the mechanism of alkaline flooding. In situ generation of surfactant from the residual oil at increased pH occurs during alkaline flooding. McGuire et al. (2005) suggested that the main mechanism of LS is generation of in situ surfactant and reduction in IFT.

An increase in the pH of around 2-3 unit in the effluent brine is commonly observed in LS water flooding. LS flooding is considered to be an alkaline flooding when the pH of the effluent reaches above 9 (Lager et al., 2006). In alkaline flooding, when acidic oil comes in contact of LS brine in an alkaline environment, natural surfactant is generated. The reactions are given below:



There are three different mechanism how the generated natural surfactant can increase the recovery of oil. First mechanism is about the reduction of interfacial and surface tensions that decreases the

capillary forces that reduces trapping of oil. The second mechanism is wettability alteration towards a more water wet condition. The third mechanism is diffusion of oil into the water phase by behaving as an emulsifying agent (McGuire et al., 2005). Whereas, HS brine has higher concentration of divalent ions (Ca^{2+}/Mg^{2+}) that prevent surfactant to precipitate causing low oil recovery, LS has low concentration of these divalent cations and help surfactant to precipitate. Thus, LS works better than HS in oil recovery according to this mechanism (Anderson, 1986a; McGuire et al., 2005).

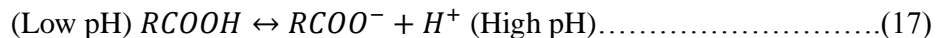
There are quite a few observations that do not have the same opinion with the mechanism recommended by McGuire et al. (2005). Core flooding of North Sea reservoir whose crude oil had a very low acid number, showed a very good recovery of oil with LS flooding though to generate natural surfactant in alkaline flooding requires an acid number greater than 0.2. Other researches with oil having low acid number showed good oil recovery that is against this mechanism (Torrijos, 2017).

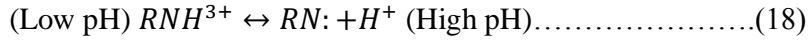
On the other hand, oil recovery was observed while very low pH change in effluent during LS flooding which indicates no natural surfactant generation. Zhang et al. (2007) and Pu et al. (2008) observed oil recovery with an insignificant increase in pH that goes against the mechanism. Cissokho et al. (2009) and Torrijos (2017) experienced no oil recovery where pH increased up to 10. All these researches make this mechanism vulnerable.

4.2.3 Desorption by pH Increase

Austad et al. (2010) proposed a chemical mechanism of LS flooding where pH increases in the system due to desorption of initially adsorbed cations from the clay surface and disturbs the initial equilibrium between crude oil, brine and rock systems in the core. This outcome produces negative charges on the clay exterior that must be charge balanced. The H^+ ion has the largest affinity towards clay minerals in reservoir condition, and by adsorption of an H^+ ion from water, molecules, creating a local pH increase.

This increase in pH will origin desorption of organic material from the clay surface. The reservoir will be less water wet if more organic materials adsorbed onto the clay surface. The system will change to more water wet when the organic material desorbs due to a change in charge because of the pH increment. The shift in charge with shift in pH can be seen from the following equations:





Thus, as the pH at the water-clay interface increases and results the discharge of organic compounds from the clay surface and the system become more water wet. As a result, it becomes easier to displace the oil and increase oil recovery. Table 4 represents the suggested mechanism for both acidic and basic organic material.

Table 4: Smart water mechanism in LS displaying how absorbed acidic and basic materials from clay mineral can be removed by desorption (Austad et al., 2010).

Organic Material	Initial Situation	Low Salinity Flooding Situation	Final Situation
Basic			
Acidic			

Austad et al. (2010) experienced that the desorption of both acidic and basic crude oil took place as the pH number increases from around 2-3 units which shows that pH augment is diminishing the adsorption of oil components to the clay surface.

4.2.4 Multicomponent ion exchange

Lager et al (2008) proposed multicomponent ion exchange mechanism (MIE) which suggested that multivalent cations present in the formation water would attach to polar components present in the oil phase forming organo-metallic complexes and propping up oil-wetness. MIE occurs by removing organic polar compounds and organo-metallic complexes from the surface and exchanging them with uncomplexed cations during LS flooding. They believed that LS effect does not happen when the formation water is barred from divalent ions during the aging process. They claimed that an ion exchange process should remove the organic material (Lager et al., 2008).

Lager et al. (2008) experienced a drop in the Mg^{2+} concentration in a larger extent than Ca^{2+} , and it was attributed to an exchange mechanism. However, Austad et al. (2010) argued that these observations might be the cause of precipitation of divalent ions within the core material. Additionally, Cissokho et al. (2009) experimented that the concentration of divalent ions is key parameter in the LSE (Cissokho et al., 2009). Figure 11 illustrates suggested mechanism of organic matter adsorbed onto clay mineral.

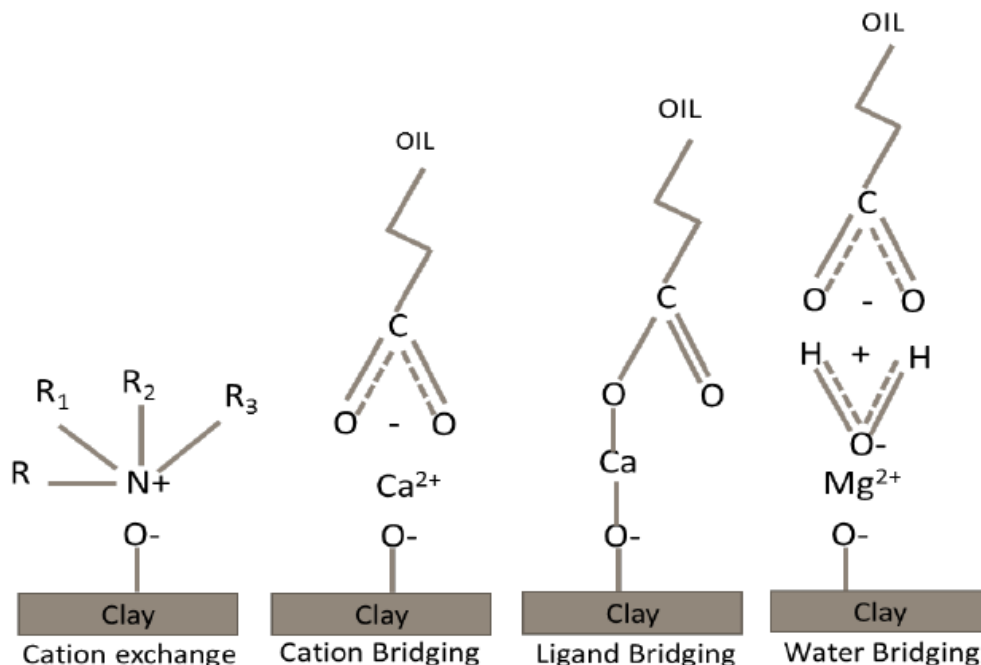


Figure 11: Attraction of divalent cations and clay surface. Redrawn from Lager et al. (2008).

4.2.5 Salting-in Salt-out effect

RezaDoust et al. (2009) proposed salting-in effect for LS water. Solubility of organic material in water is reliant on the formation of water around the hydrophobic part because of hydrogen bonds between water molecules. Water molecules can build water structure around the hydrophobic tail of the organic molecules when the salt concentration is decreased. As a result, the solubility of the material increases and causes desorption as shown in figure 12.

Salt-in effect is described as decline in salt beneath a critical ionic strength, which will increase the solubility of organic material in the aqueous phase and desorption of carboxylic material. On the other hand, salting-out is referring to reduced solubility of organic material by increased in salinity. Cations

such as Na^+ , Ca^{2+} and Mg^{2+} break up the water structure around the organic molecule and reduce the solubility (RezaDoust et al., 2009).

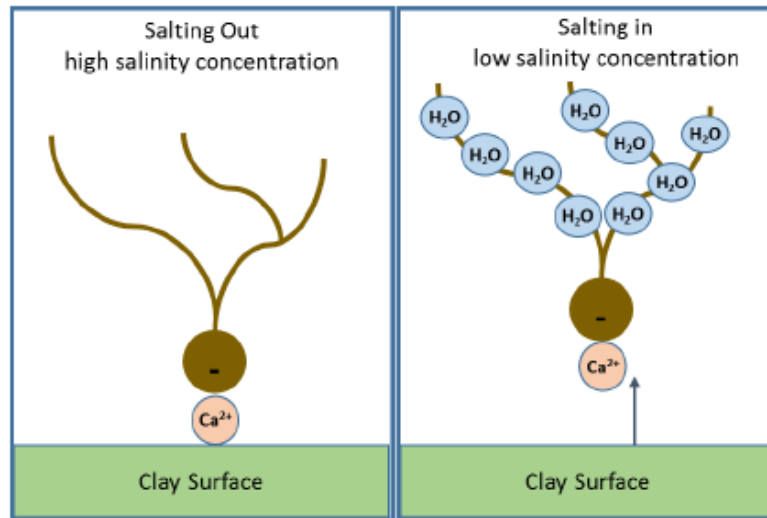


Figure 12: Illustration of salt-in and salt-out effect (RezaDoust et al., 2009).

However, this mechanism is no longer believed since the exact opposite behavior was seen when doing the adsorption experiments of quinoline onto kaolinite clay (Austad et al., 2010).

4.3 pH screening Test:

Researchers from University of Stavanger established pH screening test as a Smart water EOR potential observing method in sandstone. Instead of using oil, 100% saturated core with formation water is used at reservoir temperature and flooded with the brine which EOR potential needed to be tested. The interaction between effective surface area exposed to flooded brine and the brine is observed during this test by measuring the effluent pH, density changes, pressure difference of inlet and outlet core and the composition of produced brine. It gives information about initial wetting and reversibility of the process.

An example is shown in Figure 13 where PV flooded is shown against pH of the effluent. Rock samples which have the potential to show LS EOR effects are characterized by an initial pH below 7 because low pH favors the adsorption of polar components onto the rock surface creating mixed-wet conditions. Moreover, a significant increase in pH during LS water flooding is also a good indication of a positive EOR potential. The pH increase in sandstone will generate the conditions for desorption of polar

components and therefore changing the wettability towards a more water-wet state. Under such conditions, the Smart Water EOR effect may take place. Though oil is not used in this process, it can forecast the LS EOR effectiveness in a quick time. Nevertheless, for confirmation, oil recovery test should be used (Aksulu et al., 2012; Torrijos, 2017)

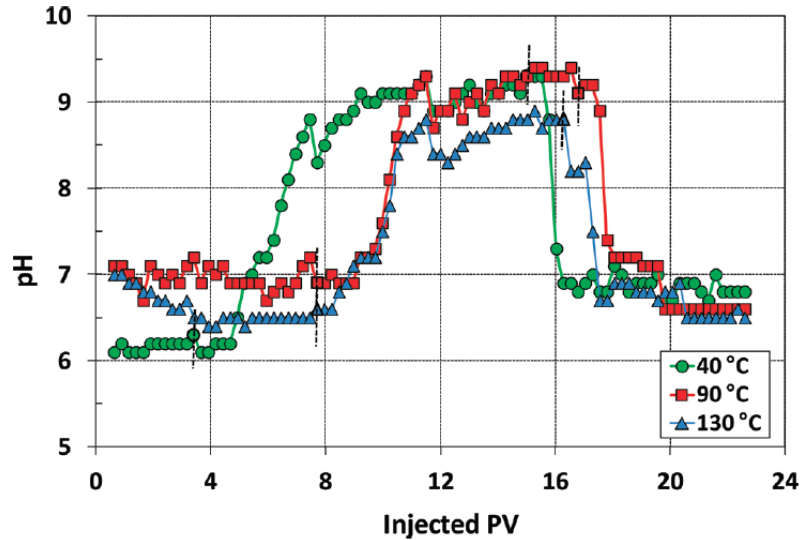


Figure 13 A typical pH screening test. Change in effluent pH versus PV-injected fluid in core OC1 at 40, 90, and 130 °C. The brine flooding sequence was HS–LS– HS. The switches of injection fluids are indicated by the dashed lines (Aksulu et al., 2012).

In this thesis, the potential EOR effect for LS and alkaline is compared by pH screening test. Alongside measuring the pH of the effluent, density change, pressure difference, composition of produced water are monitored.

5 Alkaline Flooding

Alkaline flooding is one of the oldest IOR methods used in petroleum industry and numerous researches had been done on it during 70's and 80's as there was less cost required for this method. However, due to low recovery rate, scaling problems in producing wells, reservoir damage due to chemicals and of course for other methods which give more recovery than alkaline, this method is not used much now a days. Different researches suggested that alkaline works much better when it is mixed with surfactant and polymer and many research papers have been published on alkaline, surfactant and polymer.

Due to higher oil price, heavy oil recovery became economically viable and alkaline flooding became important again because heavy oils have high contents of organic acids (saponifiable components) to react with alkalis so that surfactants (soaps) are generated in situ. However, in this thesis, alkaline flooding was compared with low salinity water flooding for conventional oil recovery as both the methods shows increase pH in effect in the core. For this reason, researches that were considered for the thesis was done only for conventional oil recovery and most of them were done in the 20th century.

In this chapter, the basic reaction of crude oil, rock and water with alkaline water is discussed. The mechanism how alkaline water worked as an IOR injection fluid in improving oil recovery is also discussed along with the comparison of different alkaline that were used for improving oil recovery previously.

5.1 Alkaline reaction with Crude oil:

Alkaline reaction with crude oil is the most important thing in alkaline IOR method.

5.1.1 In Situ Soap Generation

During the alkaline flooding, the injected alkaline water reacts with the acidic components of the crude oil. These acidic components are known as petroleum acids or naphthenic acids. Naphthenic acid is a mixture of many cyclopentyl and cyclohexyl carboxylic acids with molecular weight from 120 to around 700. It can be consisted of carboxylic acids (Shuler et al., 1989), carboxyphenols (Seifert, 1975), porphyrins (Dunning et al., 1953), and asphaltene (Pasquarelli and Wasan, 1979). The composition differs with the crude oil composition and the conditions during raffination and oxidation (Rudzinski et al., 2002).

A highly oil-soluble single pseudo-acid component (HA) is assumed in the oil. This pseudo acid component is divided into the oleic and aqueous phases and subsequent hydrolysis in the presence of alkaline to produce a soluble anionic surfactant A⁻ (Such as RCOO⁻), as shown in Figure 14.

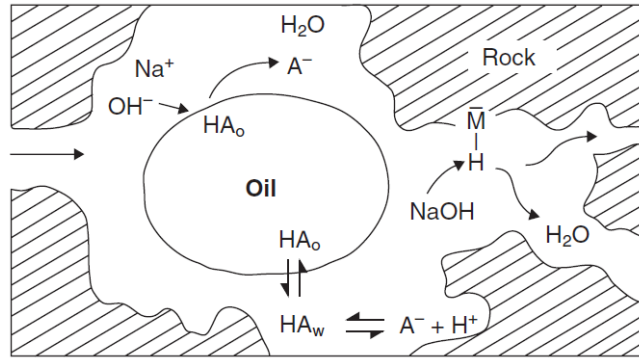
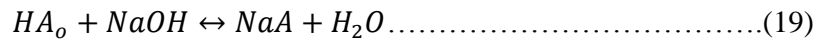
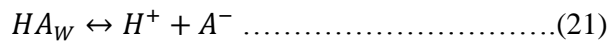
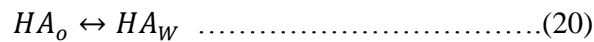


Figure 14: Schematic of alkaline recovery process. (deZabala et al., 1982).

The extraction and hydrolysis reaction is given below,



This reaction strongly depends on the pH of aqueous solution and takes place at the interface of water and oil. Fractions of organic acids in oil become ionized when it comes in in contact with alkaline water, while others remain neutral electronically. Acid soaps are formed when hydrogen bond is created between the neutral and ionized acid. Thus, the overall reaction of equation (19) is decomposed into a distribution of the molecular acid between the oleic, aqueous phases and an aqueous hydrolysis (deZabala et al., 1982).



Here, HA is a single acid, A is a long organic chain and o and w represents aqueous phases.

Zhao et al. (2002) Showed that the IFT of extracted oil (Produced oil) with same NaOH solution is higher than the crude oil. The acidic components in crude oil react with alkaline to reduce IFT.

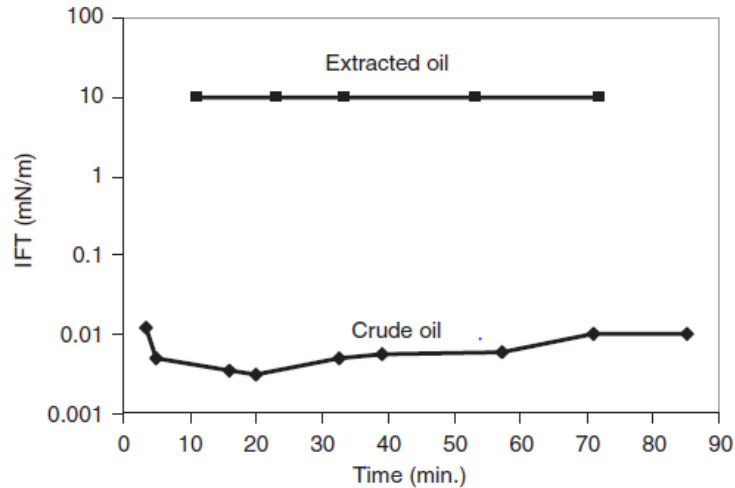


Figure 15: Change of IFT of extracted oil (Produced oil) by using alkaline solution (Zhao et al., 2002).

5.1.2 Emulsification

Creation of emulsion or emulsification mainly depends on oil water IFT. It is easy to create emulsion when IFT is low. In addition, the stability of emulsion depends on the film of the water oil interface. Because of high IFT of extracted oil with alkaline water, it is not easy to create emulsion. That's why nowadays, industry uses surfactant with alkaline water to reduce IFT between extracted oil and water to lower IFT value to create emulsification.

Huang and Yu (2002) experienced that emulsification was not completely reversible. When the dynamic IFT reached ultralow, emulsification occurred and even when dynamic IFT went up, emulsified oil droplets did not easily coalesce. Emulsification is instant and very stable in alkaline flooding. In enhanced oil recovery, minimum IFT plays an important role from this emulsification point of view. From the low IFT point of view, we may think we should use equilibrium IFT because reservoir flow is a slow process. However, the core flood results in the Daqing laboratory showed that when the minimum dynamic IFT reached 10^{-3} mN/m level and the equilibrium IFT was at 10^{-1} mN/m; the ASP incremental oil recovery factors were similar to those when the equilibrium IFT was 10^{-3} mN/m (Li, 2007). One explanation is that once the residual oil droplets become mobile owing to the instantaneous minimum IFT, they coalesce to form a continuous oil bank. This continuous oil bank can be move even when the IFT becomes high later. Then for this mechanism to work, the oil droplets must be able to coalesce before the IFT becomes high. As it will be more difficult for such a mechanism

to function in field conditions rather than in laboratory corefloods, this mechanism is not universally accepted (Sheng, 2011).

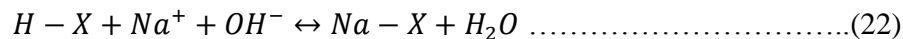
5.2 Alkaline reaction with formation water

When alkaline water come in touch of formation water in the reservoir, Precipitation of calcium and magnesium hydroxide, carbonate or silicate may happen. This precipitation forming depends on pH, ion concentration, pressure temperature and many more things. These precipitates may have positive or negative impact on improving oil recovery. Precipitates can block the pore and diverse the flow to an upswept area and increase oil recovery. On the other hand, due to precipitation, number of cation of formation water may reduce which will create more activity of surfactant and lower the IFT value (Mayer et al., 1983).

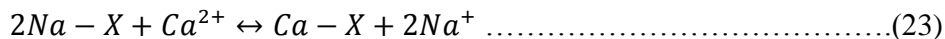
On the negative side of this, this precipitation may seriously damage the reservoir by blocking the way that the injecting water could not reach all the area of reservoir where they could reach without precipitation. Reduction of permeability will also harm the possibility of further injection of injecting fluid. Moreover, it can create scale problem in the production well as well. Even near the injecting well, it can block the pore space. To solve this, costly chemical need to be used and it will increase the operational cost.

5.3 Alkaline reaction with Rock

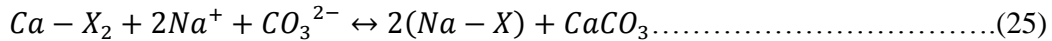
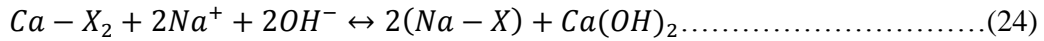
Alkaline reaction with rock is most difficult and less studied topic of alkaline flooding because of large number of reaction possibilities of rock and alkaline as the mineralogy of rock is intricate. On the other hand, clays have a huge surface area. When clays come in contact with alkaline water, clay surfaces will try to equilibrate with its new environment and exchange ion with alkaline water. As the pH of alkaline water is high, hydrogen ions of clay surface will react with hydroxide ions of alkaline water and reduce the pH of alkaline solution. As alkaline water moves through the reservoir, the alkalinity will be consumed. This can be explained by the following equation-



Where X represents mineral-base exchange sites. Similarly, for Na⁺, Ca²⁺ exchange, we have



Not only Hydrogen, but divalent like calcium and magnesium ions are also presents in clays and when calcium free alkaline water come in touch of clays, calcium or magnesium ions of the clay surface will exchange sodium ions in the alkaline solution causing calcium or magnesium precipitation. Reaction of this kind of cation exchange can be represented by following equations.



Ion exchange is a fast-reversible process but dissolution of rock by alkaline is an irreversible long-term kinetic process which can also happen. The number of possible reaction between rock and alkaline water is huge as rock has different mineralogy. Ehrlich and Wygal (1977) studied caustic consumption in different minerals and found high consumption rate for clays and less consumption for dolomite, calcite and quartz.

Holm and Robertson (1981) found the amount of Na_4SiO_4 consumed by reaction with exchangeable divalent ions on Muddy sandstone was 0.5 meq/ kg rock (0.05 lb/bbl PV). Krumrine et al. (1982) found the NaOH consumption was 40 to 160 meq/kg due to ion exchange using a mixture of 0.16% and 0.35% NaOH and NaCl, respectively.

Ehrlich and Wygal (1977) and Grim (1939) observed alkalinity loss for clays. Increase in the consumption of alkalinity was experienced with the increase in temperature, pH of the alkaline solution and contact time by Cooke et al. (1974). In general, the consumption of alkalinity is highest for kaolinite and gypsum, temperate for montmorillonite, illite, dolomite and zeolite, fairly low for feldspar, chlorite, and fine quartz, Lowest for quartz sand and Insignificant for calcite (Sheng, 2011).

Shen and Chen (1996) made a list of the alkaline consumption in rock in this order: gypsum > montmorillonite > kaolinite > illite > anorthosite (plagioclasite) > microcline > quartz > mica > dolomite > calcite.

Cooke et al. (1974) experimented that the consumption of alkalinity depends on contact time. For that reason, it can be said that laboratory experiment of core flooding cannot measure the alkalinity consumption correctly, but it is obvious that alkalinity is consumed.

5.4 Recovery mechanisms

There are many recovery mechanisms for alkaline flooding proposed by different researcher. Among them, the main and most studied mechanism is lowering the IFT by creating natural surfactant. Eight mechanisms were found about alkaline IOR. According to Radke and Somerton (1983), they are emulsification with entrainment, emulsification with entrapment, emulsification with coalescence, wettability alteration (i.e., oil wet to water wet or water-wet to oil-wet), wettability gradients, oil-phase swelling, disruption of rigid films and low interfacial tensions (Sheng, 2011). Along with the main mechanism, all other proposed mechanisms are discussed in this section.

5.4.1 Lowering IFT by generating surfactant

During flooding, alkaline water reacts with the acidic part (naphthenic acid) of crude oil and generates natural surfactant and decreases the IFT. Details of surfactant or soap generation are discussed in previous part 5.1.1.

5.4.2 Wettability alteration

This method can be classified in two- oil wet to water wet and water wet to oil wet.

5.4.2.1 Oil wet to water wet:

Oil Production increases if the wettability changes from oil wet to more water wet. This mechanism is only applied to oil wet reservoir because residual oil in water wet system is immobile and discontinuous as compared to oil wet system (Wagner and Leach, 1959). Mungan (1966a) established that alkaline flood decreases the water relative permeability and, in another experiment, he (1966b) experienced higher oil recovery in Teflon cores, which was oil wet with alkaline flooding by wettability alteration mechanism. On the other hand, many Russian researchers got similar results that showed that the cores became more water wet during alkaline flooding (Sheng, 2011).

5.4.2.2 Water wet to oil wet:

This mechanism is proposed by (Cooke et al., 1974) and it needed to be better described as this is totally opposite to the opinion that the reservoir should be made more water wet to produce more oil.

In this mechanism, a non-wetting residual oil in transformed to an uninterrupted wetting phase, providing a way for oil what otherwise would be trapped. At the parallel moment, low interfacial

tension induces development of an oil-external emulsion of water droplets in the uninterrupted, wetting oil phase. These emulsion droplets have a propensity to obstruct flow and stimulate a high-pressure gradient in the area where they generated. The high-pressure gradient, in turn, is said to surmount the capillary forces already reduced by low interfacial tension, as a result plummeting residual oil saturation more. Drainage of oil from the volume between emulsified alkaline water drops leaves behind a high water-content emulsion in which residual oil saturation may be as low as 5% PV (Sheng, 2011).

5.4.3 Emulsification and Coalescence

Emulsification and coalescence are related to instinctively generated unsteady water oil emulsion (Castor et al., 1981) or mixed emulsion. Secluded oil droplets are emulsified after coming in touch with alkaline water. The emulsified droplets join together with each other to become larger droplets while they travel in the pores; this happens because the films of water oil emulsion are not firm and can be easily split and combine to become larger. A few of the emulsified droplets are stopped at pore throats. Therefore, the mechanism of oil recovery is to boost sweep efficiency and amplify coalescence of oil drops into an uninterrupted oil bank (Sheng, 2011).

5.4.4 Emulsification and Entrainment

Low acid number, low salinity, high pH, oil water emulsion size less than the diameter of pore throat is the condition for this mechanism to work. In this mechanism, the crude oil is emulsified and reduce IFT and entrained by the flowing alkaline solution (Subkow, 1942).

5.4.5 Emulsification and Entrapment

Moderate acid number, low salinity, high pH, oil water emulsion size greater than the diameter of pore throat is the condition for this mechanism to work. In this mechanism, the emulsified oil droplets block the pore space and increase the sweep efficiency. However, Ehrlich and Wygal (1977) experimented 19 crude oils and found only one viscous crude (44.2 cP at 25°C) with a high acid number (1.39 mg KOH per gram of oil) that showed evidence of emulsification as a recovery mechanism. They suggested that the minimum acid numbers from 0.5 to 1.5 mg KOH per gram of oil are needed for the emulsification mechanism to be efficient (Sheng, 2011).

5.5 Alkalis used in alkaline flooding

Sodium carbonate, sodium hydroxide, sodium orthosilicate, sodium metaborate, sodium tripolyphosphate, ammonium carbonate, ammonium hydroxide are the most studied alkalis for alkaline flooding. The first three among those are mostly used to improve oil recovery purpose. Sodium hydroxide generates OH^- by dissociation, sodium carbonate and sodium orthosilicate through the development of weakly dissociating acids (silicic and carbonic acid, respectively) that remove free H^+ ions from solution.

As our aim is to see the pH transportation ability of different cores, we will discuss the pH of different alkalis and it is given on the figure 16.

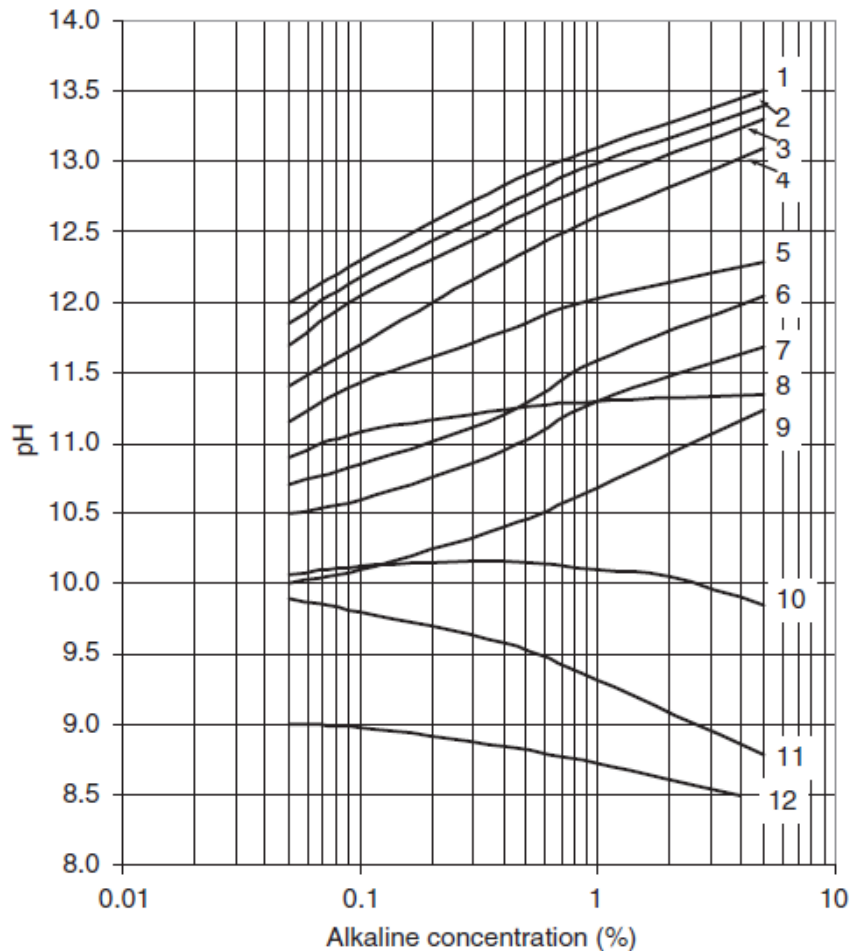


Figure 16: pH values of alkaline solutions at different concentrations at ambient condition: 1, sodium hydroxide; 2, sodium orthosilicate; 3, sodium metasilicate; 4, sodium silicate pentahydrate; 5, sodium phosphate; 6, sodium silicate $[(\text{Na}_2\text{O})(\text{SiO}_2)_2]$; 7, sodium silicate $[(\text{Na}_2\text{O})(\text{SiO}_2)_{2.4}]$; 8, sodium carbonate; 9, sodium silicate; 10, sodium pyrophosphate; 11, sodium tripolyphosphate; and 12, sodium bicarbonate (Sheng, 2011).

All three alkalis have a little difference in terms of reducing IFT during flooding (Burk, 1987; Campbell, 1982). It has also been experienced that the minimum IFT occurs over a narrow range of alkaline concentrations, typically 0.05 to 0.1 wt.% with a minimum IFT of 0.01 mN/m (Green and Willhite, 1998a). However, the only main difference of using different alkalis is they have different scale forming ability. Due to scaling problem, in many Chinese fields, only sodium carbonate was used more often. The pH of the solutions varies with salt content. However, by comparison, the pH of sodium carbonate solutions is less dependent on salinity (Labrid, 1991). Some of main properties of most common alkalis are showed in table 5.

Table 5: Properties of several common alkalis (Sheng, 2011)

Main Properties	Sodium Hydroxide NaOH	Sodium Carbonate Na ₂ CO ₃	Ammonium Hydroxide NH ₄ OH	Sodium Orthosilicate Na ₄ SiO ₄	Sodium Tripolyphosphate Na ₅ P ₃ O ₁₀
IFT Reduction	Yes	Yes	No	Yes	No
Precipitation of Ca ²⁺	Yes	Yes		Yes	
Precipitation of Mg ²⁺	Easier Than Ca ²⁺	No/ Difficult than Ca ²⁺		Yes	
Emulsifier	Good	Yes		Good	Good
Wettability alteration	Yes	Yes	Good	Yes	Yes

Chang (1976) found improved oil recovery using sodium tripolyphosphate, which is a buffer. Sodium tripolyphosphate was proposed by Olsen et al., (1990) to minimize divalent precipitation, wettability alteration and emulsification. Normally, it is not used as a primary alkali to generate natural surfactant to reduce IFT, but it is used with other alkalis mainly sodium carbonate where divalent could be a problem (Sheng, 2011).

5.6 Why sodium carbonate is used more than others?

Sodium Silicate shows better results of recovering oil but silicate precipitates even at low concentration. On the other hand, sodium carbonate precipitates are granular and less adhering on solid surfaces (Cheng, 1986). For this, in presence of hard water sodium carbonate shows less permeability damage. Both sodium silicate and sodium carbonate can create scale on the production well, but sodium carbonate scale can be easily removed by acidizing or by using inhibitors. On the other hand, there is no method exist to remove silicate scale in long term. A continuous release of carbonate ions from rock

minerals into the solution can be prevented by using sodium carbonate because carbonate ions brought by the solution oppose calcite and magnesite dissolution. Sodium carbonate represses calcium ion concentration, but not magnesium's concentration. Sodium carbonate reduces the extent of ion exchange and mineral dissolution (in sandstones) as a weaker alkali compared with sodium hydroxide because mineral dissolution increases with pH. Owing to the buffer capacity of sodium carbonate, great changes in pH are not expected provided that the system is in chemical equilibrium. The preference of a weak alkali also comes from the concern of scale in production facilities. Generally, ASP formulations use moderate pH chemicals such as sodium bicarbonate (NaHCO_3) or sodium carbonate (Na_2CO_3) rather than sodium hydroxide (NaOH) to reduce emulsion and scale problems. Chinese ASP projects have had difficulty in breaking emulsion when using a strong alkali such as NaOH (Sheng, 2011).

To diminish the corrosion dilemma and scale problem associated with inorganic alkalis such as sodium hydroxide and sodium carbonate, an organic alkali was proposed (Berger and Lee, 2006). Metaborate was proposed to impound divalent cations such as Ca^{2+} and to avoid precipitation (Flaaten et al., 2008). However, no field test is found for inorganic alkalis (Sheng, 2011).

6 Materials and method

The materials and methods used in the experimental work of this thesis are summarized in this section.

6.1 Brine

Five different kinds of brine have been used in these experiments: formation water, low saline water, alkaline water-1, 2 and 3. Ion composition and properties of the brines are listed in table 6.

Table 6: Ion composition and properties of brine

Characteristics		FW (mM)	LS (mM)	ALK-1 (mM)	ALK-2 (mM)	ALK-3 (mM)
Ion Composition	Na ⁺	1540.00	17.10	17.30	17.64	18.00
	Ca ²⁺	90.00	0.00	0.00	0.00	0.00
	Cl ⁻	1720	17.10	15.40	11.98	8.55
	CO ₃ ²⁻	0.00	0.00	.9434	2.83	4.72
Brine Properties	pH	6.25	6.05	10.40	10.67	10.85
	Density, gm/cm ³	1.067	0.998	0.998	0.998	0.998
	Salinity, ppm	103250	1000	1000	1000	1000

6.1.1 Brine Preparation

All chemical substances used to prepare the brines were reagent grade and provided by Merck laboratories. Deionized (DI) water was used for the brine preparation with a total organic content T.O.C < five ppb and resistivity of 18.2 MΩ cm.

The brines were filtered using a 0.22 μm millipore membrane filters before using to get rid of any possible particles that might block the pore inside the core. Figure 17 illustrates the filtration setup, composed of a Büchner flask, a vacuum pump and piece-filtering funnel connected to the flask through a black elastomer, as an adapter for sealing. A filter and micro filter paper had been placed in between funnels and all of them were locked together to prevent any leakage. A vacuum pump was used to draw off the brine via the filter. Finally, the filtered brine amassed into a airtight flask.

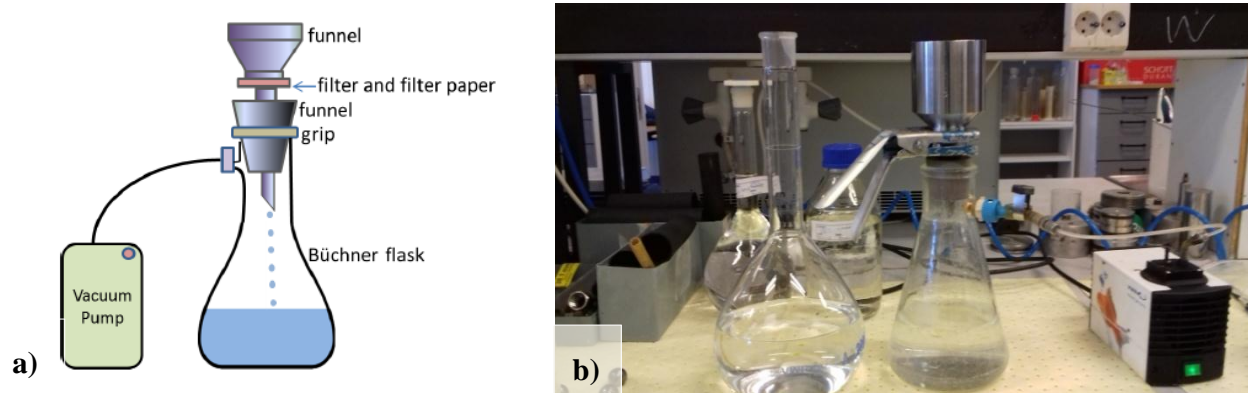


Figure 17: a) A schematic diagram of water filtration setup. b) Water filtration setup in lab.

6.2 Core Material

Three different outcrop sandstone cores have been used for this experiment: B-1, B-22 and Idaho Gray-1. B-1 and B-22 were supplied by Total E&P and known as Total outcrops. They were previously used in several studies (Austad et al. 2010, RezaeiDoust 2011, Torrijos, 2017). Idaho Gray-1 was also provided by Total E&P but it hasn't been used in any experiment before. Total E&P provided the outcrop core material together with mineralogical data composition and cation exchange capacities (CEC). In addition to the provided data, porosities and permeabilities of the cores were determined. The physical properties are given in Table 7 and mineralogical data is presented in Table 8. SEM and EDX were also done to have a closer look on the pores and to check the mineralogy. Figure 18 is showing the SEM photo of Total Outcrop B-22. In the figure, clays can be seen frequently which plays an important role in LS EOR. Core B-01 and B-22 has higher clays content, 3.4 and 2.9% more than Idaho Gray-1 respectively. Core B-01 and B-22 also has higher Quartz content (about 18% more) than Idaho Gray-1. On the other hand, Idaho Gray-1 has 22% of microcline which is absent in other two cores.

Table 7: Physical properties of Cores

Core #	PV (ml)	Porosity (Φ)	Permeability, K (mD)
B-1	16.3	20.4	na
B-22	23	20.5	135.1
Idaho Gray-1	24.26	29	971.2

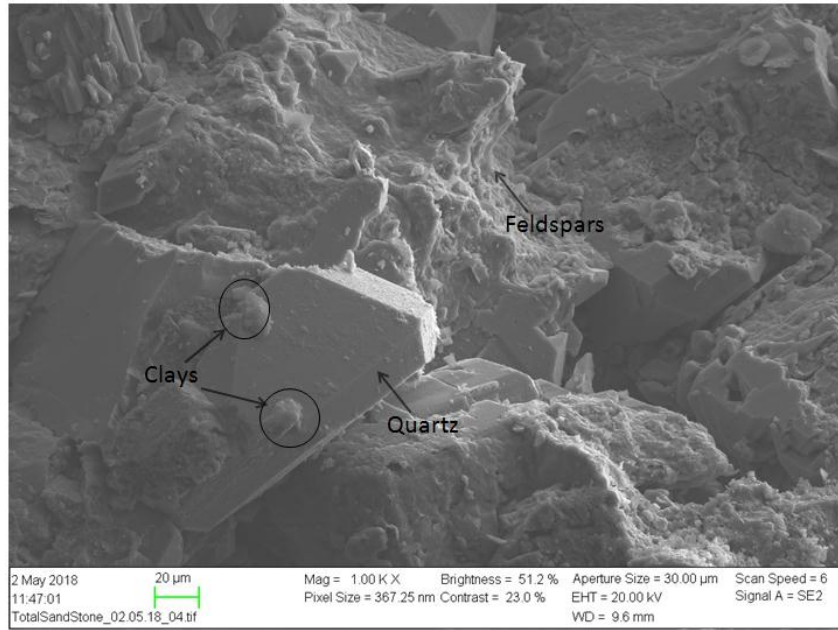


Figure 18: SEM image of core B-22

Table 8: Main mineralogical composition of cores

Mineral	B-1	B-22	Idaho Gray- 1
Quartz	58.2	56.20	39.65
Kaolinite	0.00	0.00	6.00
Chlorite	1.90	1.70	-
Illite	8.40	8.10	0.00
Smectite/Illite (R0-R1)	-	-	0.90
Albite	30.40	32.90	29.00
Microcline			22.00
Calcite	0.30	0.30	0.20
Dolomite	-	-	0.70
Others	0.80	0.80	1.55
Total clays and micas	10.30	9.80	6.90

*This includes smectite (Illite) R0 (Disordered) and/ or R1 (ordered two layers) and/or smectite.

Core B-1 and B-22 has a heterogeneous pore size distribution, as shown by Figure 19.

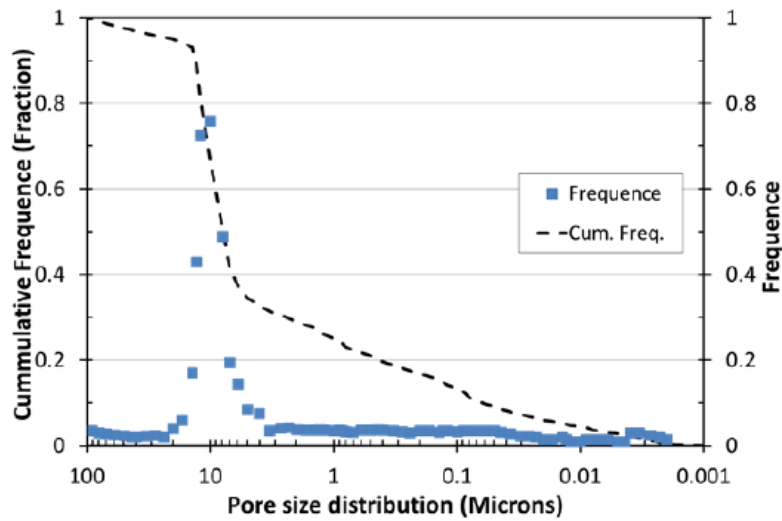


Figure 19: Pore size distribution of a core from the same block as the tested core material. Data provided by TOTAL E&P (Torrijos, 2017)

6.2.1 Core Preparation

As Core B-1 and B-22 were used before for oil flooding, they needed to be cleaned from oil. Core B-22 was provided clean before the experiment but B-1 was not clean. So, Core B-1 was cleaned by flooding kerosene, heptane and low salinity water respectively. At First, Kerosene was flushed into the core until the effluent color was acceptably clear, indicating that the core was ready for the next step of the cleaning process. Figure 20 shows the effluent of core cleaning process after flooded with kerosene. At first, the effluent was dark black indicating that the core was saturated with oil before.

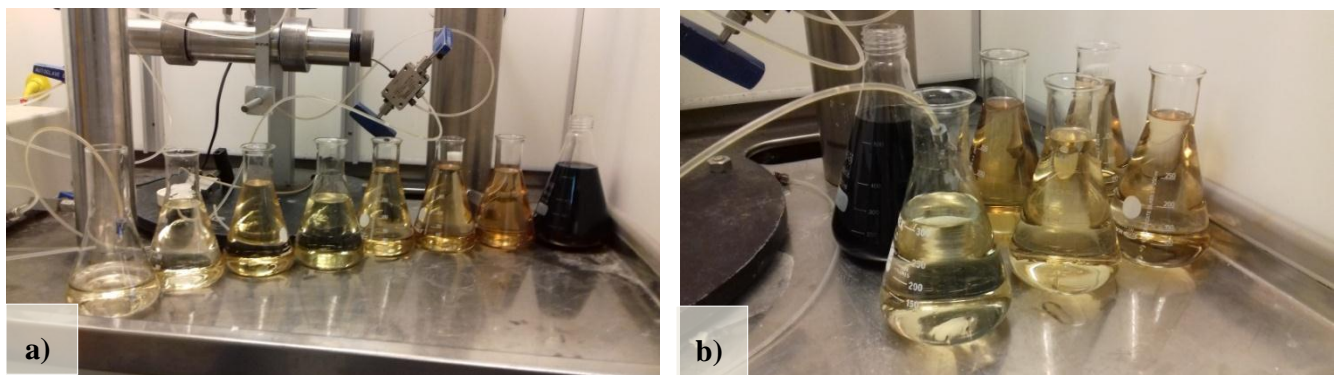


Figure 20: a) Effluent of Core cleaning with Kerosene. b) With Heptane.

The core was then flushed with heptane after completion of the kerosene injection. After clear effluent

was observed with heptane flooding, low saline water was flooded into the core to remove heptane and precipitated salts inside the cores. The schematic of cleaning setup can be seen in figure 21.

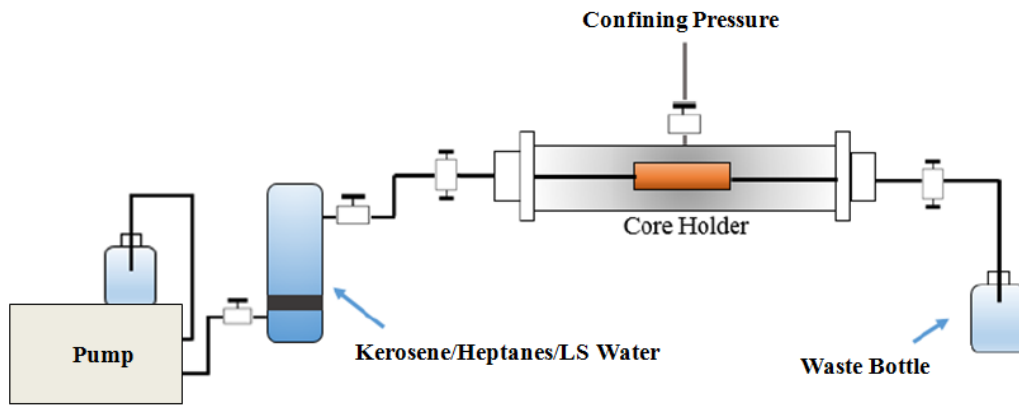


Figure 21: A schematic overview of core cleaning setup.

Finally, the core was placed in a heating cabinet at 60°C to evaporate remaining liquids in the core. The core was dried in the heating cabinet until its weight became constant by several measurements of its weight marking that all the liquids had been evaporated.

6.2.2 Saturation of Core with Brine

Firstly, the dry cores were placed over marbles inside a plastic container separately. Some marbles were placed at the bottom so that the end side of the core have some space to get contact with liquid. Then it was placed in a sealed system. A vacuum pump was used to take out the air from the system. Then the formation water was flowed through a valve, until water column became higher than the core height. Then the core remained in the system for 1 hour to become fully saturated. Figure 22 is showing the system schematic.

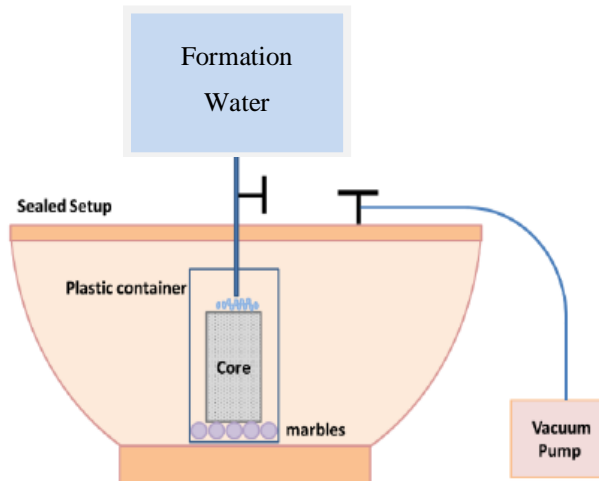


Figure 22: A schematic diagram of core saturation system.

5.2.3 Determination of Pore Volume and Porosity

The pore volume calculation was based on the weight difference between dry and 100% saturated core with formation water with known density. Dry weight was measured after the core had been cleaned and dried. The wet weight was also measured after the core had been fully saturated with formation water. The effective pore volume and the porosity of the cores were calculated from equation 26 and 27. The details of that calculation is not added to this thesis.

$$PV = \frac{W_s - W_d}{\rho_{FW}} \dots\dots\dots(26)$$

Where,

PV is the Pore volume core (cm³)

W_s is the Weight of core 100 % saturated with FW (gm)

W_d is the Weight of dry core (gm)

ρ_{FW} is the Density of FW [gm/cm³]

$$\Phi = \frac{PV}{V_b} \dots\dots\dots(27)$$

Where,

Φ is the Porosity of core (%)

PV is the Pore volume of core (cm³)

V_b is the Bulk volume of core (cm³)

6.3 Core Flooding Setup

The schematic of core flooding setup used for the experiment can be seen in figure 23(a). A piston cylinder contained the brine that was injected that was connected to a Hassler core holder showing in Figure 23(b). Steel pipes connected the piston cylinders to the inlet and outlet of the core holder. The piston cylinder containing the brine was connected to a Gilson HPLC pump that injected water into the piston cylinder, thereby displacing the brine into the tubing and through the core. Pressure of inlet and outlet was measured throughout the experiments. A backpressure of 10 bars was maintained constantly during the flooding. A confining pressure of 20 bars was applied around the rubber sleeve

containing the core. When one type of brine flooding was completed, the cylinder was disconnected, cleaned and again used for another brine.

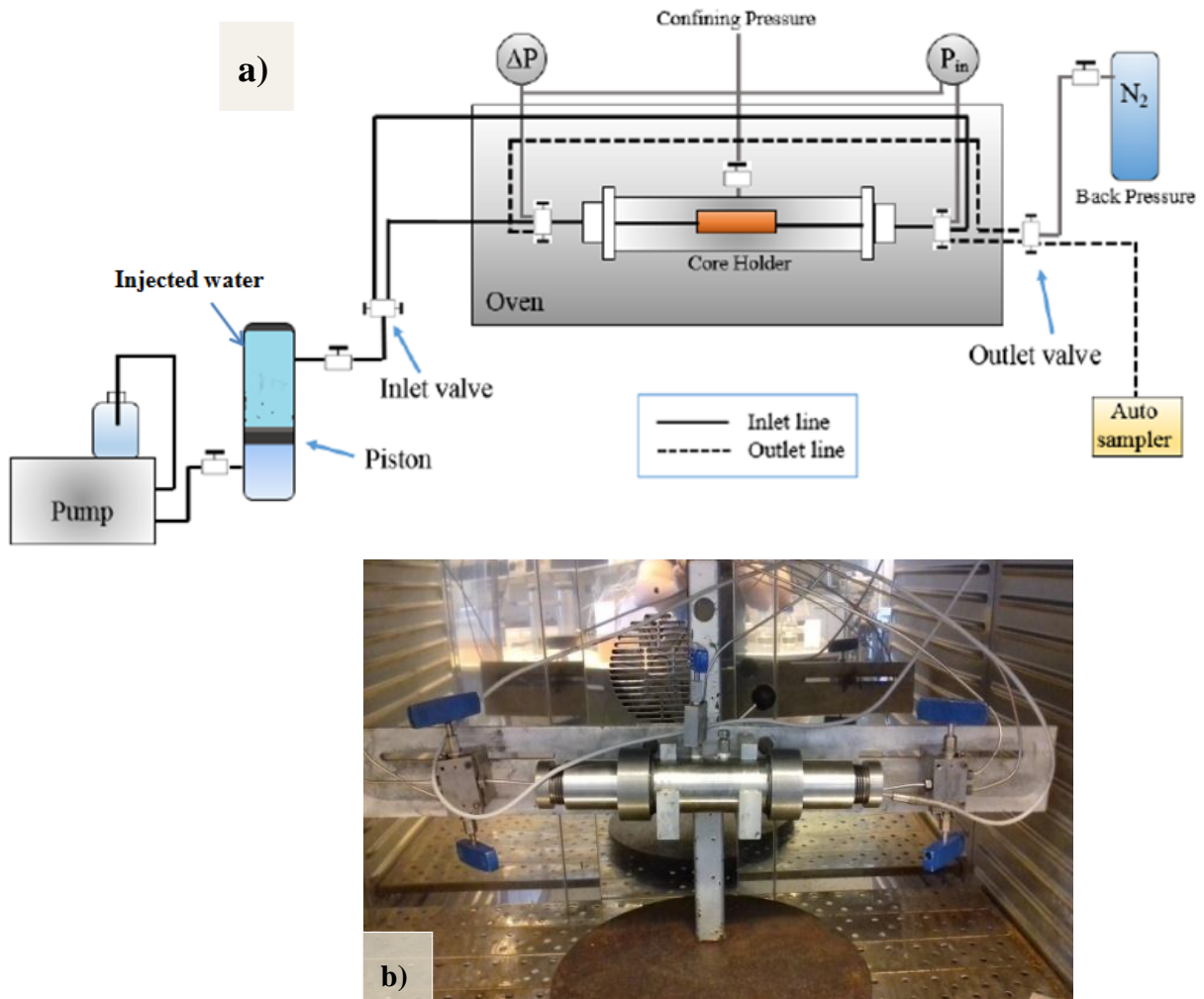


Figure 23: a) A schematic overview of core flooding setup. b) Hassler core holder

6.4 Fluid Analysis

pH, density, ion concentration was measured both for produced water and injected water. Temperature was fixed for each test and the pressure differences of inlet and outlet of the core were measured continuously. During the flooding process, the produced water (effluent) was collected by automated Automated liquid handler *Gilson GX-271* in a sealed container. Total 12 test were performed and the details of each test is given in table with test number in a chronological manner in table 9.

Table 9: pH screening tests performed during the thesis with flooding sequence and temperature in a chronological way

Core #	Flooding Sequence	Test no.	Temperature (°C)
B-22	FW - LS - ALK-1 - LS - FW	1	25
	FW - LS - ALK-1 - LS - FW	2	60
	FW - LS - ALK-1 - LS - FW	3	90
	FW - ALK-1 - FW - LS - FW	4	90
	FW - ALK-1 - FW - LS - FW	5	60
Idaho Gray-1	FW - ALK-1 - FW - LS - FW	6	60
	FW - ALK-1 - FW - LS - FW	7	90
	FW - LS - ALK-2 - LS - ALK-3 - FW	8	60
	FW - ALK-3	9	60
	FW - LS - ALK-3 - LS - FW	10	60
B-01	FW - ALK-1 - FW - LS - FW	11	60
	FW - ALK-1 - FW - LS - FW	12	90

Five tests each were performed with B-22 and Idaho Gray-1 with different flooding sequence. Only 2 tests were performed with core B-01. Flooding sequence representing which brine was flooded one after another.

6.4.1 pH Measurements

pH is the negative logarithm of hydrogen ion (H^+) concentration in the solution. At the ambient temperature, pH of neutral solution is 7, greater than 7 for alkaline and less than 7 for acidic solution. A *Mettler Toledo Seven Compact* pH meter (Figure 24(a)) was used to measure the pH. Prior to measuring the pH, the electrode was calibrated with buffer solution of pH 4, 7 and 10 to ensure the accuracy of the device. All the pH of produced water samples were measured at ambient temperature even though they were flooded at higher temperature. pH of the samples was measured just after the sealed container was opened to avoid any contamination of CO_2 with brine.

6.4.2 Density Measurements

Both the density of injected brine and produced brine were measured by *Anton Paar DMA 4500 Density Meter* (Figure 24(b)) at ambient temperature. Before measuring the density of the samples, the device was cleaned by injecting white spirit and acetone respectively. It was made sure by visual

inspection that there were no bubbles present during the measurement. Before starting the measurements, the accuracy of the device was checked by measuring the density of de-ionized water.

6.4.3 Ions Concentration Measurement

The Dionex ICS-300 Ion Chromatography (Figure 24(c)) was used to measure the ion concentration of the produced water and injected water to see the imbalance of ions during flooding. Ions can be absorbed by the core or released from the core to the brine. To ensure optimum detection of ions, the brines were diluted 500 times for LS water and 1000 times for high salinity formation water and then filtered through a 0.22 μm filter. Automated liquid handler *Gilson GX-271* was used to do the dilution process. After diluting and filtering the brine samples, they were put into different sealed bottles and placed into IC auto sampler. LS water and seawater of known composition were used as calibration reference for the device. The samples were transported through ion exchange column with the help of an elute. In the column, the ions were separated by using a stationary phase. The separated ions with elute passed through a suppressor. In the conductivity detector, each ion was found based on its conductivity measured in μS. The samples were analyzed in Chromeleon 7, where the cations and anions showed up as peaks based on their time through the column and their conductivity. The area below the curves are given in μS*min. To convert the area below the curves into concentration, mmole/liter, the following equation was used:

$$C_{sample} = \frac{C_{ref}A_{sample}D_{sample}}{A_{ref}D_{ref}} \dots\dots\dots (28)$$

Where,

C_{sample} = Concentration of sample in mmole/L

C_{ref} = Concentration of reference fluid in mmole/L

A_{sample} = Area of sample in μS*min

A_{ref} = Area of reference fluid in μS*min

D_{sample} = Dilution rate of sample

D_{ref} = Dilution rate of reference

6.5 Pressure Measurement

The pressure of the inlet and outlet of the core was measured and stored by software during each test to measure the pressure difference to see any kind of precipitation or scale. The permeability is a function of pressure difference. If there were any porosity and/or permeability loss than it would show pressure buildup or major change in the pressure data.

6.6 Scanning Electron Microscope (SEM)

The cores were photographed with Scanning Electron Microscope, *Zeiss Gemini Supra 35VP* for closer look at the sizes distribution of mineral surface. SEM is one of the most important beam technology inventions of the last century and has been developed constantly since then. Small samples were collected from the reference core and prepared with the help of Emitech K 550 before the analysis. The samples were cleaned with air to prevent erosion of the samples when they were under the influence of electronic beam in the SEM. Then the samples were coated with Palladium in an argon atmosphere to create a positive effect on the electronic conductivity of the sample (Emitech, 1999). In the device, an electronic gun bombarded them with electrons with voltage of 0.02 KV - 30 KV. Different signals were created when the beam hit the samples. Secondary electrons, backscattered electrons and X-rays are the most common used to generate an image from the deflected signals (Goldstein et al., 2003).

The SEM was equipped with an Energy-Dispersive X-ray Spectrometer (EDS) to analyze the composition. The same sample was used for this purpose. The emitted X-rays, from the sample exposed to the electron beam, are detected in a Si(Li) detector. The signals were then amplified and presented as a histogram by voltage (Goldstein et al., 2003)



Figure 24: a) pH meter, b) Density meter, c) Ion Chromatography.

7 Results

In this chapter, all the results of 12 pH scanning test are presented in the sequence how they were performed. pH of the effluent is plotted against injected PV of brine and the horizontal red dash line is representing the bulk pH of each of that brine. The vertical black dot lines are representing the change of brine such as from FW to LS or LS to ALK-1. Results of three different outcrop cores are presented separately. The flooded amount of brine was 4 PV/day for each test.

7.1 Core B-22

Figure 25 shows a pH screening test of core B-22 performed at ambient temperature by flooding in the sequence of FW - LS – ALK-1 - LS – FW. In this test each brine was flooded until a stable plateau was reached to see the reactivity level of the core with brines. However, alkaline water was not flooded more than 8 PV in this test to reduce the possibility of precipitation. Ambient temperature was used because the reaction rate between core and brine is highest at this temperature.

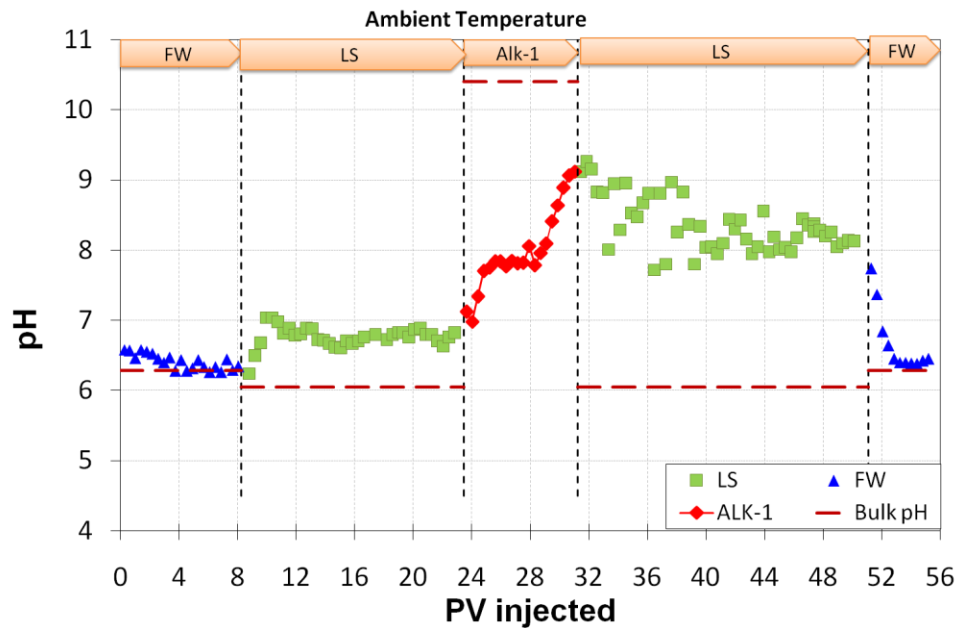


Figure 25: Test 1: pH Screening test of outcrop core B-22 at ambient temperature. Sequence of flooding: FW - LS – ALK-1 - LS – FW.

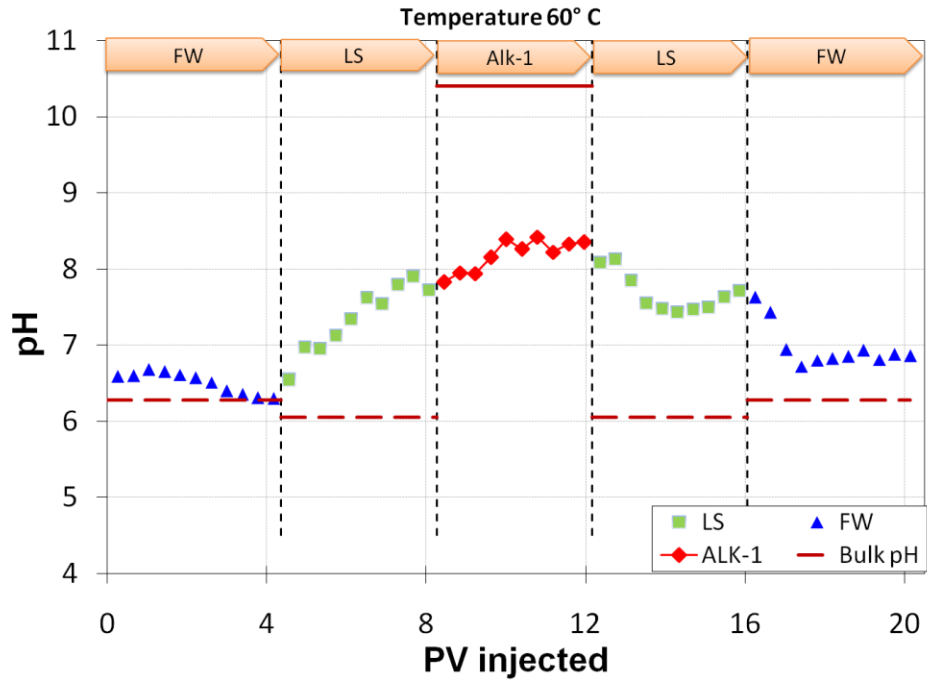


Figure 26: Test 2: pH Screening test of outcrop core B-22 at 60°C. Sequence of flooding: FW - LS – ALK-1 - LS – FW

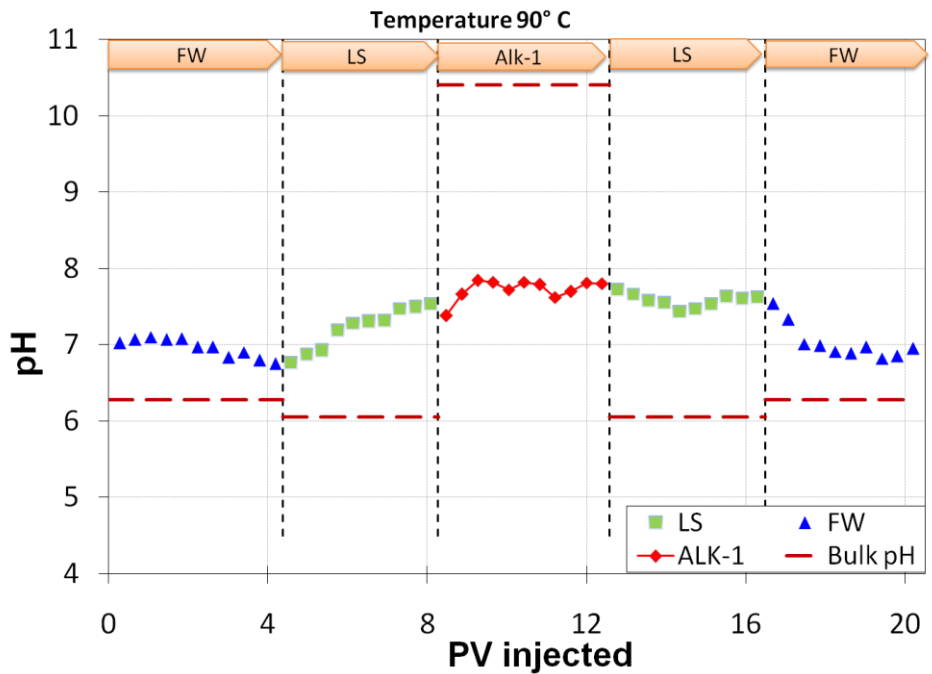


Figure 27: Test 3: pH Screening test of outcrop core B-22 at 90°C. Sequence of flooding: FW - LS – ALK-1 - LS - FW

Figure 26 shows the same kind of test that was done on test 1 but at different temperature (60°C). However, in this test only about 4 PV of each brine was flooded, as most cases in reservoir, the injected fluid for EOR does not reach 4 PV.

Figure 27 is showing the same kind of test done at test 2, but with a different temperature (90°C). The reason behind using LS between HS FW and alkaline water is the presence of Ca^{2+} in FW. Ca^{2+} could react with the alkaline and precipitate as CaCO_3 . However, in some tests, alkaline was used after FW to see what could happen. Test 4 and test 5 are the example of it. The sequence of flooding was FW – ALK-1 - FW - LS – FW and the only difference between the tests was temperature. 90°C was used for test 4 and 60°C was used for test 5. Figure 28 and 29 are showing test 4 and test 5 respectively. The black line during ALK-1 and LS is representing the slop of trend line which indicates how first the alkalinity has built up.

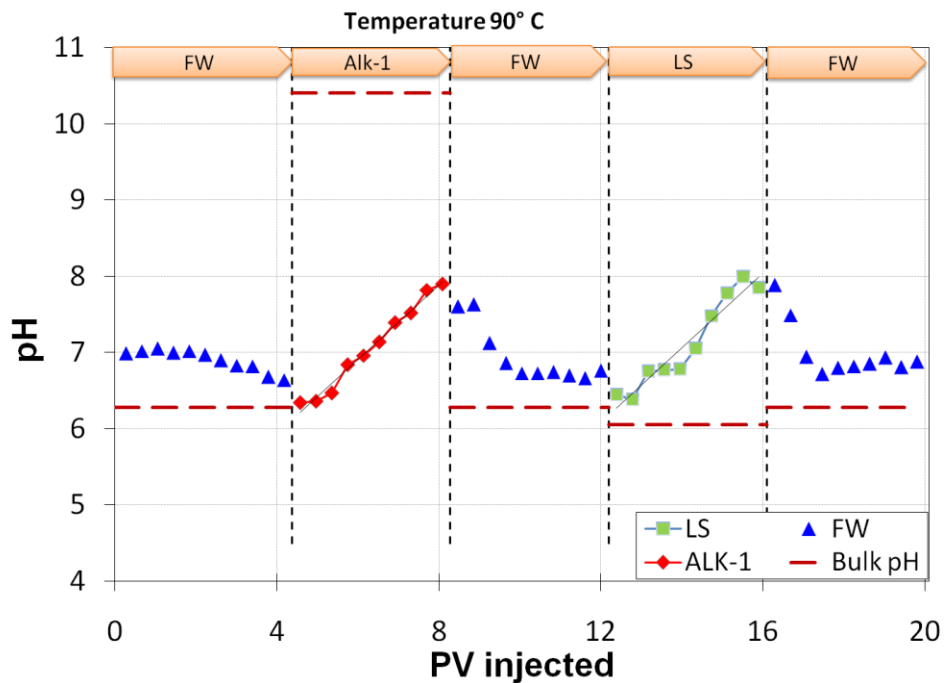


Figure 28: Test 4: pH Screening test of outcrop core B-22 at 90°C Sequence of flooding: FW – ALK-1 - FW - LS – FW

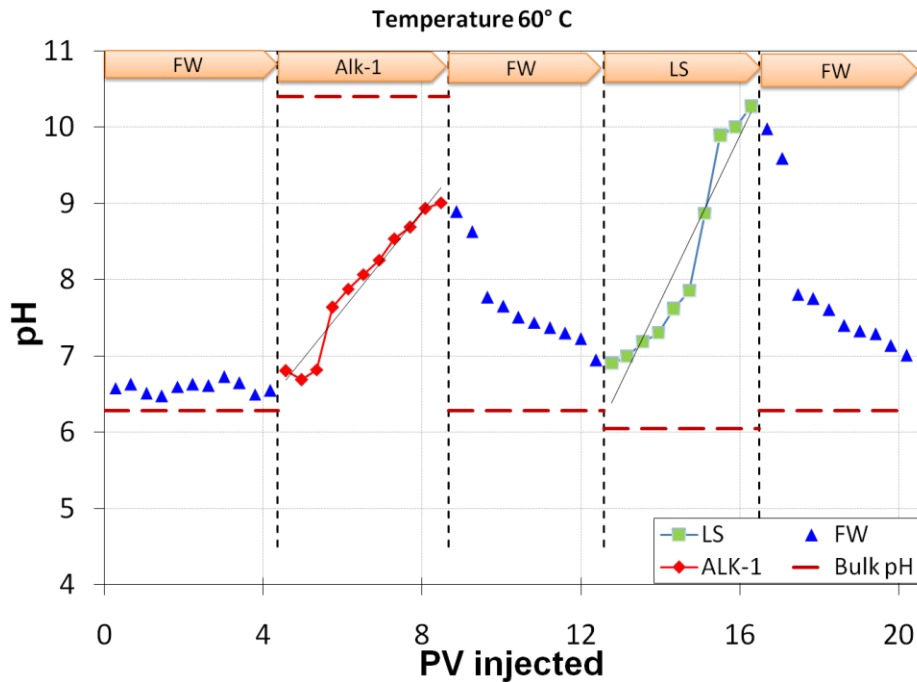


Figure 29: Test 5: pH Screening test of outcrop core B-22 at 60°C. Sequence of flooding: FW – ALK-1 - FW - LS - FW

7.2 Core Idaho Gray-1

Figure 30 to 34 are showing pH screening tests (Test 6-10) that were done with Idaho Gray-1 core at different temperatures. Figure 30 is showing test 6 that has the same temperature and flooding sequence as test 5, but with different core. Similarly, Figure 31 is showing test 7 that has the same temperature and flooding sequence as test 4. FW, LS and alkaline water has the same concentration from test 1 to 7. Figure 32 is showing test 8 which was done at 60°C for Idaho Gray-1 core and different concentration of salinity was used. After flooding the FW, LS was flooded before alkaline water to prevent possible precipitation. Alkaline (ALK-2) that was flooded after LS has 2.83 mmole (0.3 gm of Na_2CO_3 per liter solution) of CO_3^{2+} whereas, second alkaline (ALK-3) has 4.72 mmole (0.5 gm of Na_2CO_3 per liter solution) of CO_3^{2+} in this test.

Figure 33 is representing test 9 where higher concentration of Alkaline water was used just after FW. Though the plan was to flood FW after alkaline but due to precipitation problem at the producer line, the test needed be stopped.

After the precipitation problem, the outlet was cleaned and test 10 was performed with LS flooded in between FW and high concentration alkaline (ALK-3) at same temperature (60°C).

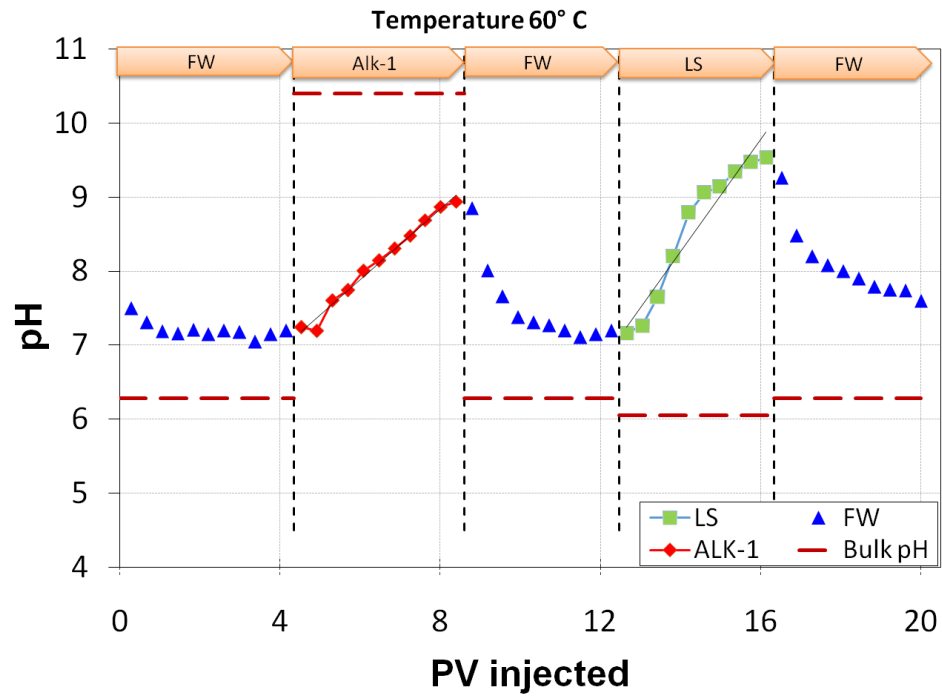


Figure 30: Test 6: pH Screening test of outcrop core Idaho Gray-1 at 60°C. Sequence of flooding: FW – ALK-1 - FW - LS - FW

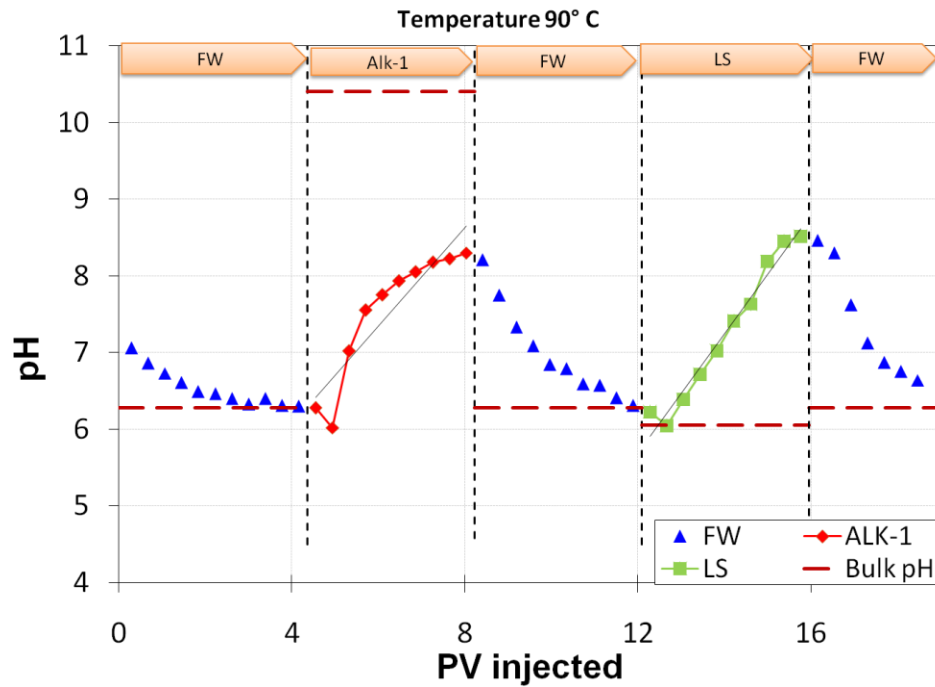


Figure 31: Test 7: pH Screening test of outcrop core Idaho Gray-1 at 90°C. Sequence of flooding: FW – ALK-1 - FW - LS - FW

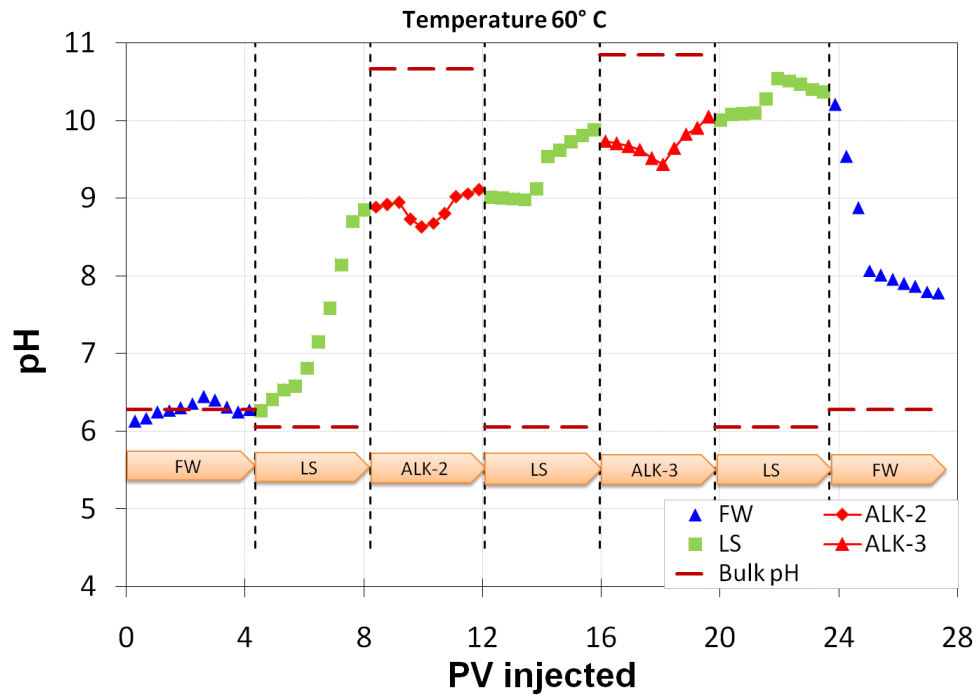


Figure 32: Test 8: pH Screening test of outcrop core Idaho Gray-1 at 60°C. Sequence of flooding: FW - LS - ALK-2 - LS - ALK-3 - FW

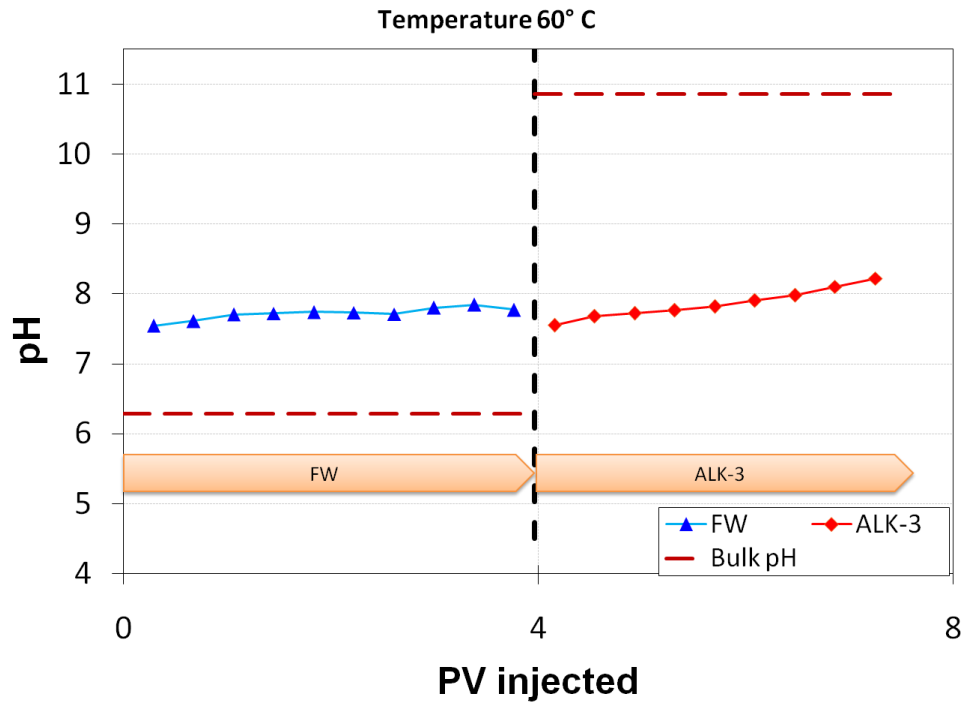


Figure 33: Test 9: pH Screening test of outcrop core Idaho Gray-1 at 60°C. Sequence of flooding: FW - ALK-3

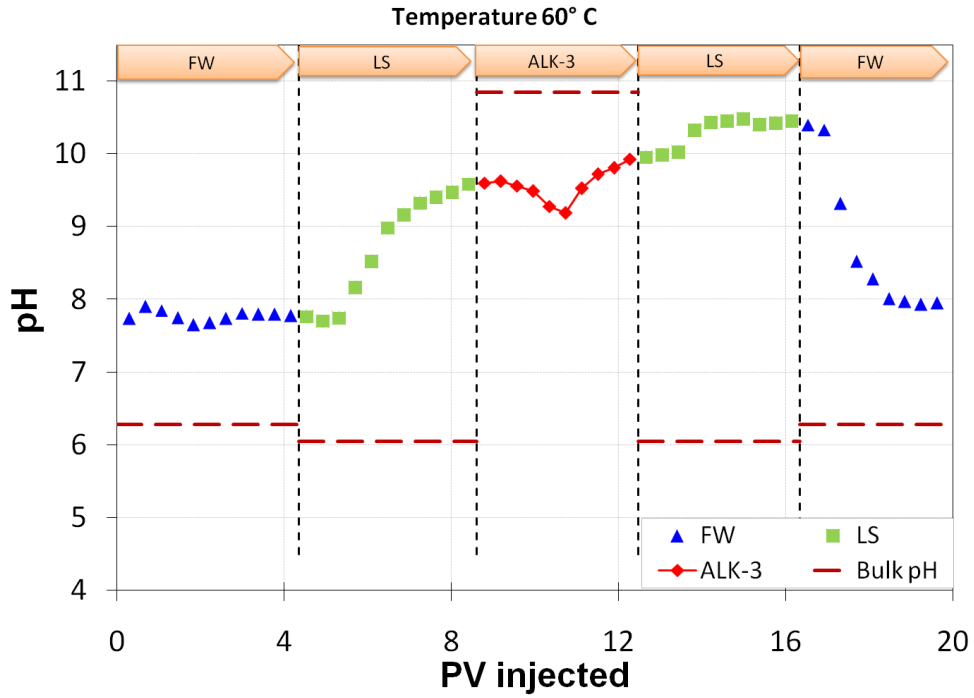


Figure 34: Test 10: pH Screening test of outcrop core Idaho Gray-1 at 60°C. Sequence of flooding: FW - LS- ALK-3 – LS – FW

7.3 Core B-01

Two tests were performed with core B-01 T 60°C and 90°C with the sequence of FW - LS- ALK-1 – LS – FW and showed in figure 35 and 36. The black straight line in most of the figures is showing the trend line of pH buildup for alkaline and LS.

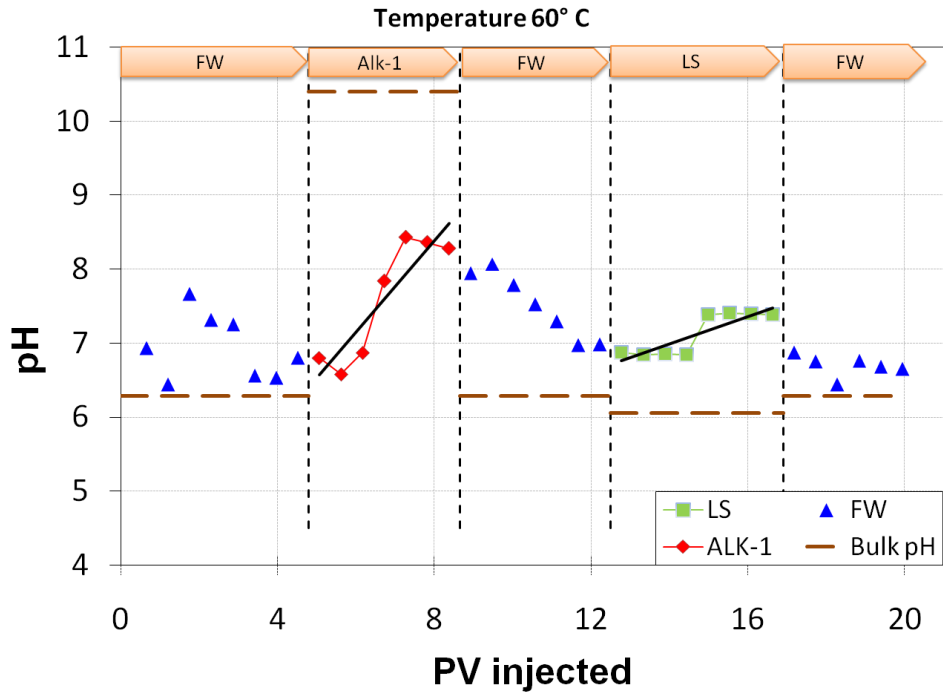


Figure 35: Test 11: pH Screening test of outcrop core B-01 at 60°C. Sequence of flooding: FW - ALK-1 -FW - LS - FW

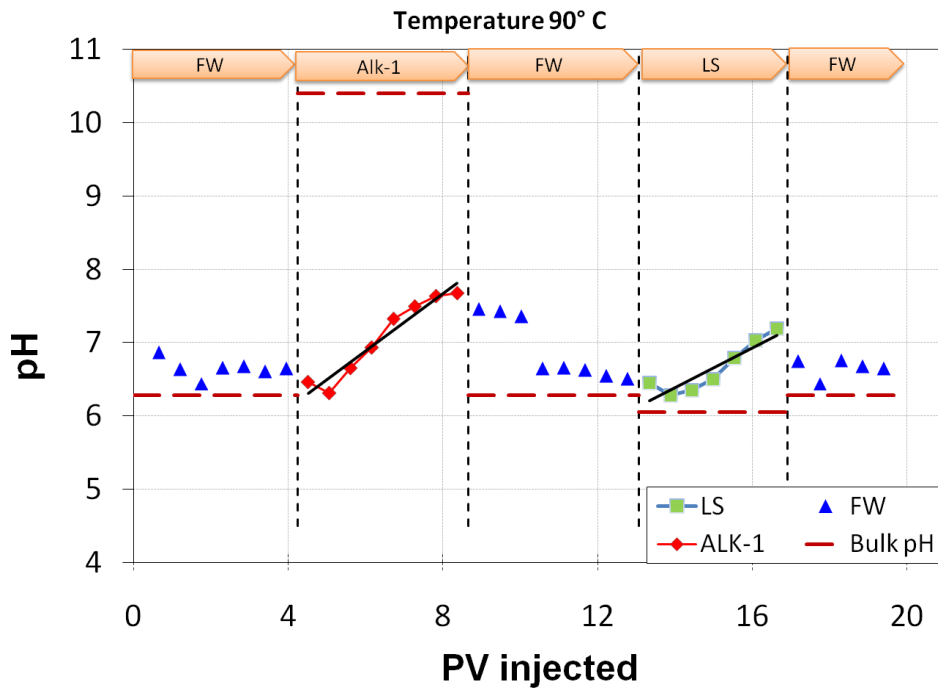


Figure 36: Test 12: pH Screening test of outcrop core B-01 at 90°C. Sequence of flooding: FW - ALK-1 - FW - LS - FW

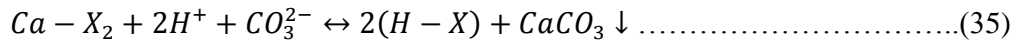
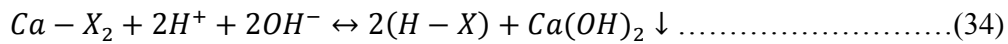
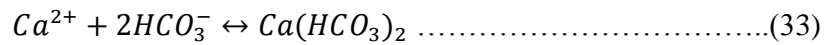
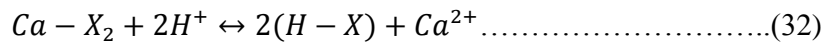
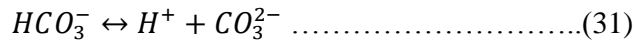
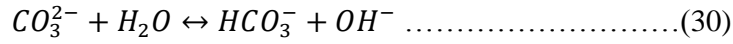
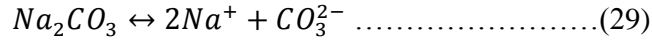
8 Discussion

Most of the pH screening tests are showing similar kind of trends for different cores though they have very different mineralogy. The pH of the effluent has not changed too much (pH around 7) from initial pH for the total formation water, whereas the bulk pH of formation water was 6.25. Effluent pH during LS flooding increased around 2 pH unit or even more from initial pH in some cases. Alkaline water is showing the same trend as LS water though alkaline water has high initial pH over 10. In the discussion part, it will be explained why the pH of the effluents changed and which mineral played vital role in pH change with the possible chemical reactions. As the previous researches showed that high pH in the core is beneficial for good EOR, it was tried to transport the pH through the cores. In case of LS water flooding, in situ pH was created in the core. However, if high pH water is injected, *can the same pH level be achieved at the effluent for alkaline water?* The answer of that question was tried to find out in this thesis.

8.1 Alkalinity Transporting Ability

It was discussed in the theory part that alkaline water creates in situ surfactant inside the core and decreases IFT whereas LS water creates in situ pH inside the core, changes the wettability to more water wet and increases oil recovery. By injecting alkaline water, if it is possible to transport the pH through the core, it is expected to have the same result of increased oil recovery as same as low salinity water alone with the alkaline effect which is lowering IFT. Therefore, alkaline water of high pH was injected and the pH was measured after flooding through the core. All the cases, it has been observed that the pH is decreased by core flooding. After flooding 4 PV, the initial pH of alkaline cannot be reached. In most cases, the pH value of the effluent was around 8 after 4 PV of alkaline injection. The highest value of effluent pH was 9 at 60°C for B-22 and Idaho Gray-1 core while injecting alkaline water when it was flooded just after formation water which can be seen in figure 29 and 30 respectively. However, in test 8 and 10 for Idaho Gray-1 core, more increase in pH can be seen (around 10) at the end of alkaline flooding. The main reason of that is LS water was flooded before the alkaline flood and the pH was built up before the alkaline water was flooded. Moreover, it can be seen that pH even decreased during alkaline flooding than LS water flooding, which was flooded just before it (Figure 32, Figure 34). From both B-22 and Idaho Gray-01 core test (figure 25-34), the pH of LS effluent was higher than the alkaline effluent. On the other hand in B-01, a high pH in alkaline effluent can be seen but it was very low (.5 pH unit). About 1.5-3 pH unit was absorbed by the minerals for all the cores in case of alkaline water flooding. As a result, it can be said that alkalinity transportation depends on the

mineralogy of the core. It is not possible to conclude on which mineral is playing the major role on absorbing the alkalinity. However, how the alkalinity is consumed by the clay minerals, which has divalent ions with it, can be expressed by following reactions (Sheng, 2011).



Firstly, Sodium carbonate (Na_2CO_3) dissociates in the water and followed by the hydrolysis reaction. OH^- , HCO_3^- and CO_3^{2-} ions are created, and they are the main reason for high pH of alkaline water. On the other hand, H^+ replaces divalent ions such as Ca^{2+} from the rock surface. Or Ca^{2+} desorbs from the clay surface to reestablish equilibrium, H^+ takes its place on the clay surface. Generating OH^- that can cause precipitation with divalent cation Ca^{2+} . In the reaction, X is denoted as clay mineral surface. By taking the proton (H^+), clays become neutrally charged. The Ca ion released from the clay surface attracts two hydrogen carbonate ions (HCO_3^-) and creates a neutral soluble calcium bi carbonate molecule [$Ca(HCO_3)_2$]. In this process, negatively charged bicarbonate is reduced and the pH of the solution reduced as well. This might be one of the causes for alkalinity consumption in the core. This process is slowed down when the most reactive clay particles gave all the divalent ions and the formation of $Ca(HCO_3)_2$ is reduced. When temperature increases to $90^\circ C$, all the test showed more alkalinity reduction. This will be discussed in the effect of temperature in chapter 8.5.

Another reason of alkalinity reduction is formation of solid particles like $CaCO_3$ and $Ca(OH)_2$ which are less soluble in water and create scale. In this research, these might be the reason for occurred scaling. These reactions are expressed by equation 34 and 35 (Sheng, 2011).

Somerton and Radke (1983) also experienced alkalinity consumption in Wilmington oil sands at 52°C. They injected sodium hydroxide of 11.2 pH but did not get the same hydroxide amount measured in the effluent even after 10 PV flooded.

Therefore, it is obvious that the alkalinity cannot be transported in a 7 cm long core in the experiment than in the field it is impossible to transport the alkalinity where the distance of the injector and producer will be few hundred meters in the reservoir.

How the presence of crude oil can affect the alkalinity consumption is not experimented in this thesis. Alkalinity consumption can be higher because of less interaction between rock and water if oil is present. But, at the same time, crude oil contains acids and bases that can also react to buffer pH. Detail discussion was presented about oil and alkaline reaction in chapter 5.1.

8.2 Low salinity water flooding effect

All the experiments in this thesis are showing increase in pH value in the effluent when LS water of pH 6.05 is injected. For Idaho Gray-1 core, the pH of LS effluent reached 9.5 pH unit and for B-22 it reached the highest of around 10.5 pH unit at 60°C. Therefore, the main question in this part is “*Why pH of the effluent increases during LS flooding?*” Many researchers had tried to find out that reason and linked it to water wetness of the rock. Researchers of Smart Water Group from University of Stavanger named it Chemical Smart Water EOR Mechanism and it is discussed in Chapter 4.2.3.

As the pH increases, the reservoir moves to more water wet and increases the potentiality of more oil recovery. Using this logic, Aksulu et al. (2012) established pH screening test as a potentiality checker of EOR in sandstone in case of low salinity smart water.

For both B-22 and Idaho Gray-1 cores have high potential for LS EOR as they are showing high pH increment during LS flooding. In case of B-22, oil recovery test was performed during the PhD project (2017) of Torrijos at the smart water lab. The result of that test supports the pH screening test that is done in this thesis.

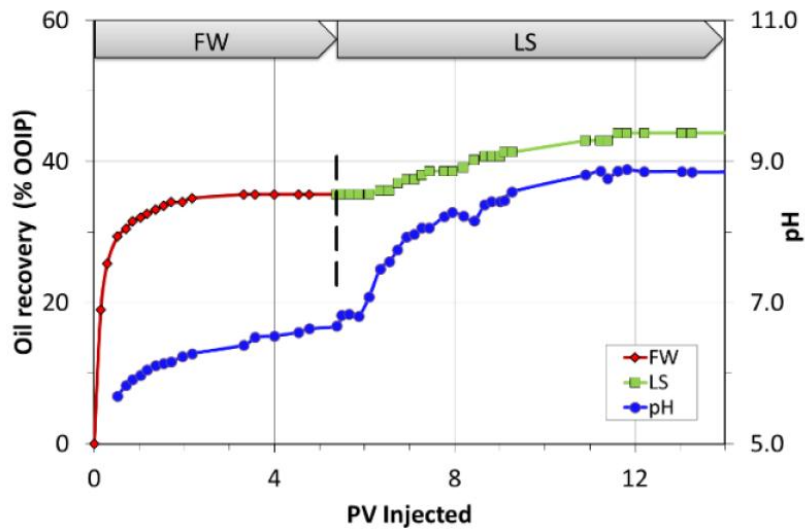


Figure 37: Oil recovery test on core B-22, with 20% water saturation and aged in crude oil at 120°C. Flooding sequence was FW-LS at 4 PV per day (Torrijos, 2017).

In this test, Torrijos (2017) used the same salinity LS what is used in this thesis. As this experiment was done at 120°C, LS effect is low (Figure 37). If we consider another core B-21 (Figure 38), which has the same mineralogy as B-22, at lower temperature (60°C), we can see more LS EOR effect. For B-22 at 120°C, LS EOR is around 8.7 % extra than high salinity formation water and for B-21 at 60°C, the recovery is 9.2% more than formation water. Therefore, it is obvious that high pH during LS flooding is the primary requirement to see EOR effect.

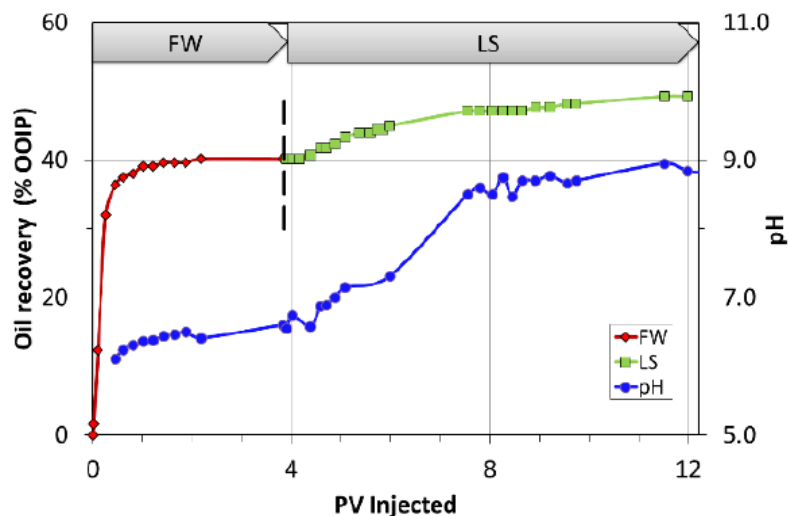
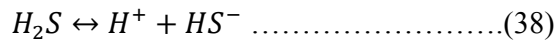
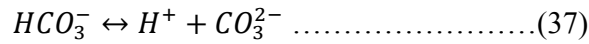


Figure 38: Oil recovery test on core B-21, with 20% water saturation and aged in crude oil at 60°C. Flooding sequence was FW-LS at 4 PV per day (Torrijos, 2017).

However, during the field test of LS EOR in Endicott field in Alaska by British Petroleum (BP) found high oil recovery without increasing the pH in the produced water. The reason behind it was CO₂ and H₂S, which were present in the crude oil and buffer the pH by following reactions (Aksulu et al., 2012).



8.3 High salinity Formation water effect on pH, wettability and EOR potential

Almost in all tests, when high salinity formation water was injected, it can be seen from the result that the pH of the formation water effluents remains in between 6 and 7 and in some cases 7.5 pH unit. *What does it mean?* Torrijos (2017) and Aksulu et al. (2012) confirmed that low pH for formation water is needed to see the effect of LS in the outcrop cores by pH screening test. High pH (>8) represents water wetness and moderate pH (6-7) represents mixed to water wet core. A high initial pH does not favor initial adsorption of polar components onto to the rock. To see the higher LS effect, experiments showed that mixed wet or a slightly water wet reservoir is necessary along with other condition. Therefore, all the effluent pH of formation water of most of the tests suggests a good LS oil recovery prospect. In most of the experiment, after flooding approximately 4 PV of LS or alkaline or 12 PV of LS, Alkaline and LS, while transferring to formation water again, it can be seen that formation water effluent has same pH as it was before. But in test 8, when we LS and different alkaline water were flooded one after another about 20 PV and a high alkaline environment of pH greater than 10 was created, effluent pH of formation water didn't go down to its previous level which was less than 7. The effluent pH of formation water of that time was around 7.8. That means with 20 PV of alkaline environment changed the reactivity of the core. In next two tests, test 9 and 10, the pH of the effluent of formation water remain the same (about 7.8). Long term water-flooding may perhaps change the reactivity of the core or saturate the surface with ions and some of them can be difficult to remove or exchange further.

8.4 Effect of Temperature

All the experiments were done in both 60°C and 90°C to see the temperature effect on the pH change and alkalinity transportation. In this section, pH of effluent at 60°C and 90°C are combined in the figure 37 and 38 for FW – ALK-1 – FW – LS – FW flooding sequence for B-22 and Idaho Gray-1 cores.

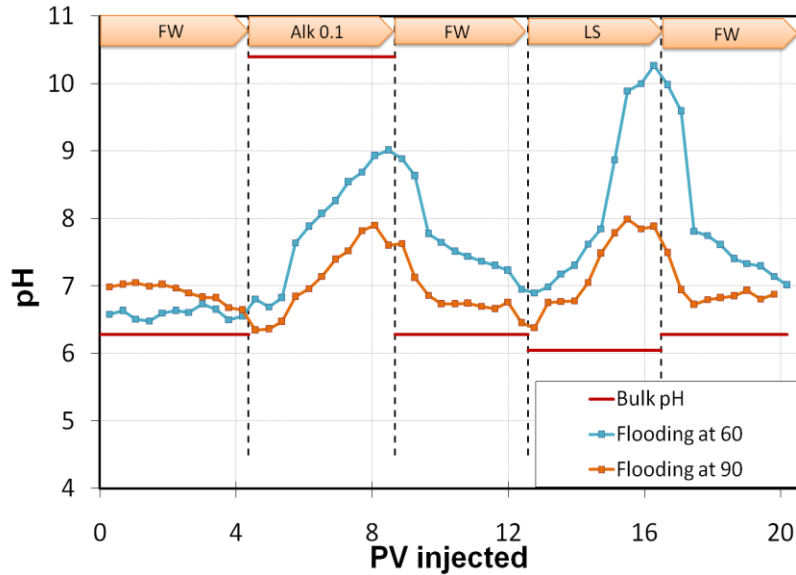


Figure 39: pH-screening test at 60°C and 90°C of B-22.

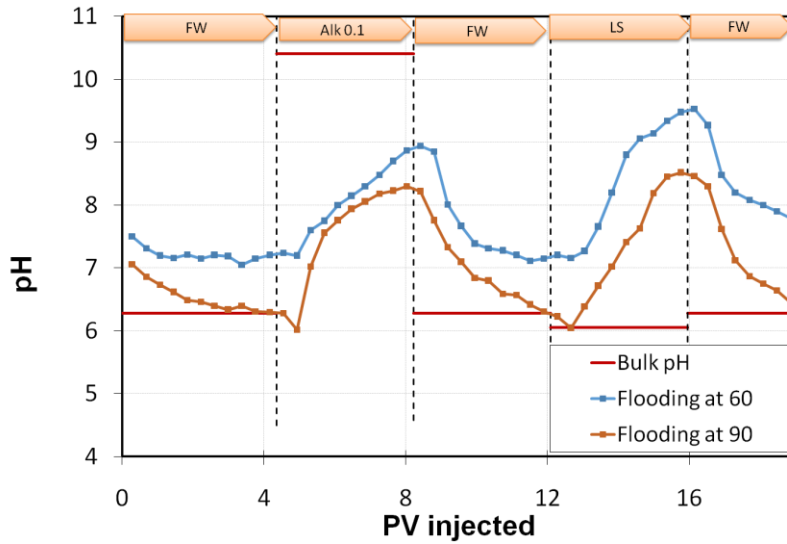


Figure 40: pH-screening test at 60°C and 90°C of Idaho Gray-1.

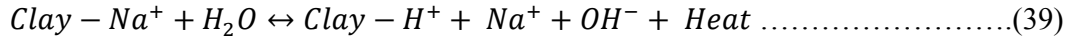
For both the core, pH of the effluent was low at high temperature compared to low temperature. For 30°C temperature difference, pH difference was roughly .5-1.0 pH unit. Though the peak of the pH for alkaline and LS were higher for lower temperature, the pH changes (ΔpH) from formation water to LS or alkaline water were same for both temperature. For Idaho gray-1, the change of pH was 1.7 at 60°C and 1.8 at 90°C from FW to ALK-1. For the same core, the change of pH from to LS was 2.3 for both 60°C and 90°C. On the other hand, for core B-22, pH difference for 60°C and 90°C were more than double. Table 10 represents the value achieved from test-4,5,6 and 7. In case of B-01, alkaline water at 60°C has higher pH change than 60°C and B-1 has around half unit change of pH in both temperature. Average value was taken for FW effluent that was flooded before alkaline water. Therefore, only for Idaho Gray-1, pH difference did not change with temperature. On the other hand, pH difference from FW to LS or alkaline depends on temperature. Hence it can be concluded that pH change of the effluent from FW to LS/ALK-1 depends on mineralogy rather than temperature.

Table 10: Comparison of pH change at different temperature for different cores.

Core	Temperature (°C)	Average pH of FW before ALK-1 flooding	Highest pH of ALK-1 flooding	Change of pH (ΔpH)	Average pH of FW before LS flooding*	Highest pH of LS flooding	Change of pH (ΔpH)
B-22	60	6.6	9.0	2.4	7.0	10.2	3.2
	90	6.9	7.9	1.0	6.7	8.0	1.3
Idaho Gray-1	60	7.2	8.9	1.7	7.2	9.5	2.3
	90	6.5	8.3	1.8	6.4	9.7	2.3
B-01	60	6.9	8.4	1.5	7.0	7.4	0.4
	90	6.7	7.7	1.0	6.6	7.2	0.6

* During changing from alkaline to FW, the effect of alkaline flooding was seen up to 3 to 3.5 PV flooded. Therefore, to have a stable pH value of FW water, only last half PV flooded was considered to calculate the average.

Though pH differences from FW to ALK/LS cannot be differentiate with temperature but the pH increment can be identified with low temperature. So, why the pH is higher at lower temperature? The ion exchange reaction of the clay is an exothermic reaction. When heat is added to the system then the reaction (39) moves to right to left according to Le Chatlier's principle. More heat in the system means less hydroxide ion in water and less pH. That is the main reason why pH at 90°C of all effluent is less than 60°C.



On the other hand for alkaline effluent, a soluble $\text{Ca}(\text{HCO}_3)_2$ is formed in the formation which reduce the pH of alkaline by taking HCO_3^- ions from the solution. However, when temperature increases, this calcium bi carbonate breaks down and give proton to the system. Though the amount of that is very low, still it decreases the pH of the solution.

Aksulu et al. (2012) found about 1.8 pH unit change in LS effluent between 40°C and 130°C in a reservoir core (Figure 41). They used low salinity NaCl (1000 ppm) brine and high salinity (100000 ppm) brine with sodium and calcium salt. This core has more than 20% clays.

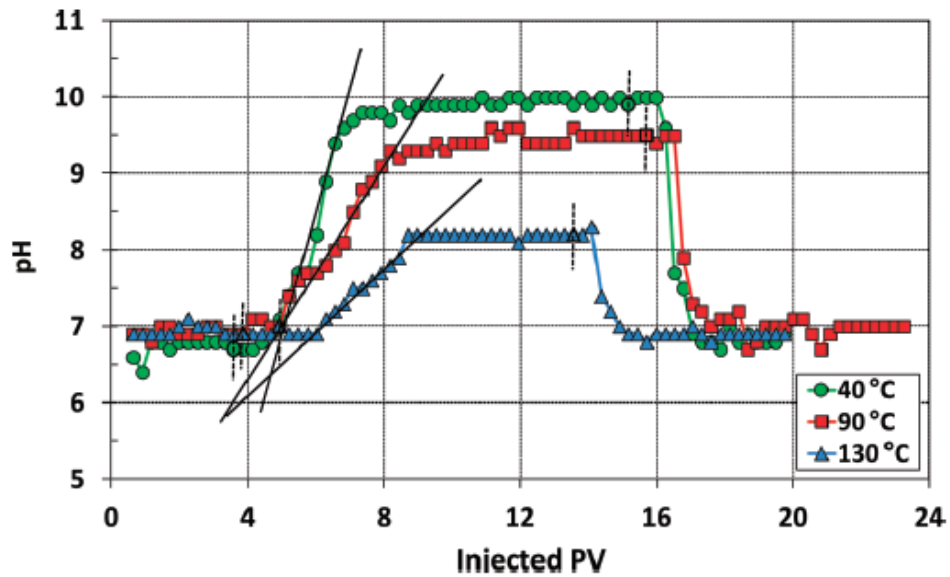


Figure 41: Comparison of effluent pH in 40°C, 90°C and 130°C in sandstone reservoir core-2 (RC-2) during pH screening test at 4 PV/day. The flooding sequence was HS-LS-HS. The dash lines indicating the slop of pH change (Aksulu et al., 2012).

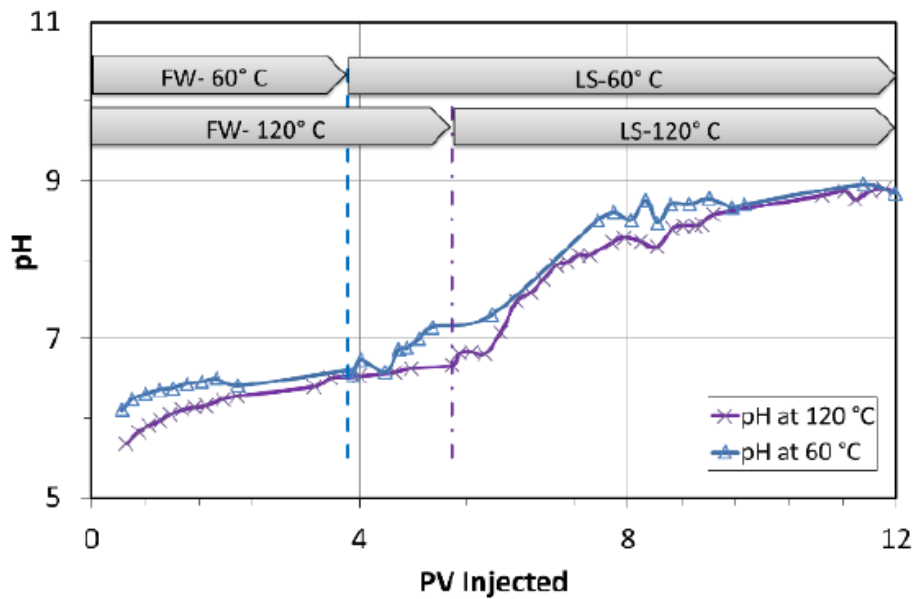


Figure 42: Comparison of effluent pH at 60°C and 120°C of B-21 during pH screening test at 4 PV/day. The flooding sequence was FW-LS (Torrijos, 2017).

However, Torrijos (2017) found similar pH for higher temperature (120°C) and lower temperature (60°C). In his research (Figure 42), he used outcrop sandstone core, which have the same mineralogy as B-22 that is used in this thesis. The LS and FW was also the same as this thesis.

Therefore, comparing researches from Aksulu et al. (2012), Torrijos (2017) and this thesis it can be said that, LS effect depends on the mineralogy of the core rather than temperature.

8.5 Effect of mineralogy

To study the effect of mineralogy for LS and alkaline brine, three different cores of different mineralogy were used in this thesis. The mineralogy of cores can be found in table 8. The mineralogy of the cores is so complex that which mineral is affecting the pH increment during LS and alkalinity consumption is difficult to say. However, from the discussion of chapter 8.4, it can be said that if a core has lower amount of clays, the pH of the effluent does not change so much because of temperature change which is also supported by aksulu et al. (2012). Moreover, Idaho gray-1 also has microcline, kaolinite and illite which are not present in other two core whereas it has less about 20% less quartz than core B-1 and B-22. According to Shen and Chen (1996) kaolinite, illite and microcline has more

ability to consume alkalinity than quartz. However, there is no conclusive evidence of more alkalinity consumption in Idaho Gray-1 in this thesis.

As the same fluid (FW/ALK/LS) was injected through the cores and produced water with different pH, it can be said that it is the minerals that plays the major role in changing pH.

8.6 Effect of Density

When the flow sequences were FW - ALK-1 - FW - LS - FW then the density was measured. As LS and ALK has the same density, it is impossible to track the density change when ALK flooded after LS. By tracking the density of effluent, the change of HS to LS brine can be identified. The homogeneousness of the core might also be visualized with density change. If the effluent density takes more time to reach the exact density of injecting fluid, then it can be said that the pore of the core is heterogeneous. Density of test 5 and test 9 for B-22 and B-1 are combined to compare the heterogeneity of core in figure 43.

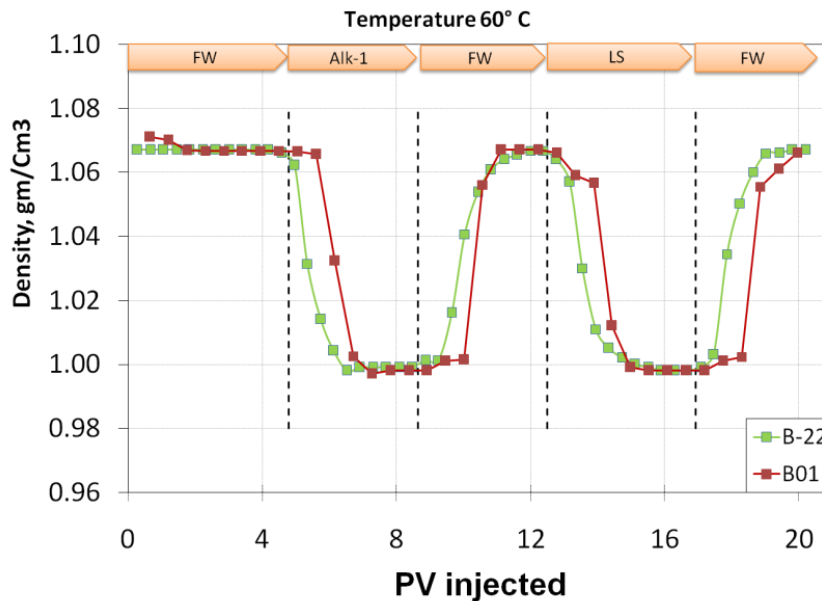


Figure 43: Density of the effluents for core B-22 and B-1 at 60°C. The flow sequence was FW - ALK-1 - FW - LS - FW.

The density of injected LS and ALK-1 were .998 gm/cm³ and 1.067 gm/cm³ for FW. The trend for density change is similar to each other for both core with slightly small variation. As B-1 and B-22 has similar kind of pore sorting, it is impossible to come to a conclusion that which core is more homogeneous or well sorted. Therefore, density change can only help to identify the change of brine in this case.

8.7 Effect of Pressure Difference during Flooding

The pressure of inlet and outlet of the core was measured and monitored during the flooding. There was no major pressure buildup or decrease in pressure difference found. Tang and Marrow (1999) found increase in pressure difference in their research and concluded it as the result of fine migration. However, in this thesis, the pressure difference was very low and the difference is almost negligible. Therefore, it can be said that there was no or negligible fine migration during LS flooding which is considered as one of the mechanism for LS EOR. Moreover, it can be said that there was no precipitation of solids during the test in the core, especially with using alkaline and LS flooding. The following figure is showing the pressure drop of test 7. The pressure drop is between 0.1 to 0.4 mbar, which is very low. For FW, pressure difference became little higher than LS and ALK-1 because it has high density and density is a function of pressure. The rest of the pressure data was collected and stored in Smart water lab, as they are not that significant.

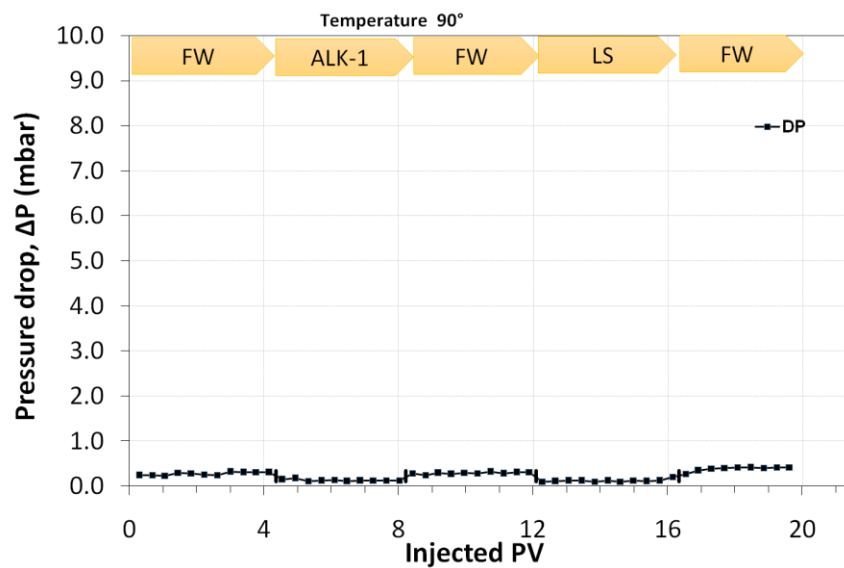


Figure 44: Pressure drop during test 7 at 90°C for Idaho Gray-1 core. Flooding sequence was FW - ALK-1 – FW – LS – FW.

8.8 Ion concentration measurement

Ion concentration was measured for the effluent of all the test to picture the inside scenario of the core. What kind of reactions is happening between the core and brines can be predicted through this. Ion chromatography test from test 1 is presented below. Measured cation concentrations and anion concentrations are showed in figure 45 and figure 46 respectively. As the formation water has high

salinity and has less impact on ion exchange, effluent of HS formation water is not included in the figure.

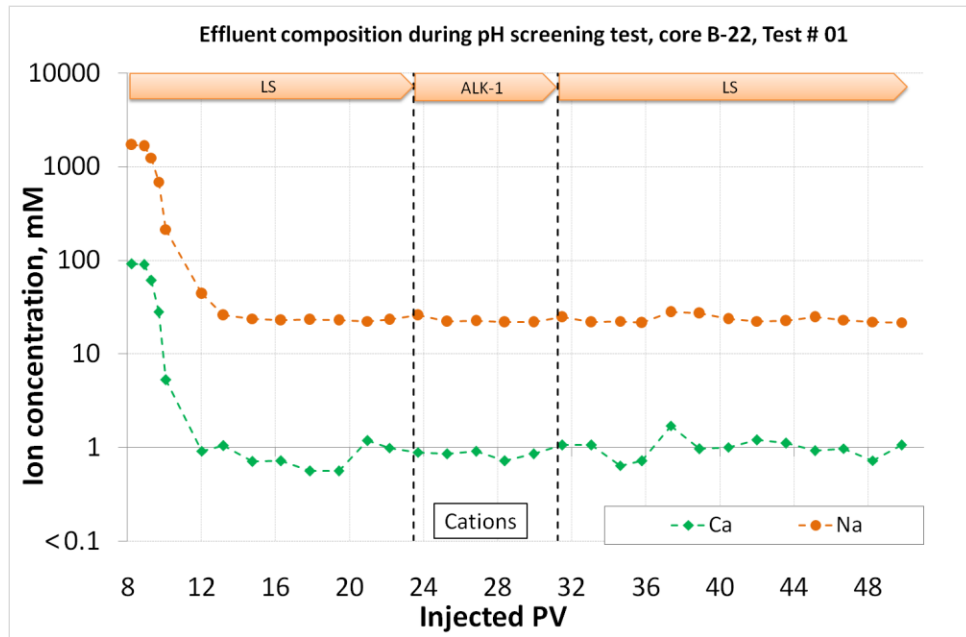


Figure 45: Cations concentration during pH screening test of core B-22, test 01 at ambient Temperature.

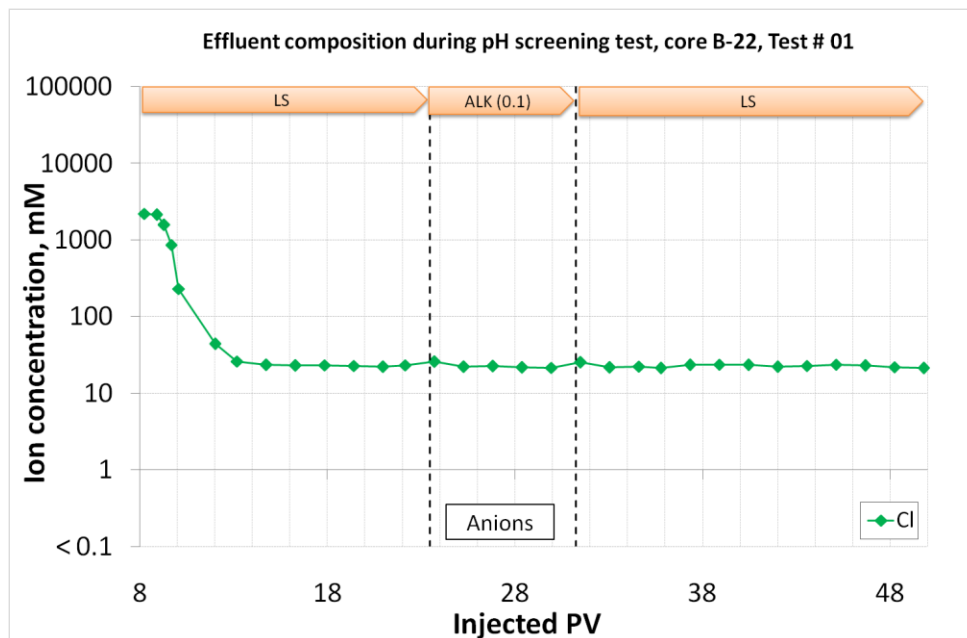


Figure 46: Anions concentration during pH screening test of core B-22, test 01 at ambient Temperature.

In case of cations, Na^+ and Ca^{2+} concentrations were measured to see if the divalent ions from the clay surface dissolved in the effluent by proton exchange from the LS or alkaline water. At 8 PV, both cations and anions were high due to formation water flooding in previous stage. As the LS flood started, the concentration went down steeply. However, there was no calcium in the LS or alkaline water, which was injected, but it can be seen that there are calcium ions in the effluent. This means, the calcium ions were coming from the core, mainly from the clays. Therefore, it can be said that chemical mechanism of Smart water (Austad et al., 2010) is one of the main mechanisms behind the pH increase in the LS flooding in sandstone. However, the core has just been flooded by FW containing Ca^{2+} , thus some Ca^{2+} has exchanged on the mineral surfaces, and those ions are now being exchanged back. This might also cause the presence of Ca^{2+} in alkaline and LS effluent. As Ca^{2+} was exchanged with H^+ from FW, the concentration of proton increased and the pH of the effluent of FW decreased. The concentration of Ca^{2+} was very low, but it was enough for pH change as two protons (H^+) were needed to replace that ion. Both in case of LS and alkaline water effluent, no suspicious result was found during the other test. For that reason, the data of other Ion Chromatography tests were not processed.

8.9 Scale Problems

Scaling problem is very common in alkaline flooding and it was discussed before in the alkaline flooding chapter. In this thesis, we had an issue with scale problems in the outlet of the producer during test 9. However, it was not sure whether HS formation water, LS or alkaline was responsible for that problem. But from the previous experiences of flooding in the Smart Water Lab and the literature review suggests that there is a very small chance of precipitation in case of HS and LS water flooding.

During test 9, when alkaline water with high concentration of carbonate flooded just after HS formation water that has calcium, by which calcium carbonate might form and precipitate. In figure 33, in test 9, the experiment was stopped after 7 PV of flooding due to a sudden pressure buildup. Later it was found that the distributor of producer was blocked by salt. As LS flooding never experienced this type of scale, it can be predicted that alkaline water was the main reason behind this scale.

On the other hand in test 8, that was done just before test 9, an alkaline environment was created by flooding LS, alkaline, LS, Alkaline, LS respectively. In that test, pH of the effluent reached highest 10.5 and after that, while flooding formation water, the pH didn't go down to its bulk pH. The pH of the FW effluent was around 7.8, which means that the alkalinity made the core less reactive or there is a precipitation. In test 9, the pH of alkaline didn't increase which indicating precipitation of $\text{Ca}(\text{OH})_2$

or CaCO_3 . However, in naked eye, no particle was found in the effluent, but the pH loss and sudden pressure drop indicate precipitation. Now it should be discussed why precipitation is causing drop in pH. pH of the alkaline effluent can be reduced by two ways, by forming $\text{Ca}(\text{HCO}_3)_2$ or by precipitating $\text{Ca}(\text{OH})_2$ or CaCO_3 which is expressed by equation 34 and 35 and discussed briefly at section 8.1. Therefore, if precipitation happens, pH of the effluent of alkaline will reduce more than bulk pH that is supported by test 9 and 10.

Theoretically, if higher concentration of alkali is used, the chance of precipitation will increase as there will be more CO_3^{2-} in the solution that might react with Ca^{2+} either from clay surface or from FW. Test 9 is a good example of precipitation as higher concentration was used. However, without this test, there is no other evidence that can say high concentration of alkali can create more precipitation than low concentration.

In conclusion, it can be said that alkaline creates precipitation or scaling problems, which may cause damage the production well or the reservoir.

8.10 Comparison between LS and Alkaline EOR potential

According to pH screening tests, as both alkaline and LS water has similar kind of pH increment in the effluent it can be said according to Aksulu et al. (2012) that both the brine has same potential of EOR in the used sandstone outcrop core. However, in some cases, LS has higher potential of better EOR than alkaline flooding as LS showed more pH increment. As it is mentioned before, without considering the minerology of the reservoir, it is not convenient to conclude that which one is better. Moreover, it also depends on the properties of oil as discussed before. However, before going for a recovery test, it is recommended to have a quick experiment of pH screening test. As pH screening test is indicating pH increment in the effluent, it is suggested to experiment recovery test using different types of oil.

8.11 Economical Analysis

In case of oil recovery, operational cost of different EOR methods are very important in the low oil price scenario. According to BP (British Petroleum), an additional 42 million barrels of oil from Clair Ridge field in UK can be produced at an additional cost of \$3 per barrel using LoSal® EOR (LS is

known as this name) (BP,2014). In that section, it is tried to find out a rough estimation of money that is needed to produce an extra barrel of oil in case of alkaline water flooding.

The general thumb rule of water flooding suggests 10 barrels of water produce 1 barrel of oil. If 0.1 gm of Na_2CO_3 is used as alkaline along with 0.9 gm of NaCl to make ALK-1 to inject then if we assume we have double oil production (2 barrels) then 159 gm of Na_2CO_3 is needed for 10 barrels of water which produces 2 barrels of oil.

According to Sigma-Aldrich Norway AS (accessed in 30 May, 2018), Price of 1000 gm Sodium Carbonate (ACS reagent grade) = 522 NOK including taxes. The price of Sodium Carbonate can be reduced upto 50% if it is purchased in huge amount in industrial basis which is lower in quality.

Therefore, to produce 1 barrel of extra oil, 41.5 NOK/ 5.1 \$ is needed. In addition, the price of NaCl is needed to be considered along with other operation cost and investment cost. Any kind of extra chemical injected is costly for EOR whereas NaCl is a kind of salt which is very cheap and environmental friendly.

Therefore, it can be said that using LS water as EOR fluid is more economical than alkaline if they have similar effect on oil recovery.

9. Conclusion

A series of pH screening tests were performed in this thesis with 100% water saturated sandstone outcrop cores at different temperature. The findings of the thesis are:

- In-situ generation of alkaline condition in the reservoir by injecting LS water seemed to have a larger potential for EOR purposes than transporting alkalinity by injecting high pH alkaline water through the reservoir.
- When injecting an alkaline solution with high bulk pH, the alkalinity cannot be transported even through a 7 cm long outcrop core as the minerals of the core consume most of the alkalinity. Therefore, it is impossible to transport the alkalinity in field scale where the distance between injector and producer is several hundred meters. However, which mineral consumes more alkalinity cannot be determined exactly with pH screening test.
- Mineralogy of sandstone affects both LS and alkaline pH change in the effluent as well as EOR potential of both fluids more than temperature change.
- The reason behind LS EOR is “Desorption by pH Increase” by Austad et al. (2010) rather than “Fine migration” by Tang and Morrow (1999) that is confirmed by Ion chromatography test and pressure measurement during the flooding. Though any EOR test was not performed but experiment from Torrijos (2017) support that statement. Moreover, pH the reason of pH increment during LS flooding matches the chemical mechanism of Austad et al (2010).

Recommendations for future work

There are several recommendations for future works that will be useful for EOR team at the University of Stavanger according to experimental findings presented in this thesis:

- The combination of LS effect and alkaline effect cannot be seen by pH screening test. Therefore, oil recovery test for both alkaline and LS water need be done along with measuring IFT of produced oil to investigate the IFT effect for alkaline and LS.
- Different alkaline such as sodium hydroxide or sodium orthosilicate can be used for pH screening test if precipitation risk can be minimized to see the alkaline transportability.
- The impact of clay in LS EOR is well established. pH screening test with alkaline water should be performed to sandstone core where there are no reactive clays to investigate the impact of clays on Alkaline by comparing with this result presented in the thesis.

NOMENCLATURE

λ_D	Mobility of the displacing fluid ($m^2/ Pa.s$)
d	Mobility of the displaced fluid ($m^2/ Pa.s$)
μ_w	water viscosity (Pa.s)
μ_o	Oil viscosity (Pa.s),
σ	Interfacial tension (IFT) (N/m)
Φ	Porosity
θ_c	Contact angle between the phases ($^\circ$)
Π	Disjoining pressure,
σ	Interfacial tension between two fluids
AN	Acid number
ALK	Alkaline
ASP	Alkaline, surfactant and polymer
BET	Brunauer – Emmet –Teller
BN	Base Number
CBR	Crude oil, Brine and Rock
CEC	Cation exchange capacity
DI	Deionized water
EOR	Enhanced oil recovery
E	Global/Total displacement efficiency
E_D	Microscopic displacement efficiency
E_V	Macroscopic (volumetric) displacement efficiency
FW	Formation water
HS	High salinity

IFT	Interfacial tension
IOR	Improved Oil Recovery
J^*	Leverett dimensionless entry pressure.
J	Mean surface curvature.
k	Permeability (m^2)
k_{rw}	Relative permeability of water (m^2)
k_{ro}	Relative permeability of oil (m^2),
LS	Low salinity
M	Mobility ratio
MIE	Multi -component ion exchange
NSO	Oxygen, Nitrogen and Sulfur
OOIP	Original oil in place
P_c	Capillary pressure (Pa)
P_o	Pressure in the oil phase at interface (Pa),
P_w	Pressure in the water phase at interface (Pa),
ppm	Parts per million
r_c	Pore radius of capillary (m)
SEM	Scanning Electron Microscope
S_{or}	Residual oil saturation
S_{wi}	Irreducible water saturation.
TDS	Total Dissolved Solid
WAG	Water Alternating Gas
wt%	Weight percent

References

Abdullah, N.B., 2016. Reservoir wetting in sandstone reservoirs, adsorption of polar basic oil components onto quartz and feldspar minerals. Master's Thesis. University of Stavanger.

Aghaeifar, Z., Strand, S., Austad, T., Puntervold, T., Aksulu, H., Navratil, K., Storås, S. and Håmsø, D., 2015. Influence of formation water salinity/composition on the low-salinity enhanced oil recovery effect in high-temperature sandstone reservoirs. *Energy & Fuels* 29(8): 4747-4754.

Ahmed, T., 2010. Principles of Waterflooding Reservoir Engineering Handbook (Fourth Edition) (pp. 909-1095). Boston: Gulf Professional Publishing.

Ahmed, T., and McKinney, P.D., 2005. 4 - Performance of Oil Reservoirs Advanced Reservoir Engineering (pp. 291-325). Burlington: Gulf Professional Publishing.

Aksulu, H., Håmsø, D., Strand, S., Puntervold, T. and Austad, T., 2012. Evaluation of Low-Salinity Enhanced Oil Recovery Effects in Sandstone: Effects of the Temperature and pH Gradient. *Energy & Fuels*, 26(6), 3497-3503.

Alroudhan, A. R., Vinogradov, J. and Jackson, M.D., 2015. Zeta potential in carbonates at reservoir conditions-application to IOR. Paper presented at the 18th European Symposium on Improved Oil Recovery, Dresden, Germany., 14-16 April.

Anderson, W. G., 1986a. Wettability Literature Survey - Part 1: Rock/oil/brine interactions and the effects of core handling on wettability. *Journal of Petroleum Technology*, 38(10), 1125-1144.

Anderson, W. G., 1986b. Wettability literature survey - Part 2: Wettability measurement. *Journal of Petroleum Technology*, 38(11), 1246-1262.

Anderson, W. G., 1986c. Wettability literature survey - Part 4: Effects of wettability on capillary pressure. *Journal of Petroleum Technology*, 39(10), 1283-1300.

Armstrong, R.T., Georgiadis, A., Ott, H., Klemin, D. and Berg, S., 2014. Critical capillary number: desaturation studied with fast X-ray computed microtomography. *Geophysical Research Letters* 41(1): 55-60.

Austad, T., 2013. Chapter 13 - Water based EOR in carbonates and sandstones: new chemical understanding of the EOR potential using “Smart Water”. Enhanced oil recovery field case studies. J. J. Sheng. Boston, Gulf Professional Publishing: 301-335.

Austad, T., and Milter, J., 1997. Spontaneous imbibition of water into low permeable chalk at different wettabilities using surfactants. Paper presented at the International Symposium on Oilfield Chemistry.

Austad, T., RezaeiDoust, A., & Puntervold, T., 2010. Chemical mechanism of low salinity water flooding in sandstone reservoirs. Paper presented at the SPE improved oil recovery symposium.

Bavière, M., 1991. Basic concepts in enhanced oil recovery processes (Vol.33): Springer.

Berger, P.D. and Lee, C.H., 2006. Improved ASP process using organic alkali. Paper SPE 99581 at the SPE/DOE Seventh Symposium on Enhanced Oil Recovery, Tulsa, 22-26 April.

Boston, W.G., Brandner, C.F. and Foster, W.R., 1969. Recovery of oil by waterflooding from an argillaceous, oil-containing subterranean formation. US Patent 3,740,956, 7 October.

BP. 2014. Low salinity water brings award for BP. Retrieved from <https://www.bp.com/en/global/corporate/bp-magazine/innovations/offshore-technology-award-for-clair-ridge.html>

Brady, P. V., Morrow, N.R., Fogden, A., Deniz, V., Loahardjo, N. and Winoto, 2015. Electrostatics and the low salinity effect in sandstone reservoirs. *Energy & Fuels* 29(2): 666-677.

Buckley, J. S., 1994. Chemistry of the crude oil/brine interface. Proceedings of the 3rd International Symposium on Evaluation of Reservoir Wettability and Its Effect on Oil Recovery, Laramie, WY, USA, 21-23 September.

Buckley, J. S., 1995. Asphaltene precipitation and crude oil wetting SPE Advanced Technology Series 3(1): 53-59.

Buckley, J. S., 2001. Effective wettability of minerals exposed to crude oil. *Current opinion in Colloid & Interface Science* 6(3): 191-196.

Buckley, J. S. and Fan, T., 2007. Crude oil/brine interfacial tensions 1. *Petrophysics* 48(3).

Buckley, J. S. and Liu, Y., 1998. Some mechanisms of crude oil/brine/solid interactions. *Journal of Petroleum Science and Engineering* 20(3-4): 155-160.

Buckley, J.S., Liu, Y., and Monsterleet, S., 1998. Mechanisms of wetting alteration by crude oils. *SPE Journal*, 3(01), 54-61.

Buckley, J.S. and Morrow, N.R., 2010. Improved oil recovery by low salinity Water-flooding: A Mechanistic Review, presentation at the 11th International Symposium on Reservoir Wettability. University of Calgary, Calgary, Alberta, Canada, 6-9 September.

Buckley, J. S., Takamura, K. and Morrow, N.R., 1989. Influence of electrical surface charges on the wetting properties of crude oils. *SPE Reservoir Engineering* 4(3): 332-340.

Burk, J.H., 1987. Comparison of sodium carbonate, sodium hydroxide and sodium orthosilicate for EOR. *SPERE*. (February), 9-16.

Carroll, D., 1959. Ion exchange in clays and other minerals. *Geological Society of America Bulletin* 70(6): 749-779.

Castor, T.P., Edwards, J.B. and Passman, F.J., 1981a. Response of modify control agents to shear, electronical and biological stress.

Chang, H.L., 1976. Oil recovery by alkaline waterflooding, Canadian Patent No. 1037863, 24 February.

Campbell, T.C., 1981. The role of alkaline chemicals in oil displacement mechanisms.

Chapman, D. L., 1913. LI. A contribution to the theory of electrocapillarity. *The London, Edinburgh, and Dublin philosophical magazine and journal of science*, 25(148), 475-481.

Chen, H.L., Lucas, L.R., Nogaret, L.A.D, Yang, H.D. and Kenyon, D.E., 2000. Laboratory monitoring of surfactant imbibition using computerized tomography. Paper SPE 59006 presented at the SPE International Petroleum Conference Villahermosa, Mexico., February 1-3.

Cheng, K.H., 1986. Chemical consumption during alkaline flooding: A comparative evaluation. Paper SPE 14944 presented at the SPE/DOE Seventh Symposium on Enhanced Oil Recovery, Tulsa, 20-23 April.

Cissokho, M., Boussour, S., Cordier, P., Bertin, H. and Hamon, G., 2009. Low salinity oil recovery on clayey sandstone: experimental study. Paper presented at the International Symposium of the Society of Core Analysts, Noordwijk, The Netherlands, 27-30 September.

Cooke, C.E., Williams, R.E. and Kolodzie, P.A., 1974. Oil recovery by alkaline waterflooding, JPT (February), 1365-1374.

Craig, F.F., 1971. Basic water-oil flow properties of reservoir rock. In S. o. P. E. o. AIME (Ed.), The reservoir engineering aspects of waterflooding (pp. 12-28). Dallas, TX, USA: Henry L. Doherty Memorial Fund of AIME.

Crundwell, F., 2015. The mechanism of dissolution of the feldspars: Part I. Dissolution at conditions far from equilibrium. Hydrometallurgy, 151, 151-162.

Derjaguin, B., and Landau, L., 1941. The theory of stability of highly charged lyophobic sols and coalescence of highly charged particles in electrolyte solutions. Acta Physicochim. URSS, 14(633-52), 58.

Derjaguin, B.V., Churaev, N.V., and Muller, V.M., 1987. Chapter 8: The Derjaguin-Landau-Verwey-Overbeek (DLVO) theory of stability of lyophobic colloids. Surface Forces. J. A. Kitchener. New York, Consultants Bureau.

deZabala, E.F., Vislocky, J.M., Rubin, E. and Radke, C.J., 1982. A chemical theory for linear alkaline flooding. SPEJ (April), 245-258.

Didier, M., Chaumont, A., Thibaut, J., Bondino, I. and Hamon, G., 2015. Contradictory trends for smart water injection method: role of pH and salinity from sand/oil/brine adhesion maps. Paper SCA2015-005 presented at the International Symposium of the Society of Core Analysts, St. John's Newfoundland and Labrador, Canada, 16-21 August.

Dunning, H.N., Moore, J.W. and Denekas, M.O., 1953. Interfacial activities and porphyrin contents of petroleum extracts. *Ind. Eng. Chem.* 45 (August), 1758-1765.

Ehrlich, R. and Wygal, R.J., 1977. Interaction of crude oil and rock properties with the recovery of oil by caustic waterflooding. *SPEJ* (August), 263-279.

Elsevier, 2016. Enhanced oil recovery – Do you have the right EOR strategy?. Retrieved from <https://www.elsevier.com/rd-solutions/industry-insights/oil-and-gas/enhanced-oil-recovery>

Emitech., 1999. Technical brief - sputter coating incorporating emitech K500, K550, K575 And K675X. Retrieved from https://crn2.3it.usherbrooke.ca/guide_sb/appareils/Emitech/SputterCoating.pdf

Fatt, I. and Jr., W.A.K., 1959. Effect of fractional wettability on multiphase flow through porous media. *SPE Journal of Petroleum Technology*, 11(10): 71-76.

Flaaten, A.K., Nguyen, Q.P., Zhang, J.-Y., Mohammadi, H. and Pope, G.A., 2008. Chemical flooding without the need for soft water. Paper SPE 116754 presented at the SPE Annual Technical Conference and Exhibition, Denver, 21-24 September.

Goldstein, J., Newbury, D., Joy, D., Lyman, C. and Echlin, P., 2003. *Scanning electron microscopy and x-ray microanalysis* (3rd ed.). New York: Springer Science.

Green, D.W., & Willhite, G.P., 1998a. *Enhanced Oil Recovery* (4th ed.): Henry L. Doherty Memorial Fund of AIME, Society of Petroleum Engineers.

Green, D.W., & Willhite, G.P., 1998b. Introduction to EOR Processes *Enhanced Oil Recovery* (4th ed., pp. 1-11). Richardson, TX, USA: Henry L. Doherty Memorial Fund of AIME, Society of Petroleum Engineers.

Green, D.W., & Willhite, G.P., 1998c. Macroscopic Displacement of Fluids in a Reservoir. In F. Poettmann & F. Stalkup (Eds.), *Enhanced Oil Recovery* (4th ed., pp. 79-99). Richardson, TX, USA: Henry L. Doherty Memorial Fund of AIME, Society of Petroleum Engineers.

Green, D.W., and Willhite, G.P., 1998d. Microscopic Displacement of Fluids in a Reservoir. In F. Poettmann and F. Stalkup (Eds.), Enhanced Oil Recovery (4th ed., pp. 12-35). Richardson, TX, USA: Henry L. Doherty Memorial Fund of AIME, Society of Petroleum Engineers.

Grim, R.E., 1939. Properties of clays, Recent Marine Sediments. AAPG, Tulsa, PP. 466-495.

Guo, H., Dou, M., Hanqing, W., Wang, F., Yuanyuan, G., Yu, Z., Yansheng, W., and Li, Y., 2015. Review of capillary number in chemical enhanced oil Recovery. Paper SPE 175172 presented at the 2015 Oil and Gas Show and Conference, Mishref, Kuwait, 2015/10/11/.

Gouy, M., 1910. Sur la constitution de la charge électrique à la surface d'un électrolyte. J. Phys. Theor. Appl., 9(1), 457-468.

Holm, L.W. and Robertson, S.D., 1981. Improved micellar/polymer flooding with high-pH chemicals. JPT 33(1), 161-172.

Hirasaki, G. J., 1991. Wettability: fundamentals and surface forces. SPE Formation Evaluation 6(2): 217-226.

Huang, Y.-Z. and Yu, D.-S., 2002. Mechanisms and principles of physicochemical flow.

IDF, 1982. Clay chemistry. Technical manual. Aberdeen, UK, International Drilling Fluids Limited.

Israelachvili, J.N., 2011. Electrostatic Forces Between Surfaces in Liquids Intermolecular and Surface Forces (3rd ed., pp. 291-340): Academic Press.

Israelachvili, J.N., and McGuiggan, P.M., 1988. Forces between surfaces in liquids. Science, 241(4867), 795.

Jaafar, M., Nasir, A.M., and Hamid, M., 2014. Measurement of isoelectric point of sandstone and carbonate rock for monitoring water encroachment. Journal of Applied Sciences, 14(23), 3349-3353.

Jadhunandan, P.P. and Morrow, N.R., 1995. Effect of wettability on waterflood recovery for crude-oil/brine/rock systems. SPE Reservoir Engineering 10(1): 40-46.

Jahn, F., Cook, M. and Graham, M., 2008. Reservoir Description Hydrocarbon Exploration and Production (2nd ed., pp. 95-171). Amsterdam: Elsevier.

Krumrine, P.H., Falcone, J.S. and Campbell, T.C., 1982. Surfactant flooding 2: the effect of alkaline additives on permeability and sweep efficiency. SPEJ (December), 983-992.

Labrid, J., 1991. The use of alkaline agents in enhanced oil recovery processes.

Lager, A., Webb, K.J. and Black, C.J., 2006. Low salinity oil recovery-an experimental investigation. Paper SCA 2006-36 presented at the International Symposium of the Society of Core Analysis, Trondheim.

Lager, A., Webb, K. J. and Black, C.J., 2007. Impact of brine chemistry on oil recovery. Paper presented at the IOR 2007-14th European Symposium on Improved Oil Recovery.

Lager, A., Webb, K.J., Collins, I.R. and Richmond, D.M., 2008. LoSal™ enhanced oil recovery: evidence of enhanced oil recovery at the reservoir scale. Paper SPE 113976 presented at the 2008 SPE/DOE Improved Oil Recovery Symposium, Tulsa, OK, USA, 19-23 April.

Li, H.-B., 2007. Advances in alkaline-surfactant-polymer flooding and pilot tests. Science Press.

Ligthelm, D.J., Gronsveld, J., Hofman, J., Brussee, N., Marcelis, F., and van der Linde, H., 2009. Novel waterflooding strategy by manipulation of injection brine composition. Paper presented at the EUROPEC/EAGE Conference and Exhibition.

Mayer, E.H., Berg, R.L., Carmichael, J.D. and Weinbrandt, R.M., 1983. Alkaline injection for enhanced oil recovery-a status report. JPT (January), 209-221.

McGuire, P., Chatham, J., Paskvan, F., Sommer, D. and Carini, F., 2005. Low salinity oil recovery: An exciting new EOR opportunity for Alaska's North Slope. Paper presented at the SPE Western Regional Meeting.

- Molnes, S.N., 2017. Evaluation of cellulose nanocrystals as a green “Smart Water” additive in enhanced oil recovery from sandstone reservoirs. Dr. Ing. Thesis, University of Stavanger, Dr. Ing. Thesis.
- Morrow, N.R., 1979. Interplay of capillary, viscous and buoyancy forces in the mobilization of residual oil. *JCPT* 18(3).
- Morrow, N.R. and Buckley, J., 2011. Improved Oil Recovery by Low – Salinity Waterflooding. *Journal of Petroleum Technology*, 63(5), 106-112.
- Morrow, N.R., Tang, G.-q., Valat, M. and Xie, X., 1998. Prospects of improved oil recovery related to wettability and brine composition. *Journal of Petroleum Science and Engineering*, 20(3), 267-276.
- Muggeridge, A., Cockin, A., Webb, K., Frampton, H., Collins, I., Moulds, T. and Salino, P., 2014. Recovery rates, enhanced oil recovery and technological limits. *Philosophical Transactions of the Royal Society A: Mathematical, Physical and Engineering Sciences*, 372(2006).
- Mungan, N., 1966a. Certain wettability effects in laboratory waterfloods. *JPT* (February), 247-252.
- Mungan, N., 1966b. Interfacial effects in immiscible liquid-liquid displacement in porous medium. *SPEJ* (September), 247-253.
- Nichols, G., 2009. *Terrigenous Clastic Sediments: Gravel, Sand and Mud Sedimentology and Stratigraphy* (2nd ed., pp. 5-27). West Sussex, UK: Wiley-Blackwell.
- Olsen, D.K., Hicks, M.D., Hund, B.G., Sinnokrot, A.A. and Sweigart, C.N., 1990. Design of a novel flooding system for an oil-wet Central Texas carbonate reservoir. Paper SPE 20224 presented at the SPE/DOE Seventh Symposium on Enhanced Oil Recovery, Tulsa, 22-25 April.
- Pasquarelli, C.H. and Wasan, D.T., 1979. The effect of film-forming materials on the dynamic interfacial properties of crude oil-aqueous system. Paper presented at the Third International Conference on Surface and Colloid Science, Stockholm, 20-25 August.
- Pettijhon, F.J., 1975. *Sedimentary rocks*. New York., Harper & Row Limited, ISBN 9780060451912.

Pu, H., Xie, X., Yin, P. and Morrow, N.R., 2008. Application of coalbed methane water to oil recovery by low salinity waterflooding, Paper SPE 113410 presented at the 2008 SPE Improved Oil Recovery Symposium, Tulsa, OK, USA.

Rao, D.N., 1999. Wettability effects in thermal recovery operations. *SPE Reservoir Evaluation & Engineering* 2(5): 420-430.

RezaeiDoust, A., Puntervold, T., and Austad, T., 2011. Chemical verification of the EOR mechanism by using low saline/smart water in Sandstone. *Energy & Fuels*, 25(5), 2151-2162.

RezaeiDoust, A., Puntervold, T., Strand, S. and Austad, T., 2009. Smart Water as wettability modifier in carbonate and sandstone: A discussion of similarities/differences in the chemical mechanisms. *Energy & Fuels* 23(9): 4479-4485.

Riley, J., 2010. Charge in Colloidal Systems. In T. Cosgrove (Ed.), *Colloid Science: Principles, Methods and Applications* (pp. 14-35). Bristol, UK: John Wiley & Sons.

Rudzinski, W.E., Oehlers, L. and Zhang, Y., 2002. Tandem mass spectrometric characterization of commercial naphthenic acids and a Maya crude oil. *Energy Fuels* 16 (5), 1178-1185.

Salathiel, R.A., 1973. Oil recovery by surface film drainage in mixed-wettability rocks. *Journal of Petroleum Technology* 25(10): 1216-1224.

Seifert, W.K., 1975. Carboxylic acids in petroleum sediments. *Progress in Chemistry of Natural Products*, Springer-Verlag.

Shen, M.-D. and Chen, Z., 1996. Chemical behavior of minerals in alkaline solutions.

Sheng, J., 2011. *Modern chemical enhanced oil recovery: Theory and practice*. Burlington, Mass: Gulf Professional.

Sheng, J., 2014. Critical review flow of low salinity water flooding. *Journal of Petroleum Science and Engineering*, 120,216–224.

Shi, L., Olsson, M.H.M., Hassenkam, T. and Stipp, S.L.S., 2016. A pH Resolved View of the Low Salinity Effect in Sandstone Reservoirs. *Energy & Fuels*, 30(7), 5346-5354.

Shular, P.J., Kuehne, D.L. and Lerner, R.M., 1989. Improving chemical flood efficiency with micellar/alkaline/polymer process. *JPT* (January), 80-88.

Standnes, D.C. and Austad, T., 2000. Wettability alteration in chalk: 1. Preparation of core material and oil properties. *Journal of Petroleum Science and Engineering* 28(3): 111-121.

Somerton, W.H. and Radke, C.J., 1983. Role of clays in the enhanced oil recovery of petroleum from some California sands. *JPT* (March), 643-654.

Stern, O., 1924. The theory of the electrolytic double-layer. *Z. Elektrochem*, 30(508), 1014-1020.

Strand, S., 2005. Wettability alteration in chalk - A study of surface chemistry. PhD Thesis. Dr. Ing., University of Stavanger.

Subkow, P., 1942. Process for the removal of bitumen from bituminous deposits, US Patent No. 2,288,857,7 July.

Taber, J.J., Martin, F.D. and Seright, R.S., 1997. EOR screening criteria revisited-part1: introduction to screening criteria and enhanced recovery field projects. *SPE Reservoir Engineering* 12(3): 189-198.

Tang, G.Q. and Morrow, N.R., 1997. Salinity, temperature, oil composition, and oil recovery by waterflooding. *SPE Reservoir Engineering* 12(4): 269-276.

Tang, G.-Q., and Morrow, N.R., 1999. Influence of brine composition and fines migration on crude oil/brine/rock interactions and oil recovery. *Journal of Petroleum Science and Engineering*, 24(2), 99-111.

Torrijos, I.D.P., 2017. Enhanced oil recovery from sandstones and carbonates with “Smart Water”. Dr. Ing. Thesis, University of Stavanger, Dr. Ing. Thesis.

Velde, B.B. and Meunier, A., 2008. The origin of clay minerals in soils and weathered rocks. Berlin, Germany, Springer.

Verwey, E., and Overbeek, J. T. G., 1955. Theory of the stability of lyophobic colloids. *Journal of Colloid Science*, 10(2), 224-225.

Wagner, O.R. and Leach, R.O., 1959. Improving oil displacement efficiency by wettability adjustment. *Trans AIME* 216, 65-72.

Wang, W. and Gupta. A., 1995. Investigation of the effect of temperature and pressure on wettability using modified pendant drop method. Paper SPE 30544 presented at the Annual Technical Conference & Exhibition Dallas, Texas, USA, 22-25 October.

Winoto, W., Loahardjo, N., Xie, S.X., Yin, P. and Morrow, N.R., 2012. Secondary and tertiary recovery of crude oil from outcrop and reservoir rocks by low salinity waterflooding. Paper SPE 154209 presented at the eighteenth SPE Improved Oil Recovery Symposium, Tulsa, Oklahoma, USA, 14-18 April.

Worden, R.H. and Morad, S., 2003. *Clay mineral cements in sandstones*: Blackwell Pub.

Yildiz, H.O., Valat, M. and Morrow, N.R., 1999. Effect of brine composition on wettability and oil recovery of a Prudhoe Bay crude oil. 38(1).

Yong, R.N., Nakano, M. and Pusch, R., 2012. *Environmental soil properties and behaviour*. Boca Raton, USA, Taylor & Francis, ISBN 978-1-4398-4530-1.

Zhang, Y., and Morrow, N.R., 2006. Comparison of secondary and tertiary recovery with change in injection brine composition for crude oil/sandstone combinations. Paper presented at the SPE/DOE Symposium on Improved Oil Recovery.

Zhang, Y., Xie, X. and Morrow, N.R., 2007. Waterflood performance by injection of brine with different salinity for reservoir cores. Paper presented at the SPE Annual Technical Conference and Exhibition.

Zhao, S., Zhang, L., Luo, L. and Yu, J.Y., 2002. Synergy between displacement agents and the active components of crude oils.

Zolotukhin, A.B., & Ursin, J.-R. 2000. Classification of EOR methods introduction to petroleum reservoir engineering (pp. 299-305). Kristiansand: Norwegian Academic Press (HøyskoleForlaget).